

University of Alberta

**The New Compact Torque Multiplier (CTM) for
Bolt Joints Tightening in Mining Equipment**

by

Richard W. Sobieski 

A thesis submitted to the Faculty of Graduate Studies and Research
in partial fulfillment of the requirements for the degree of

Master of Science
in
Mining Engineering

The Department of Civil and Environmental Engineering

Edmonton, Alberta
Spring 2007



Library and
Archives Canada

Bibliothèque et
Archives Canada

Published Heritage
Branch

Direction du
Patrimoine de l'édition

395 Wellington Street
Ottawa ON K1A 0N4
Canada

395, rue Wellington
Ottawa ON K1A 0N4
Canada

Your file *Votre référence*
ISBN: 978-0-494-30027-5
Our file *Notre référence*
ISBN: 978-0-494-30027-5

NOTICE:

The author has granted a non-exclusive license allowing Library and Archives Canada to reproduce, publish, archive, preserve, conserve, communicate to the public by telecommunication or on the Internet, loan, distribute and sell theses worldwide, for commercial or non-commercial purposes, in microform, paper, electronic and/or any other formats.

The author retains copyright ownership and moral rights in this thesis. Neither the thesis nor substantial extracts from it may be printed or otherwise reproduced without the author's permission.

AVIS:

L'auteur a accordé une licence non exclusive permettant à la Bibliothèque et Archives Canada de reproduire, publier, archiver, sauvegarder, conserver, transmettre au public par télécommunication ou par l'Internet, prêter, distribuer et vendre des thèses partout dans le monde, à des fins commerciales ou autres, sur support microforme, papier, électronique et/ou autres formats.

L'auteur conserve la propriété du droit d'auteur et des droits moraux qui protègent cette thèse. Ni la thèse ni des extraits substantiels de celle-ci ne doivent être imprimés ou autrement reproduits sans son autorisation.

In compliance with the Canadian Privacy Act some supporting forms may have been removed from this thesis.

Conformément à la loi canadienne sur la protection de la vie privée, quelques formulaires secondaires ont été enlevés de cette thèse.

While these forms may be included in the document page count, their removal does not represent any loss of content from the thesis.

Bien que ces formulaires aient inclus dans la pagination, il n'y aura aucun contenu manquant.


Canada

Dedication

To my
lovely family:
Grace, Roma, and Jacob;
and in memory of my parents
Katarzyna and Wladyslaw Sobieski.

Abstract

This thesis presents a detailed design concept, and analyses, of kinematics and forces-based methods for the design of compact epicyclic planetary type gear trains torque multiplier for the tightening of bolt joints mining equipment.

The new design is a hand-held Compact Torque Multiplier (CTM), which is superior in parameters (e.g. dimensions, weight, output rpm and diameter) and performance with existing off-the-shelf items, including SA6AM and SA8AM.

In order to ultimately assess the performance of the CTM under different geometrical conditions, knowledge of the kinematics of interior gear assembly of the conventional CTM is required. To determine the kinematics, a model approach was used. The computed and empirical geometrical and kinematical values were in concordance with ISO and AGMA revealed standards.

The new CTM has the abilities to improve human working conditions by reducing the noise and vibration levels, and improving the quality of tightening bolt joints, which reduces joint failure occurrences caused by inadequate tightening.

Acknowledgments

I wish to express my thanks to Dr. J. Z. Szymanski, PhD. P. Eng, for giving me the opportunity to identify and work on this research project.

Without his advice and dynamism he has shown as peer leader in research, this particular project would not have taken place.

Table of Contents

SECTION	Page
1. INTRODUCTION	
1.1. Objectives of the project	1
1.2. Structure of study	3
2. POWER SUPPLY	
2.1. Power supply sources	4
2.2. Air motor benefits	5
2.3. Air motor requirements for CTM	6
2.4. Characteristics of vane air motors	7
2.5. Analyses of air motors data	10
2.6. Shaft-rotor speed control	15
2.7. Silencing	15
2.8. Discussion	16
3. GEAR ARRANGEMENTS	
3.1. Parallel axis arrangements – General Consideration	17
3.2. Kinematics parameters of planetary gear set	18
3.3. Design of the planetary gear drives with parallel axis gears	20
3.4. Epicyclic planetary gear arrangement	21
3.5. Simple epicyclic planetary gear train	21

4. ANALYTICAL CONSIDERATION OF THE PROPOSED DESIGN

4.1.	Geometry considerations of the design	23
4.2.	Space criteria for planetary gear design	
4.2.1.	Coaxiality	25
4.2.2.	Assembly	25
4.2.3.	Neighborhood criteria	26
4.3.	Gear calculations for new design	
4.3.1.	The first stage selected data	27
4.3.2.	The second stage mechanical parameters of the CTM	29
4.3.3.	The third stage parameters of the CTM	30
4.4.	Determination of the critical frequency for the first stage of the CTM	31
4.5.	Torsion and bending effect – third sun gear	32
4.6.	Windage and bearing losses	33
4.7.	Effective air pressure for applicable output torque of the CTM	34
4.8.	Materials	37
4.9.	Lubricant for CTM 1100	39

5. DESIGN OF THE NEW COMPACT TORQUE MULTIPLIER

5.1.	GPS surface texture for first and third carrier for the CTM 1100	40
5.2.	Final design of the new CTM 1100	44
5.3.	The CTM 1100 and the existing worldwide bolt tightening tools	43

6.	CONCLUSIONS and RECOMMENDATIONS for FUTURE WORK	46
7.	REFERENCES	48
8.	APPENDICES	51
A;	GEAR GEOMETRY	54
B.	GEOMETRY of MATING GEARS	73
C;	NOTATION, SYMBOLS and ABBREVIATIONS, on base AGMA 6123-A83	83
D;	NOTATION, SYMBOLS and ABBREVIATIONS, on base ISO 6336-1, 1996	88
E;	FORMULAS RELATING to INDIVIDUAL GEARS	95
F;	TOOTH THICKNESS and MEASUREMENTS	99
G;	CALCULATIONS	103
H;	MATERIALS and LUBRICANT	125

List of Tables

	Title	Page
Table 1.	Air motors performance data at maximum operating pressure: 6.2 bar	13
Table 2.	Air motors performance data at minimum operating pressure: 4.8 bar	14
Table 3.	Ratio available for simple epicyclic gear arrangements	21
Table 4.	Selected geometrical parameters of the first stage of the CTM	27
Table 5.	Selected mechanical parameters of the first stage of the CTM	28
Table 6.	The list selected mechanical parameters of the second stage of the CTM	29
Table 7.	The list of selected mechanical parameters for the third stage of the CTM	30
Table 8.	General properties of the major materials used for CTM 1100	38
Table 9.	Bolt tightening tools commercially available in the world	45

List of Figures

	Title	Page
Figure 1	Air motor flow diagram	4
Figure 2	Air motor characteristics and performance curve	7
Figure 3	CTM 1100 air motor theoretical performance graph	8
Figure 4	Performance graph Ingersoll Rand air motor SM6AM	9
Figure 5	Performance graph Ingersoll Rand air motor SM8AM	9
Figure 6	Elasticity of motor	10
Figure 7	Simple gear arrangement with parallel axis	17
Figure 8	Epicyclic gear arrangements	19
Figure 9	Simple epicyclic gear train, solar, star and planetary	22
Figure 10	Velocity and speed ratio diagram	24
Figure 11	Planets neighborhood spacing criteria	26
Figure 12	CTM 1100 first stage torsion frequency graph	31
Figure 13	Bending and torsion acting in last sun gear	32
Figure 14	Graph representing power losses in third stage	33
Figure 15	CTM 1100 Input – Output/Output Torque diagram	34
Figure 16	Pressure drop and effect to applied output torque	37
Figure 16	First carrier with GPS symbols	40
Figure 17	Third carrier with GPS symbols	40
Figure 18	Surface profile	42

Figure 19	Surface parameters	42
Figure 20	Local slope profile	42
Figure 21	Assembly of CTM 1100 with air motor and section view of planetary gear set	44

1. INTRODUCTION

1.1. Objectives of the Project

The primary objectives of this research can be summarized as:

- Minimizing the CTM, including general dimensions, outside diameter, overall length, and weight (the relationship between the sun gear diameter and the gear ring diameter);
- Developing the CTM to be able to tighten bolt joints with high torque accuracy, repeatability, and generate sufficient torque applied to bolt joints; and,
- The design CTM mechanism should be able to provide the following output parameters:
 - o Output torque of 1100 Nm; and,
 - o Output shaft free speed of 100 rpm.

The new CTM designed will:

- Improve the tightening quality of bolt joints;
- Reduce harmful vibrations and effects on the human body;
- Achieve the minimum operating noise level; and,
- Reduce operating and capital costs.

The current literature available for epicyclic gear trains arrangements provides clear explanations for its kinematics solutions, ISO [5, 7, 8, 9 and 10] and ANSI/AGMA [1, 2, 3, and 4] standards, which cover industrial and mobile applications of external and internal gears.

Unfortunately, there are no publications to date that present simple and comprehensive design criteria and analytic techniques for hand-held tool utilizing planetary gear sets.

This dissertation develops techniques, which provide a potential solution for the unique design of hand-held tools with planetary gear trains.

The developed methodology provides relationships between the magnitude of output torque, bolt fastening torque, and tension forces that detail problems required future study.

1.2. Structure of Study

The findings of the current study will provide knowledge and sufficient information to enable the design and operation of the hand-held Compact Torque Multiplier (CTM), including performance parameters and the model developed. The developed model links dimensional settings with the predicted operating performance parameters. In Section 2, the general and basic information related to the fundamental data of available power supply, air sources, and hydraulic has been discussed. This section also discusses the selection of air motors and analyzes the air motors data.

Fundamental information related to epicyclic gear arrangements and their behaviors, as well parallel axis problem in gear setup, is discussed in Section 3.

The analytical portion of this work contains summaries of geometrical and strength gear data, critical frequency, torsional and bending effect, and the influence of a drop in air pressure and its effect on output torque. Axial forces in bolt joint and materials selected are also subjects covered in Section 4. The design portion covers Geometrical Product Specification (GPS), parallelism, perpendicularity, and concentricity in planetary carriers, including surface finishing and radial transition from one plane to another. Removing unnecessary material without jeopardizing the strength of the part and component reduces the rotating mass. This is covered in Section 5. Discussion and review of current available tools on the market is enclosed in Section 6. Conclusive comments and recommendations for further studies are given in the same section. References, referring to the most recent and updated textbooks that helped develop the literature review in this study, are covered in Section 7.

2. POWER SUPPLY

2.1. Power supply sources

Pneumatic-air motors are compact in relation to their power and the ease with which they are controlled within a wide range of shaft rotation speeds; this is largely due to their favorable torque characteristics. Air motors can withstand severe operation conditions, including heat, moisture, dirt, and vibrations. When applied for bolting joint, the most important factor for these motors is that they can be loaded to stall without damage. A full list of the benefits is presented in Section 2.2. Additionally, the most important benefit, which must be pointed out separately, is that they do not emit toxic gases, and do not involve any risk of explosion.

The vane motor, design, and operating principles are illustrated in Figure 1.

The compression stroke is divided by a number of vanes that can retract into the rotor; compression strokes are formed by the relative motion between a rotor and a stator. In short, the rotor is equipped with radial slots in which vanes slide, and is eccentrically mounted relative to the stator.

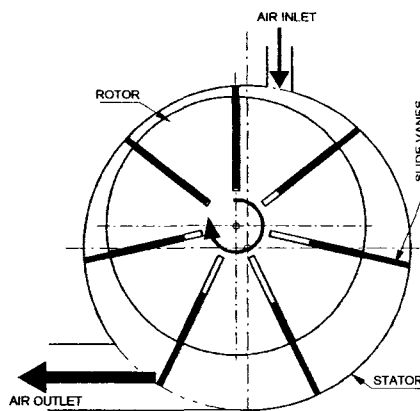


Figure 1. Air motor flow diagram

These vanes of the motor are compressed against the outer wall by centrifugal force, and either the springs or the working pressure. The vanes form cells that expand and contract with the movement of the rotor.

The compression volume could be expressed by:

$$V_l = 4 * \pi * r_{avg} * e * b \quad (1)$$

Where:

r_{avg}	Average radius of vanes (mm)
e	Eccentricity of rotor (mm)
b	Length of the vanes (mm)

2.2. Air Motor Benefits

The air motor benefits can be itemized as:

1. Favorable torque behavior for bolt joint applications allows the torque to increase up to a maximum at standstill value.
2. Can be operated to the stalling torque value. This prevents the possibility of failure because of overload.
3. Could be equipped with the pressure regulator, which controls the pressure of the compressed air supplied, and can regulate the stalling torque value.
4. Small compact dimensions, low weight, and fatigue free.

5. **Powerful and uncomplicated design guarantees long life and excellent performance of air motor and tools.**
6. **Insensitive to operating environmental influences such as dust, external moisture, temperature, etc.**
7. **High operational safety – air is harmless and there is no static build-up; it can be used in an explosive area.**
8. **No potential for overheating because the expanding compressed air cools the tool.**
9. **Simple for daily servicing, maintenance and repair (requiring a few daily oil drops).**
10. **There is a minimal cost for the replacement of the air motor.**
11. **For proper performance and to achieve full benefits from its characteristics, the air pressure should not be less than 6.3 bar at operating time.**
12. **Noise level should be less than 85 dB, which is the legislative limit in Alberta [24].**

2.3. Air Motor Requirements for CTM

To achieve the desired output torque of 1100 Nm and 100 rpm the air motor should meet the following criteria:

- Shaft free speed of 7500 rpm;
- Minimum input torque of 15.0 Nm; and,
- Input power of 3kW.

2.4. Characteristics of vane air motors

All air motors, regardless of design and configuration, have some characteristics in common. This can be illustrated in the torque/power-shaft output speed diagram in

Figure 2. When its runs unload, the torque is zero and the maximum shaft-rotor speed (free speed, idling speed) is attained. As soon as the motor is loaded, the torque supplied by the motor increases linearly while the shaft-rotor speeds drops. The more the motor is loaded, the greater is the torque supplied; these are great benefits of the air motor, and explain the positive creep pull of the van air motor. The fact that the torque increases with decreasing shaft-rotor speed produces very good low speed characteristics. This is particularly useful in the toughest bolt joint applications since the air motor will not be damaged by stalling torque. The air motor can also withstand a certain amount of forced reverse rotations. The output power, which is a function of torque and shaft-rotor speed, attains its maximum value at approximately half of the free/idling speed.

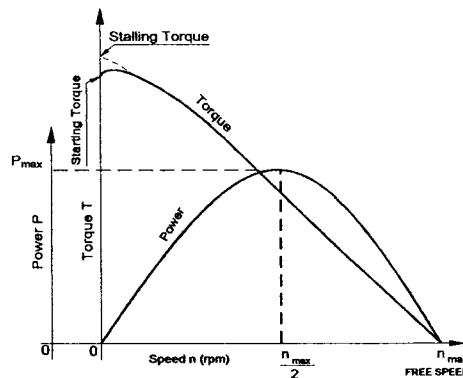


Figure 2. Air motor characteristics and performance curve

Considering Ingersoll Rand Company [18], two types of air motors are suitable with performance characteristics as shown in Figure 4 and 5.

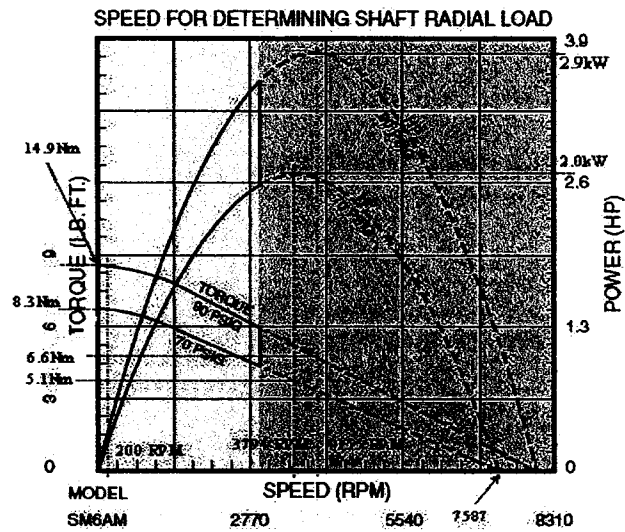


Figure 4. Performance graph, Ingersoll Rand air motor model SM6AM [18]

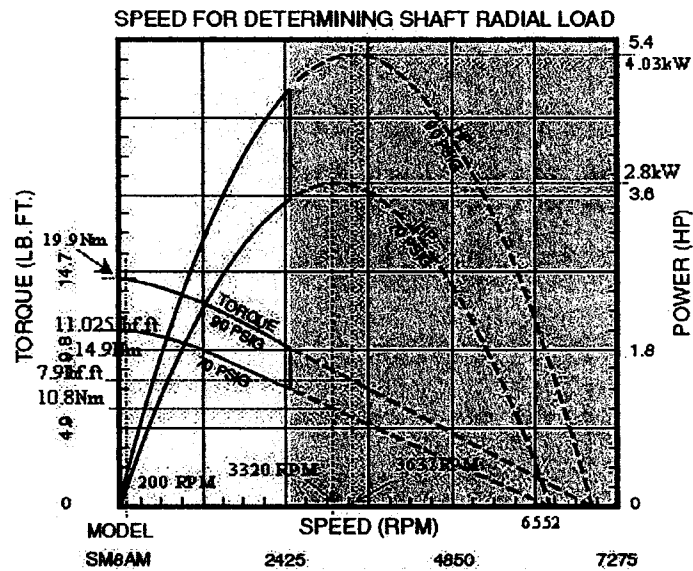


Figure 5. Performance graph, Ingersoll Rand air motor model SM8AM [18]

2.5. Analyses of Air Motors Data

Loads imposed on CTM and the air motor change rapidly. The load variations are usually caused by imperfections of crest of thread, scratches, rust, paint, or other types of obstacles in the bolt joint. In mining equipment, bolt joints are working in extremely rough conditions. The air-powered tools require great flexibility for torque transfer in order to adjust to unexpected resistances. The rate of change of motor rotation required to overcome increasing torque in case of air motors is lower with the steep torque characteristic curve. Taking this into consideration, air motors are not very “elastic” compared to a combustion engine. Flössel introduced the “elasticity of engine” approach in Germany around 1950 during an evaluation of off road vehicles powered by gasoline and diesel engines [17].

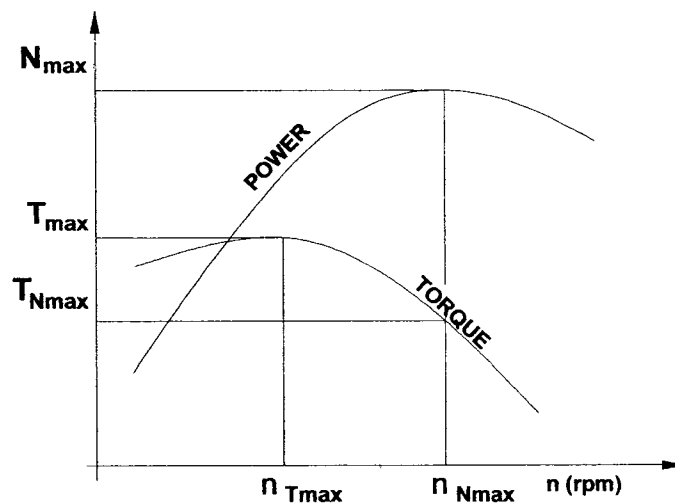


Figure 6. Elasticity of motor

The following give the definitions of the elasticity factors for combustion engines and motors [17]:

- Elasticity of torque is defined as the ratio of the maximum torque to the torque at maximum power produced by the motor.

$$e_{T_{\max}} = \frac{T_{MAX}}{T_{N_{\max}}} \quad (3)$$

Where:

T_{\max} = Maximum torque

$T_{N_{\max}}$ = Torque at maximum power.

- Elasticity of revolution is defined as the ratio of the maximum rpm to the rpm at maximum torque produced by the motor.

$$e_{rpm} = \frac{n_{N_{\max}}}{n_{T_{\max}}} \quad (4)$$

Where:

$n_{N_{\max}}$ = Revolution of motor at maximum power

$n_{T_{\max}}$ = Revolution at maximum torque.

- Then, elasticity of the motor is defined as a multiplication of $e_{T_{\max}}$ and e_{rpm} :

$$E_M = e_{T_{\max}} * e_{rpm} \quad (5)$$

In order to evaluate particular motor ability, the following elasticity expression has been introduced:

$$\Phi_M = e_{T_{\max}} - \frac{1}{e_{rpm}^2} \quad (6)$$

The value of Φ_M allows assessment of different manufacturer's motors.

Using these elasticity equations, the performance characteristics of the motors were evaluated. Please see Figures 3, 4, and 5, as well as Tables 1 and 2.

It can be seen that the CTM 1100 is more elastic than other air motors at lower air pressure (e.g. 4.8 bar). The selected model is insensitive to large and small drops in air pressure and will certainly be the best choice.

However, if keeping a constant maximum pressure of 6.2 bar, the SM8AM will be the better choice.

Table 1. Air motors performance data at maximum operating pressure: 6.2 bar

		AIR MOTOR MODEL			
		@ 6.2 bar	SM6AM	SM8AM	CTM1100
TORQUE	T_{\max} [Nm]	14.9	19.9	15.1	
	$T_{N\max}$ [Nm]	6.6	7.9	8.0	
REVOLUTION	$n_{N\max}$ [rpm]	4155	3637	3750	
	$n_{T\max}$ [rpm]	200	200	285	
ELASTICITY of AIR MOTOR	TORQUE	$e_{T\max} = \frac{T_{MAX}}{T_{N\max}}$	2.258	2.519	1.888
	REVOLUTION	$e_{rpm} = \frac{n_{N\max}}{n_{T\max}}$	20.775	18.185	13.158
		$E_M = e_{T\max} * e_{rpm}$	46.910	45.808	24.842
FUNCTION of ELASTICITY		$\Phi_M = e_{T\max} - \frac{1}{e_{rpm}^2}$	2.256	2.516	1.886

Table 2. Air motors performance data at lower pressure: 4.8 bar

		AIR MOTOR MODEL			
		@ 4.8 bar	SM6AM	SM8AM	CTM1100
TORQUE	T_{ax} [Nm]	8.3	14.9	12.08	
	T_{imex} [Nm]	5.1	10.8	7	
REVOLUTION	Nomad [rpm]	3794	3320	3300	
	T_{ax} [rpm]	200	200	255	
ELASTICITY of	TORQUE	$e_{T_{max}} = \frac{T_{MAX}}{T_{N_{max}}}$	1.627	1.380	1.726
	REVOLUTION	$e_{rpm} = \frac{n_{N_{max}}}{n_{T_{max}}}$	18.970	16.600	12.941
	AIR MOTOR	$E_M = e_{T_{max}} * e_{rpm}$	30.864	22.908	22.336
FUNCTION Of ELACTICITY		$\Phi_M = e_{T_{max}} - \frac{1}{e_{rpm}^2}$	1.626	1.378	1.724

2.6. Shaft-rotor speed control

The throttle control or the pressure valve controlling restriction at the inlet and outlet determines the speed of the air motor at a given torque. Pressure control valves are more common controlling devices for vane air motors. They must allow sufficient air volume flow and pressure into the motor to overcome the resisting torque of the load and internal losses. The given mean pressure can thus be achieved by an adjustable or variable flow of restrictors either on the inlet or the outlet side of the air motor.

For hand-held tools, air motors must have the ability to generate torques in both directions, i.e. clockwise and counterclockwise, with the same proficiency.

2.7. Silencing

Air motors for hand-held tools are silenced in the exhaust air being passed through the rotor which is equipped with vanes and several chambers controlling direction of airflow. The chambers have a special profile and certain directions to achieve a maximum performance with a minimum of volume of air motor. During long continuous operations of expansion motors, the risk of freezing air at the exhaust-silencer system must be considered. The degree of the silencing system, or devices, are limited by the available space on the handle of the air motor; please see Figure 21. Simply put, the silencer is the resistant in which the exhaust air is discharged into a larger volume and then put through a porous outlet material. To achieve good results, the best efficient silencer must have low outlet velocity and good absorbent in the chamber.

2.8. Discussion

The concept of engine elasticity, proposed by Flössel [17], can be applied directly to vane air motors used for CTM 1100. Data for the three-selected vane air motors is shown in Figure 3, Table 1, and Table 2. Analyzing the motors elasticity factors yields the following conclusions:

- The best motor will be the one with characteristics of CTM 1100;
- As the best choice, the CTM 1100 should be chosen;
- The second alternative will be SM6AM air motor made by Ingersoll Rand;
and,
- The last option will be model SM8AM air motor made by the same manufacturer.

Data from the graphs for SM6AM and SM8AM models suggest that:

- The following comments are in order after investigation of SM6AM and SM8AM performance graphs;
- The magnitude of torque and power after interpolation were marked on the appropriate axis;
- Value of rpm at maximum torque and power were written on the graphs;
- Torque value at 0 rpm is usually lower, ~ 5 to 7% of maximum torque; and,
- Stall value is an important part of the performance of the air motor during the tightening of the bolt or nuts; its value is 5 to 10% higher than the maximum torque.

3. GEAR ARRANGEMENTS

3.1. Parallel Gear Axis Arrangements – General Consideration

The most common gear arrangements are those containing a pinion and gears on a parallel axis.

The teeth for these kinds of arrangements could be spur, helical, or herringbone [15].

A simple gear train contains a pinion-driver and a gear-driven.

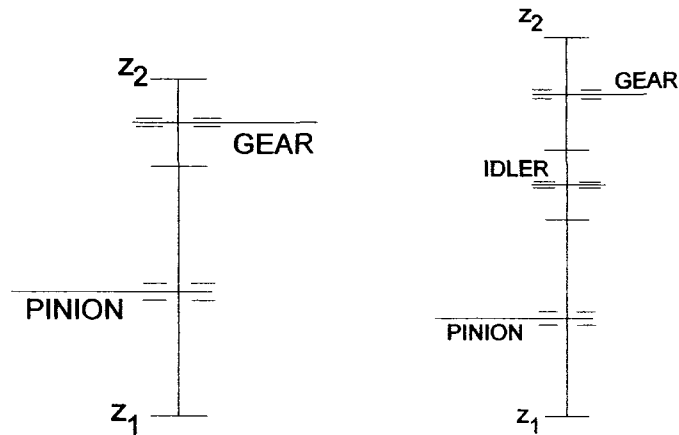


Figure 7. Simple gear arrangement with parallel axis

The ratio for the design is equations (1) and/or B.10 (Appendix B):

$$u = \frac{z_2}{z_1} = \frac{d_{b2}}{d_{b1}} \quad (7)$$

For compound gear arrangements, the ratio is:

$$u = u_1 * u_2 * u_3 \dots, \quad (8)$$

$$u = \frac{z_{21}}{z_{11}} * \frac{z_{22}}{z_{12}} * \frac{z_{23}}{z_{13}} \dots, \quad (9)$$

Where: u_1 = Ratio of the first stage

u_2 = Ratio of the second stage

u_3 = Ratio of the third stage

z_{11} = Number of pinion teeth for the first stage

z_{12} = Number of pinion teeth for the second stage

z_{13} = Number of pinion teeth for the third stage

z_{21} = Number of gear teeth for the first stage

z_{22} = Number of gear teeth for the second stage

z_{23} = Number of gear teeth for the third stage.

3.2. Kinematics parameters of the planetary gear set [15]

In planetary gear sets, two-reference systems exist:

- Absolute ω_{x_0} ; and,
- Relative (assigned to carrier planet) ω_{y_0} .

Absolute angular velocity of an element planetary gear could be calculated as a sum of the absolute velocity and the relative velocity of carrier planet.

In general, Willis's method (Robert Willis published his findings in 1857 in "Principles of Mechanism," but this reference was not possible to obtain) presents a solution for the rotational speeds in the planetary gear (See Figure 8).

$$\frac{\omega_X - \omega_o}{\omega_Y - \omega_o} = \frac{\omega_{Xo}}{\omega_{Yo}} = u_{oXY} \quad (10)$$

Where:

ω_{Xo} = Absolute angular velocity

ω_{Yo} = Relative angular velocity of carrier

u_{oXY} = Internal epicyclic ratio

X = Central axis (theoretical center line of sun gear)

Y = Axis of planet.

Note: when carrier planets are locked, the internal ratio is $u_{oXY} = \left(\frac{\omega_X}{\omega_Y} \right)_{\omega_o=0}$.

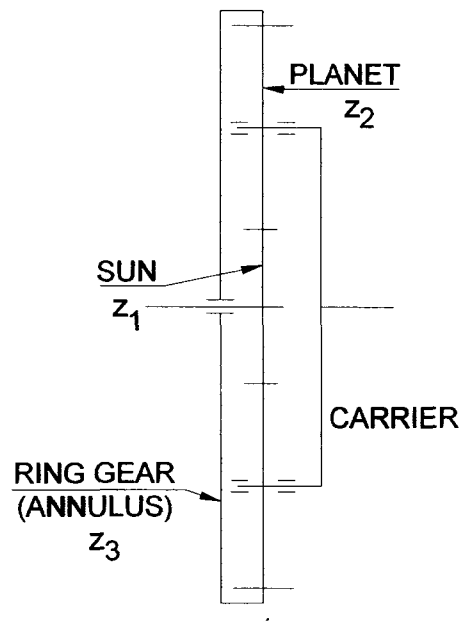


Figure 8. Epicyclic gear arrangements

For simple gear arrangements, the following relations are true [15]:

1. Regardless of the number of idlers, the ratio is always the number of teeth in the output gear divided by the number of teeth in the input pinion.
2. An idler does not change the gear ratio of the gear train; it does, however, change the direction of rotation of the output gear.
3. The ratio of the output torque to the input torque is equal to the inverse of the speed ratio.

3.3. Design of the Planetary Gear Drives with Parallel Axis

During the design process of the parallel axis planetary gear train, the following rules should be considered:

- A. Uniform tooth load distribution across the tooth flank is one of the most important factors; parallelism and perpendicularity of the bearings and shafts to each other must exist.
- B. To reduce excessive windup, designing relatively long shafts or narrow pinions should be avoided.
- C. Maintain equal torque through every power path.
- D. Minimize bearing loads in idlers.

3.4. Epicyclic Planetary Gear Arrangement

Every epicyclic planetary gear arrangement contains four basic elements or parts:

- Sun gear and pinion with external teeth;
- Planet gear with external teeth or gears;
- Carrier planet, element-holding planet or planets; and,
- Gear ring with internal teeth, also known as an annulus.

3.5. Simple Epicyclic Planetary Gear train

A simple epicyclic planetary gear train could be arranged in the following combinations:

Table 2. Ratio available for simple epicyclic gear arrangements with: $z_1=17$, $z_2=22$, $z_3=$

65

CASE	INPUT	FIXED	OUTPUT	ROTATION	OVERALL RATIO	AVAILABLE RATIO	RATIO RANGE
A	Sun	Carrier	Ring gear	Opposite	$u = \frac{z_3}{z_2}$	2.955	2:1 to 11:1
B	Sun	Ring gear	Carrier	Same	$u = \frac{z_3}{z_2} + 1$	3.955	3:1 to 12:1
C	Ring gear	Sun	Carrier	Same	$u = \frac{z_2}{z_3} + 1$	1.338	1.2:1 to 1.7:1
D	Ring gear	Carrier	Sun	Opposite	$u = \frac{z_2}{z_3}$	0.338	NOT PRACTICAL
E	Carrier	Ring gear	Sun	Same	$u = \frac{z_2}{z_2 + z_3}$	0.253	NOT PRACTICAL
F	Carrier	Sun	Ring gear	Same	$u = \frac{z_3}{z_2 + z_3}$	0.747	NOT PRACTICAL

The following are schematic representation of the simple epicyclic gear train arrangements:

Fixed carrier – output gear ring - setup called star, case A

Fixed ring gear – output carrier, setup called planetary, case B

Fixed sun gear – output carrier - setup called solar, case C

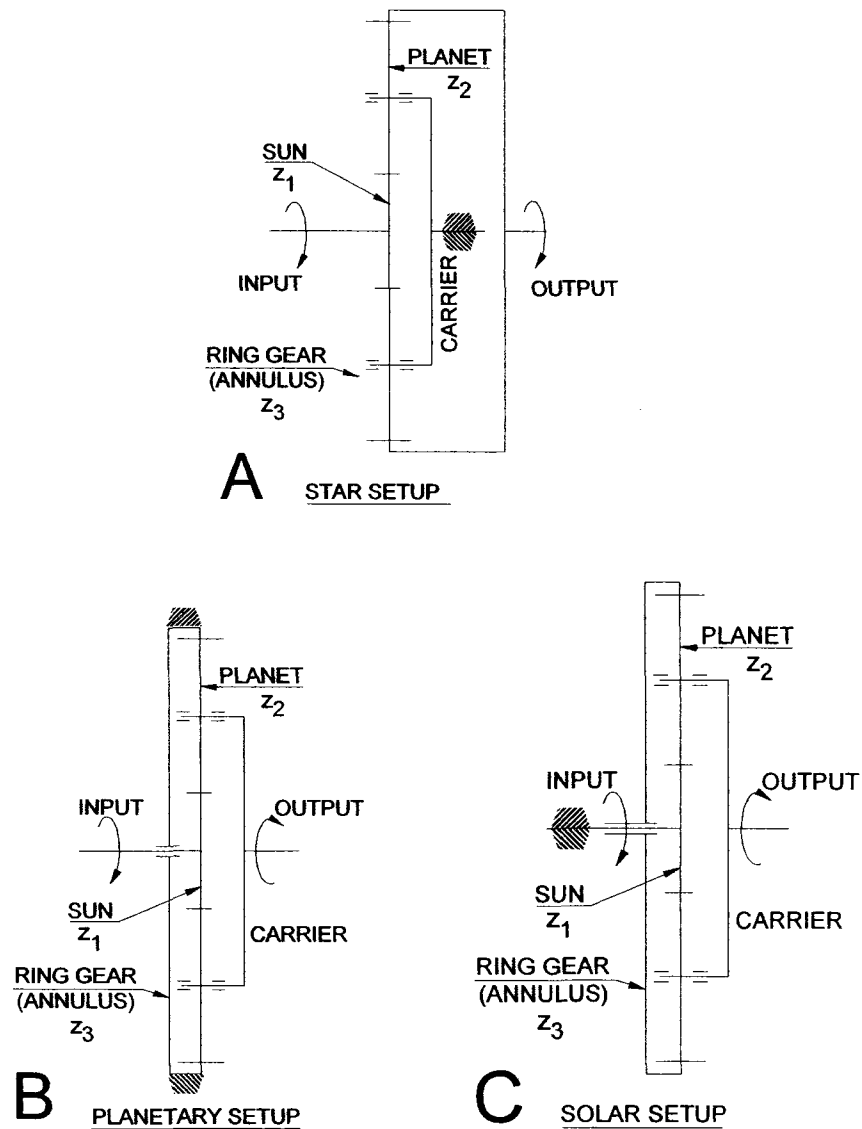


Figure 9. Simple epicyclic gear train: star, planetary and solar

4. ANALYTICAL CONSIDERATION OF THE PROPOSED DESIGN

An *epicyclic* gear train has a sun gear mounted on a moving "arm" that can rotate itself as well as the gears. The arm can be an input or an output element, and can be held fixed or allowed to rotate. A simple, but very common, epicyclic train is the sun-and-planet epicyclic train, shown in Figures 7 and 10. Three planetary gears are used for mechanical reasons; they may be considered as one when describing the actions of the gearing. The sun gear, the arm, or the ring gear may be input or output links.

4.1. Geometry Considerations of the Design

The average human hand span, measured between the thumb and the four fingers, is approximately 70 mm. Considering this rule, the outside diameter of the new CTM should not exceed 70 mm

From Figure 10, it is possible to find the length of the arm of the carrier, which is equal to:

$$A_{\text{int(}ext)} = \frac{z_1 + z_2}{2} = \frac{z_1 + \left(\frac{z_3 - z_1}{2} \right)}{2} = \frac{z_3 + z_1}{4} \quad (11)$$

The torque equilibrium is:

$$T_{out} = T_{in} * \left(\frac{\omega_{Xin}}{\omega_{Yout}} \right) = T_{in} \left(1 + \frac{z_1}{z_3} \right) \quad (12)$$

Where:

ω_{Xin} = Input absolute angular velocity

ω_{Yout} = Output relative angular velocity of carrier

T_{out} = Output torque

T_{in} = Input torque

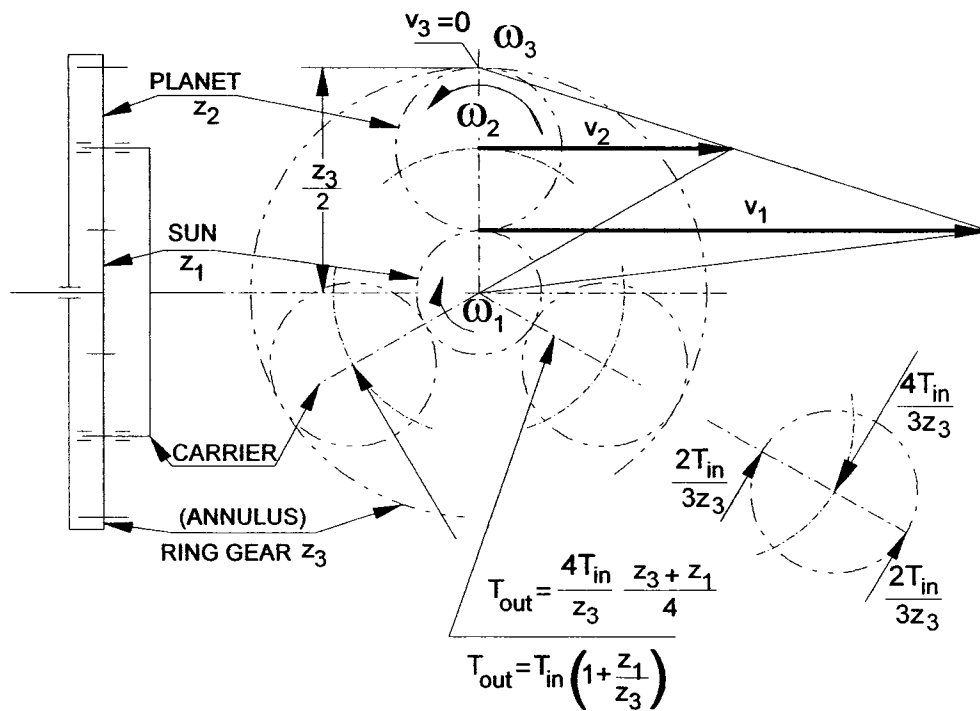


Figure 10. Velocity and torque ratio diagram

4.2. Space Criteria for Planetary Gear Design [2]

4.2.1. Coaxiality

Sun, planet, and gearing axes must meet the equation (see also Figure 11):

$$a_{SP} = -a_{PR} \quad (13)$$

Where:

a_{SP} = Distance between the centerline of the sun gear and the planet

a_{PR} = Distance between the centerline of the planet and the gear ring.

4.2.2. Assembly

The gear assembly criteria must satisfy the following equation for all stages:

$$\frac{z_S + z_R}{z_{CP}} = I_T \quad (14)$$

Where:

I_T = Result must be an integer

z_S = Number of teeth of the sun gear

z_R = Number of teeth of the ring gear

z_{CP} = Number of planets.

4.2.3. Neighborhood criteria

All planets on every stage must satisfy the following equation:

$$(z_p + z_s) * \sin \frac{\pi}{z_{CP}} > z_p + z_{CP} \cdot \quad (15)$$

All nomenclature of indexing is the same as above.

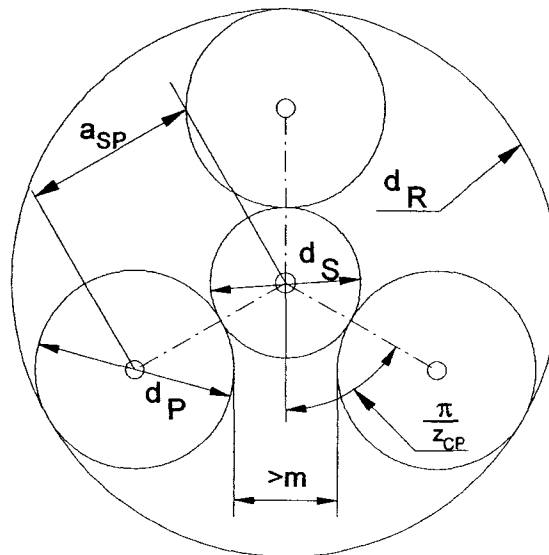


Figure 11. Planets neighborhood criteria and spacing

4.3. Gear Calculations for the new Design

All calculations were conducted on the basis of ISO standard method B. Power losses and specific sliding was calculated on the basis of ANSI/AGMA standards [2, 3, 5, 7, 8, 9, 10, 11].

Note: Those standards are not compatible and not interchangeable.

To achieve the smallest outside diameter, an imperial module, rather than a metric one, was used.

4.3.1. The First Stage Selected Data

Table 4 complies the most important geometrical parameters of the first stage of Compact Torque Multiplier

Table 4. Selected geometrical parameters of the first stage of Compact Torque Multiplier (selected detailed calculations in Appendix G)

DESCRIPTION	SYMBOL	UNITS	SUN	PLANET	RING
Number of teeth	Z		17	19	-55
Pitch Dia	D	mm	17.992	20.102	58.190
Root Dia	D_R	mm	15.350	17393	60.921
Base circle Dia	D_b	mm	16.306	18.224	52.755
Tip Dia	D_{os}	mm	20.108	22.225	56.092
Circular tooth thickness	t_s	mm	1.662	1.662	1.662
Clearance min. basic	c	mm	0.263	o.263	o.263
Pressure angle	α	deg	25.000	25.000	25.000
Normal module	m	mm	1.058	1.058	1.058
Center distance	a	mm	19.05	19.05	19.05

Table 5 list the most significant mechanical parameters of the first stage of the Compact Torque Multiplier.

Table 5. Selected mechanical parameters of the first stage of CTM

DESCRIPTION	SYMBOL	UNITS	SUN	PLANET	RING
Rated power	P	kW	3.14	-3.14	0.0
Rotational speed	n	1/min	7500	1771	0.0
Torque	T	Nm	3.998	-16.93	12.93
Face width	F	mm	8.0		
Compressive stress – fatigue	$\sigma_{H\lim}$	MPa	1419.0	1342.0	789.0
Maximum shear stress at tooth root	$\sigma_{C\lim}$	MPa	418.0	396.0	233.0
Contact ratio S/P	ε_{SP}		1.392		
Contact ratio P/R	ε_{PR}			1.474	
Specific sliding S/P	v_o		0.670	0.703	
Specific sliding P/R	v_i			0.908	0.551
Number of planets	z_{cp}			2	

4.3.2. The Second Stage Mechanical Parameters of the CTM

Table 6. The list selected mechanical parameters of the Compact Torque Multiplier

DESCRIPTION	SYMBOL	UNITS	SUN	PLANET	RING
Rated power	P	kW	8.3	-8.3	0.0
Rotational speed	n	1/min	1771	418.2	0.0
Torque	T	Nm	44.75	-189.5	144.8
Face width	F	mm	12.0		
Compressive stress – fatigue	σ_{Hlim}	MPa	1789.0	1692.0	994.0
Maximum shear stress at tooth root	σ_{Clim}	MPa	528.0	499.0	293.0
Contact ratio S/P	ϵ_{SP}		1.392		
Contact ratio P/R	ϵ_{PR}			1.474	
Specific sliding S/P	v_o		0.670	0.703	
Specific sliding P/R	v_i			0.908	0.551
Number of planets	z_{cp}			2	

4.3.3. The Third Stage Parameters of the CTM

Table 7 shows determinate and selected parameters of the third stage of the designed Compact Torque Multiplier.

Table 7. List of selected mechanical parameters for the third stage of the CTM

DESCRIPTION	SYMBOL	UNITS	SUN	PLANET	RING
Rated power	P	kW	11.38	-11.38	0.0
Rotational speed	n	1/min	418.0	98.7	0.0
Torque	T	Nm	260.0	-1101.0	841.1
Face width (active)	F	mm	16.0		
Compressive stress – fatigue	σ_{Hlim}	MPa	3194.0	3022.0	1776.0
Maximum shear stress at tooth root	σ_{Clim}	MPa	942.0	891.0	524.0
Contact ratio S/P	ϵ_{SP}		1.392		
Contact ratio P/R	ϵ_{PR}			1.474	
Specific sliding S/P	v_o		0.670	0.703	
Specific sliding P/R	v_i			0.908	0.551
Number of planets	z_{cp}			3	

4.4. Determination of the critical frequency for vibration for the first stage of the CTM

It is necessary to determine the magnitude of the critical speed of the first train CTM, as it could run in the future with higher initial rotating speeds. For these calculations, it was convenient to use Holzer method. For detailed calculations, see Appendix G.

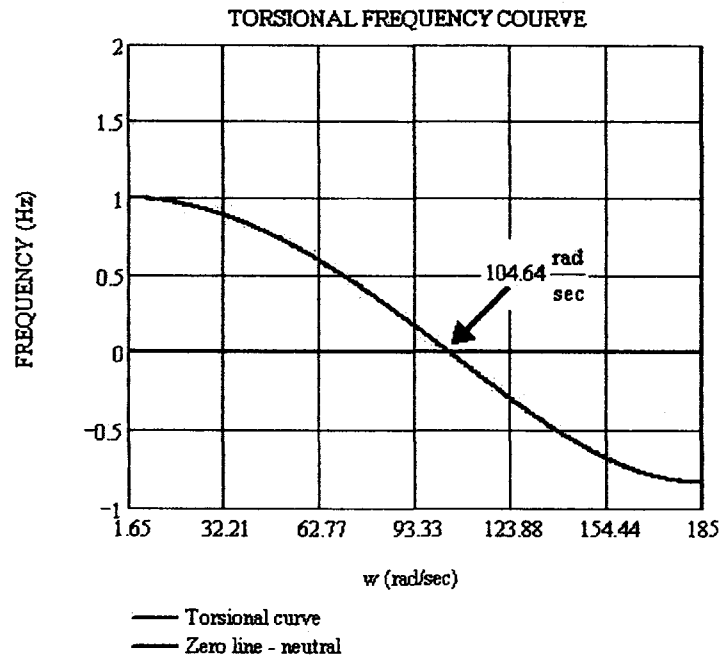


Figure 12. CTM 1100: first stage torsion frequency graph

The critical magnitude speeds of this gear train system correspond to the intersection of natural frequencies, with the horizontal at point zero. This results in zero on the 1st harmonic torsional frequency curve. It can be seen from Figure 12 that the first natural frequency of CTM in this model is 104.64 rad/sec. Also from Figure 12, it is evident that the frequency value for the designed CTM 1100 is 104.64 rad/sec, which is less than the critical value of 125.0 rad/sec.

4.5. Torsion and Bending Effect – Third Sun Gear

On base ISO 6336 standard [7], the torsion and bending of the last stage and necessary backlash were calculated and verified; the results are represented in Figure 13. For detailed calculations, see Appendix G.

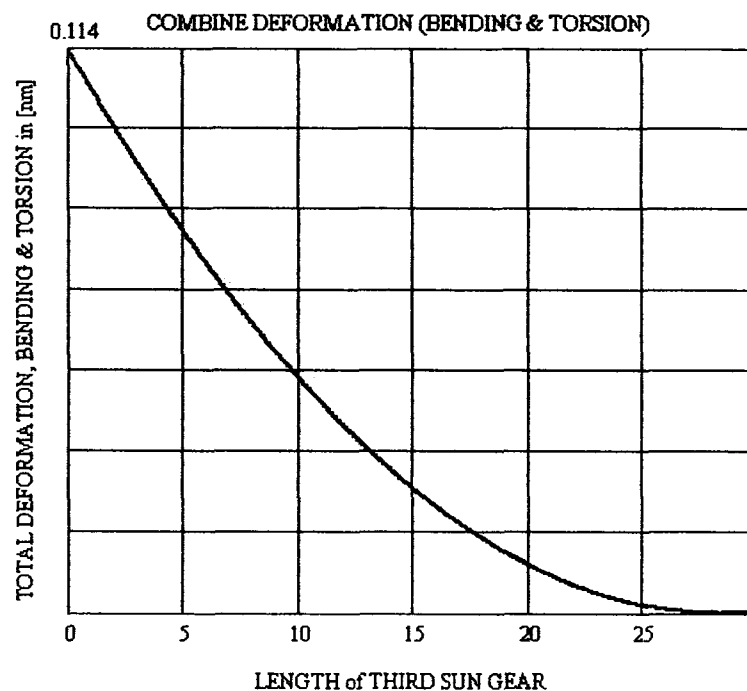


Figure 13. Bending and torsion acting in last sun gear

Maximum deformation is at the end of the sun gear; contact with the planets is 0.114mm (from Table 3). Clearance min. basics are 0.263 mm and there is 0.153 mm of clearance left.

Initial clearances are important factors and they must be considered at the beginning of the design process.

4.6. Windage and Bearing Losses

Planetary gears, with parallel gear sets, always have a tendency to windage.

Windage is caused by the fact that the input torque comes from one end and the output torque comes from the opposite end. The mechanism must be in balance in such way that the active forces must be equal to the reaction ones. Calculation of windage was conducted on the basis of ANSI/AGMA 6123-A88 [2]. Figure 14 shows the relationship between power losses vs. gear design factor for the third stage of CTM.

For detailed calculations, see Appendix G.

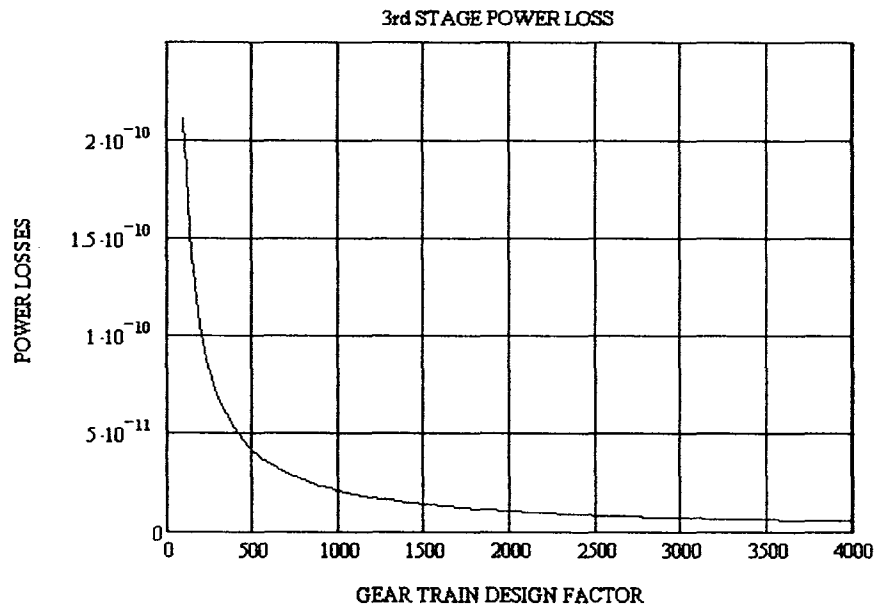


Figure 14. Graph representing power losses in third stage

From Figure 14, it is clear that that the CTM bearings exert a very small resistance and the magnitude of power loss of 3×10^{-6} W can be considered negligible.

4.7. Effective Air Pressure Range for Applicable Output Torque of CTM

Figure 15 shows minimum and maximum torque available from a CTM 1100 air motor (see Figure 3, air motor theoretical performance graph for minimum and maximum output torque), regulated by the pressure regulator from 6.2 bar to 4.8 bar.

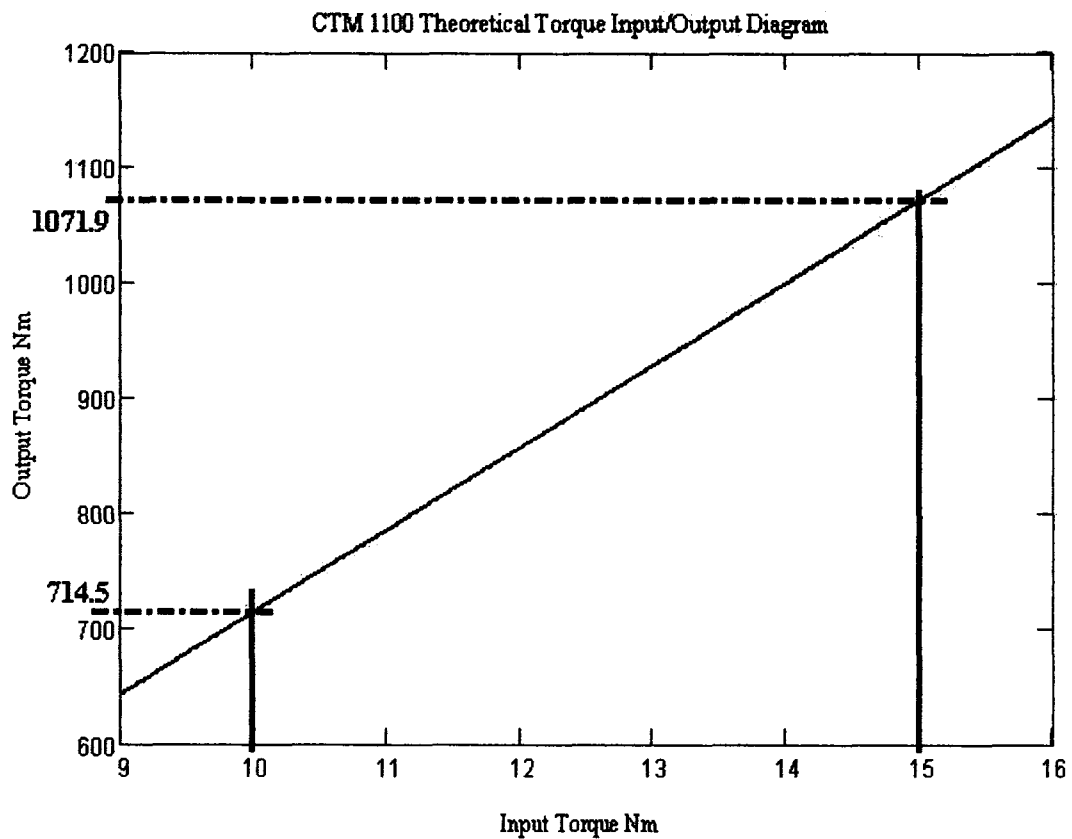


Figure 15. CTM 1100 Input/Output Torque diagram

Figure 16 shows influences of the variation of output torque and its effects to tighten bolts or axial loads generated by the applied torque. Line 1 (dashed line) was generate on the base of the common equation [19]:

$$T = k * D * F \quad (16)$$

Where:

$$k = k_1 + k_2 + k_3$$

k_1 = represents the torque factor losses by friction on the bearing surface of the nut or bolt, approximately 50% [19]

k_2 = this factor represents the losses due to friction on the contact thread flanks, approximately 40% loses of total torque [19]

k_3 = the useful factor of applied torque [19], about 10% of total torque

D = bolt nominal size [mm]

F = bolt tension [kN].

In accordance with SAE J 1701M [19, Table 1], k factor ranges from 0.05 to 0.35. For torque calculations, the value of “k” was equal to 0.2.

By rearranging equation (16), the value of applied bolt tension can be calculate

from:

$$F = \frac{T}{k * D}. \quad (17)$$

In accordance with VDI 2230 [20], the following equation was used to generate line (2) in Figure 16:

$$F_m = \frac{2 * T}{(D_N * f_N) + (C_A * D_P)} \quad (18)$$

Where:

D_N = nominal bolt diameter [mm]

f_N = coefficient of friction between bearing nut or bolt and washer

C_A = dimensionless thread angle factor (see equation 19)

D_P = pitch diameter of the bolt thread.

$$C_A = \frac{\tan(\beta + \phi)}{\cos \alpha} \quad (19)$$

Where:

β = helix angle of the thread [deg]

ϕ = thread coefficient of friction; see equation (20)

α = thread angle [deg]

$$\phi = a \tan(f_T) \quad (20)$$

Where:

f_T = friction coefficient between threads.

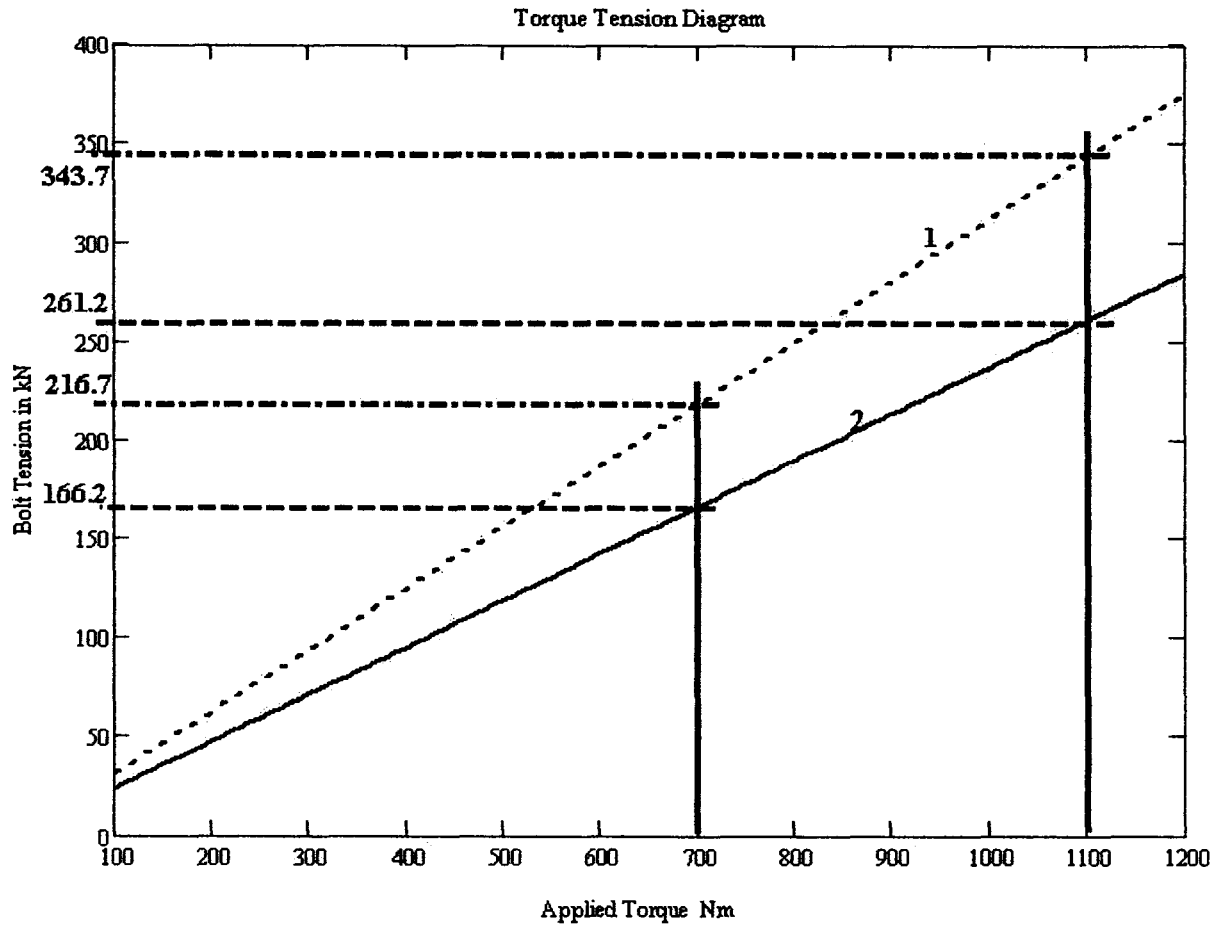


Figure 16. Pressure drop and effect to applied output torque

4.8. Materials

The CTM will be made from a few different ferrous and non-ferrous materials [15, 21, 22] which were carefully selected to achieve maximum performance durability and reliability with a relatively low cost. The tensile strength of carbon steel can be correlated with the hardness. The tensile strength value in conversion tables are, however, averages and as such should never be used for tensile testing [15].

Table 8. General properties of the major materials used for CTM 1100

	⁽¹⁾ NOMINAL HARDNESS Rockwell C	MODULUS of ELASTICITY (Young's MODULUS)	YIELD STRENGTH	ULTIMATE TENSILE STRENGTH	HARDEN- ABILITY
MATERIAL	UNITS				
	F = 1471N	MPa	MPa	MPa	
ANSI-4140	32.0	1970.0	655.0	1020.0	VERY GOOD
ANSI-4340	38.0	1970.0	860.0	1280.0	VERY GOOD
VascoMax C-300	32.0	189650.0	1693.0	1771.0	VERY GOOD
VascoMax C-350	35.0	199950.0	2037.0	2139.0	VERY GOOD

Note: ⁽¹⁾nominal hardness measured at annealed condition of steel

An important aspect in choosing a material for gears for the new torque multiplier is its hardenability. Hardenability is related to the ability of a material to fully harden to martensite structure through to the center of the part.

4.9. Lubricant for CTM 1100

Rotating elements, bearings, gears, and shafts can operate reliably and they must be adequately lubricated to prevent direct contact between two bodies.

The oil is a material that is to separate the two bodies in a state of relative motion.

The main functions of the lubricant are to:

- prevent direct contact between these bodies;
- reduce friction and wear;
- transfer the generating heat during running of the gears;
- act as a sealant;
- prevent corrosions; and,
- reduce noise.

The most favorable operating temperature is from 0°C to 50°C, where the minimum amount of lubricant required for reliable gear and bearings is at operating requirements.

In the case of CTM 1100, the function of oil also transfers the heat generated during normal and excessive loads on gears and bearings, so the amount of oil is larger than the gear and bearing requirements.

For lubrication of CTM 1100, synthetic oil 0W-30 is recommended [23].

5. DESIGN of NEW COMPACT TORQUE MULTIPLIER

In order to protect the filed patent application, only the geometrical profile and Geometrical Product Specification (GPS) data is provided in this section [12, 13, & 14].

5.1. GPS surface texture for first and third carrier of CTM

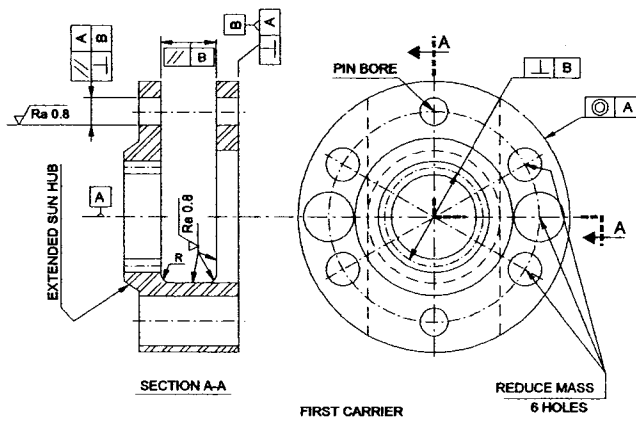


Figure 16. First carrier with GPS symbols

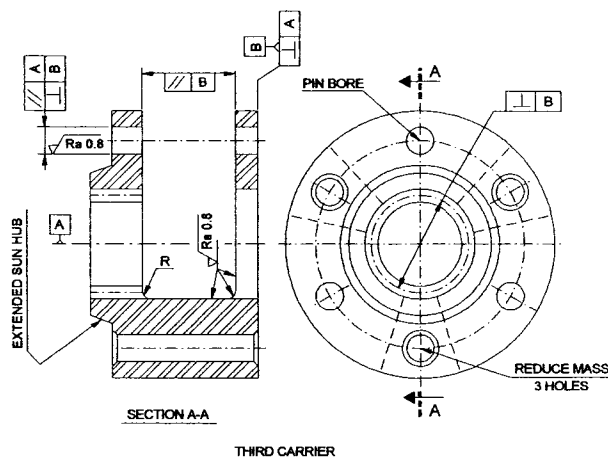


Figure 17. Third carrier with GPS symbols

To achieve long life, good durability, and reliability of planetary gear sets, the required geometrical criteria must be met during the design and manufacturing process. It should be verified during the quality control and inspection process.

It is required to establish a datum or data. In this case, datum 'A' will be designated as primary, and 'B' as secondary.

Both data are extremely critical for efficiency and performance of the planetary mechanism. In this case, datum 'A' is primary on this axis, and all elements are rotating with balance.

In order to reduce rotating mass, unnecessary material was removed from Figure 16, which represents the first carrier that the element is rotating with 5126 rpm. It bore through 6 holes and, at the same time, was reduced by the weight of the compact torque multiplier (CTM). Smooth transition is required from one plane to another in both Figures 16 and 17. The transition was marked as 'R.'

Every radial transition requires a smooth surface finishing to reduce and minimize the stress of the concentration area. This was marked with a triangle symbol with the number $Ra 0.8$ while the number $0.8\mu m$ represented surface texture finished in accordance with ISO and ANSI standard nomenclature [12, 13, & 14].

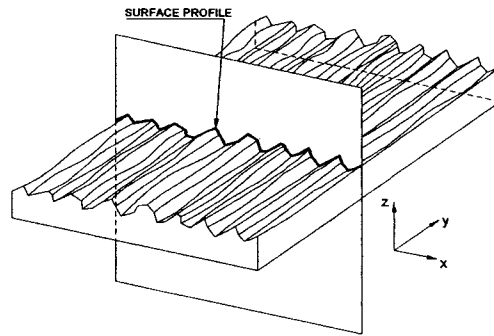


Figure 18. Surface profile

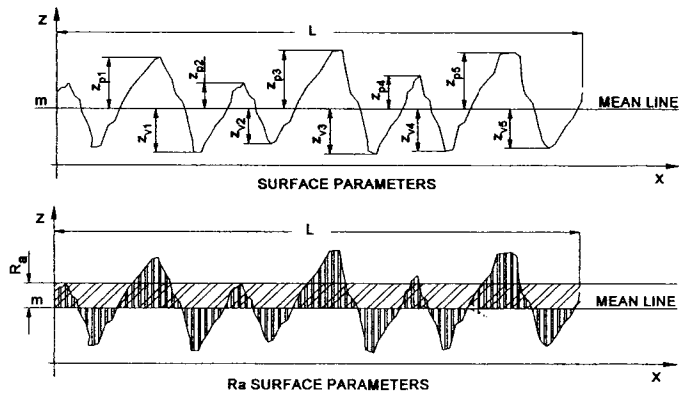


Figure 19. Surface parameters

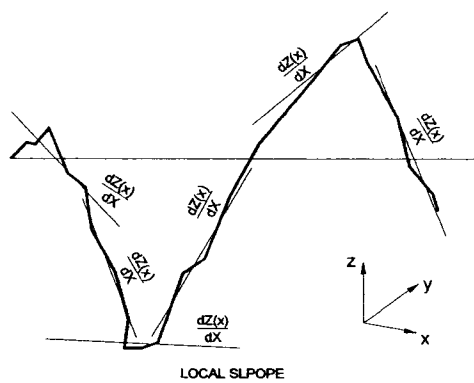


Figure 20. Local slope profile

From Figure 20, it is possible to determine the local surface slope and profile with following formula [14]:

$$\frac{dz_j}{dx} = \frac{1}{60\Delta X} (z_{j+3} - 9z_{j+2} + 45z_{j+1} - 45z_{j-1} + 9z_{j-2} - z_{j-3}) \quad (21)$$

Where:

z_i = height of the i th profile point

ΔX = spacing between adjacent profile points

and the arithmetic mean deviation of the assessed element profile could be expressed by the formula:

$$R_a = \frac{1}{l} \int_0^l |Z(x)| dx \quad (22)$$

Where:

l = sample length (Figure 19).

5.2. Final design of the new CTM 1100

For patent protection, only the essential components of the CTM 1100, shown in Figure 21.

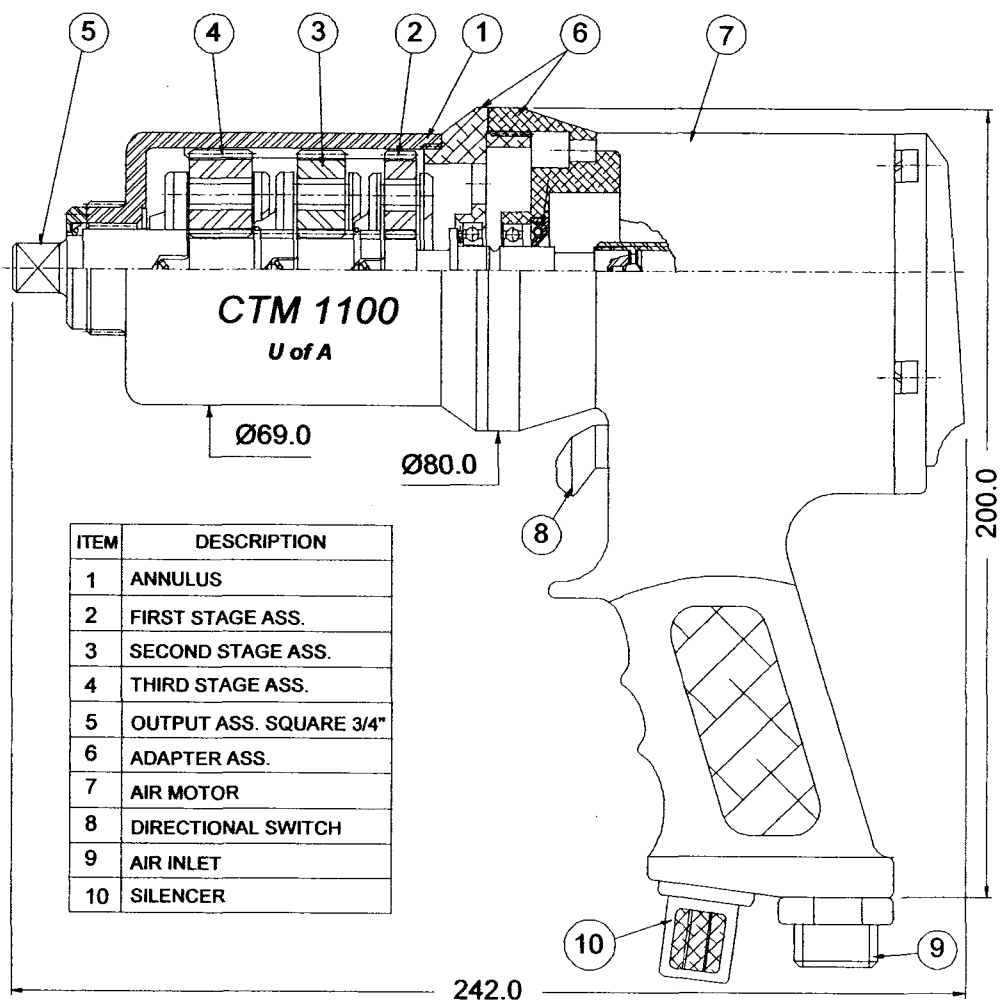


Figure 21. Assembly, CTM 1100 with air motor and section view of planetary gear set

5.3. The CTM 1100 and the existing bolt tightening tools

Table No. 9 lists the major parameters of the commercially available tools for bolt tightening and the designed CTM 1100 multiplier.

Table No. 9. Bolt tightening tools commercially available

TYPE/SIZE	Square. 3/4" DRIVE				
	CTM ⁽⁵⁾ 1100	PT72 ⁽¹⁾ 1000	PT72 ⁽²⁾ 1000 AUT	RAD ⁽³⁾ 800NG	Mountz ⁽⁴⁾ CLD 95
WEIGHT Without Reaction Arm. kg, (lb)	3.4 (7.5)	4.7 (10.4)	7.0 (15.4)	4.3 (9.5)	7.5 (16.5)
OUTSIDE DIAMETER mm [in]	69.0 (2.7)	72.0 (2.8)	72.0 (2.8)	72.0 (2.8)	85.0 (3.3)
LENGTH Without AIR MOTOR mm [in]	200.0 (7.9)	301.0 (11.85)	373.0 (14.65)	197.0 (7.75)	277.0 (10.9)
OUTPUT TORQUE Nm, (lbf*ft)	~1080.0 (~796.0)	~1000.0 (~738.0)	~1000.0 (~738.0)	~1100.0 (811.0)	1080.0 (~796.0)
OUTPUT -RPM @ 7000 INPUT	92.0	15.0	75.0	30.0	13.0

NOTES:

- (1) The manufacturer of this tool is Norbar Torque Tools Ltd. www.norbar.com
- (2) Two speed the manufacturer of this tool is Norbar Torque Tools Ltd. www.norbar.com
- (3) The manufacturer of this tool is New World Technologies Inc. www.radtorque.com
- (4) The manufacturer of this tool is Mountz Inc. www.eturque.com
- (5) The CTM 1100 - Compact Torque Multiplier,
is the invention of the University of Alberta.

6. CONCLUSIONS and RECOMMENDATIONS for FUTURE WORK

6.1 Conclusions

6.1.1. The new design of the Compact Torque Multiplier incorporates a novel compact solution and analyzes methodology of epicyclic planetary type gear trains for applications in hand held bolt-tightening devices.

6.1.2. The developed Compact Torque Multiplier – CTM showed superiorities over the existing commercially available devices in the following aspects:

- The CTM 1100 weight of 3.4 kg is 20% to 220% lighter
- The CTM 1100 outside diameter of 69 mm is 4% to 23% smaller
- The CMT 1100 total length of 200 mm is 38% to 86% shorter
- The CMT 1100 output torque of 1080 Nm has about the same magnitude
- The CMT 1100 output speed of 92 rpm is 707% larger than rpm of the slowest
- Noise level of CTM 1100 should be determined on physical tests to confirm data
- Accuracy and repeatability must be confirmed on model in laboratory tests

6.1.3. During the design stage of the Compact Torque Multiplier, all calculated and assumed empirical values of variables that were obtained in accordance with ISO and ANSI/AGMA standards.

6.1.4. The new approach, based on the elasticity of critical factors, is thorough and conclusive for selecting the air motor used in hand-held tool powering applications.

6.1.5. The new presented methodology for defining the air motor characteristics is a unique and promising effort in this engineering field.

6.1.6. The effect of the developed pressure drop analysis in this new designed CTM on the output torque is of paramount importance for the designing and application of these types of devices.

6.2. Recommendations for future work

Since the purpose of this work was to develop a CTM for use in mining industry, the following recommendations suggested regarding design changes dependent on the outcome of the future prototype performance and industrial test results.

6.2.1. The pre-production unit of CTM should be prototype tested to verify full conformance to its design, function and performance.

6.2.2. Using the same technique the CTM can be re-engineer to the second generation prototype, bringing to the table current technologies for materials in addition, specification upgrades, building CTM more update.

6.2.3. In order to verify the magnitude of the predicted natural frequencies of the CTM system when exited by dynamic bolt tightening load and applied torque modal analysis using solid modeling techniques and numerical model analysis tools is recommended.

7. REFERENCES

1. ANSI/AGMA 1012-F90, American National Standard -
Gear Nomenclature, Definitions of Terms with Symbols.
2. ANSI/AGMA 6123-A88, American National Standard -
Design Manual for Enclosed Epicyclic Metric Module Gear Drives
3. ANSI/AGMA 2002-B88, American National Standard -
Tooth Thickness Specification and Measurements
4. ANSI/AGMA 2004-B89, American National Standard - Gear Materials
and Heat Treatment Manual
5. ISO 701 - 1976, International gear notation - Symbols for geometrical data
6. ISO 1122-1 - 1998, Glossary of terms - Part 1 Geometrical definitions
7. ISO 6336-1 - 1996, Calculation of load capacity of spur and helical gears,
Part 1, Basic principles, introduction and general influence factors
8. ISO 6336-2 - 1996, Calculation of load capacity of spur and helical gears,
Part 2, Calculation of surface durability (pitting)

9. ISO 6336-3 - 1996, Calculation of load capacity of spur and helical gears, Part 3, Calculation of tooth bending strength
10. ISO 6336-5 - 1996, Calculation of load capacity of spur and helical gears, Part 5, Strength and quality of materials
11. ISO TR 10064-1 - 1992, (Technical Report) Cylindrical gears - Code of inspection practice - Part 1; Inspection of corresponding flanks of gear teeth
12. ISO 1101.2 - 2004, Geometrical Product Specifications, (GPS) - Geometrical tolerancing - Tolerances of form, orientation, location and run-out
13. ISO 1302-2002 Geometrical Product Specifications (GPS) - Indication of surface texture in technical product documentation
14. ISO 4287 - 1997 Geometrical Product Specifications, (GPS) - Surface texture - Profile method Terms, definitions and surface texture parameters
15. Dudley's Gear Handbook, by Dennis P. Townsend, published by McGraw – Hill, Inc. Second Edition, 1992, ISBN 0-07-017903-4
16. Theory of Vibration with Application, by William T. Thompson, published by Prentice Hall, Englewood Cliffs, New Jersey 07632, ISBN 0-13-914532-X

17. Bergsteigfähigkeit und Literleistung, (Climbing Ability of a Vehicle and Engine Capacity), by Flössel. W., Stuttgart, 1950
18. Industrial Air Motors, published by Ingersoll Rand. www.airmotors.com
19. SAE J1701M – Torque-Tension Tightening for Metric Series Fasteners, published by The Engineering Society for Advancing Mobility Land Sea and Space International, 400 Commonwealth Drive, Warrendale, PA 15096-0001,
20. VDI 2230 – 2000, February 2003, Systematic Calculation of High Duty Bolted Joints, Joints with One Cylindrical Bolt, published by VDI – Richtlinien,
21. Engineering Properties of Steel, by Philip D. Harvey editor, published by American Society for Metals, ISBN 0-87170-144-8
22. Allvac VascoMax catalog. www.allvac.com
23. Petro-Canada, Lubrication Handbook 2005
24. Alberta's OH & S Act, Regulation and Code, OCCUPATIONAL HEALTH and SAFETY ACT Revised Statutes of Alberta 2000 with Alberta Regulation 62/2003, published by Queen's Printer Bookstore. www.gov.ab.ca/qp

8. APPENDICES

Title	Page
A. Gear geometry	54
B. Geometry of mating gears	73
C. Notation, symbols and abbreviations, on base AGMA 6123-A88	83
D. Notation, symbols and abbreviations, on base ISO 6336-1, 1996	88
E. Formulas relating to individual gears	95
F. Determination of base tooth thickness, tools, and measurements	99
G. Calculations	103
H. Materials and lubricants	125

List of Figures

	Title	Page
Figure A.1	Base circle and involute	52
Figure A.2	Analogy and comparison of involute and rope drive	53
Figure A.3	Involute helicoids tooth flank surface of a helical gear with base helix angle β_b and base lead angle γ_b	55
Figure A.4	Gear tooth nomenclature	56
Figure A.5	Gear diameters nomenclature	56
Figure A.6	Relation of spur gear basic rack and rack cutter	58
Figure A.7	Tooth traces on interference cylinder and pitch plane	59
Figure A.8	Basic rack profile	61
Figure A.9	Basic rack profile with undercut	61
Figure A.10	Tooth profile without modification addendum $x * m = 0$	63
Figure A.11	Tooth profile with modification addendum $x * m > 0$	64
Figure A.12	Tooth profile with modification addendum $x * m < 0$	65
Figure A.13	Tooth form generated by generating rack profile	66
Figure A.14	Generated tooth profile without adequate addendum modification, cutter interference	67
Figure A.15	Approximate determination of loss of involute due to cutter interference	68
Figure B.16	Mating gears with center distance modification $y * m$	73
Figure B.17	Distance g_{inv}' along the line of action defined by geometry mating gear	79

Figure F1	Equidistant base thickness involute tooth	97
Figure F2	Base tangent length W_5 , on a spur gear	98

List of Tables

Title	Page
Table A1. Base parameters	57
Table A2. Minimum number of teeth	69
Table E1. Formulas relating to individual gears	92
Table E2. Formulas relating to external spur and helical gears pairs	95

A. GEAR GEOMETRY

A.1 Basic Concepts: Geometry of Single Gears

Gears are toothed wheels that rotate about their axis; motion is equivalent to the rolling contact between solids of revolution, enclosed by pitch cylinders. The teeth of a mathematically determined shape are spaced uniformly about the circumference of a gear so that one gear meshes with a second gear. A rotary motion is transmitted from one gear to another with a continuous and constant angular velocity ratio by the continuous engaging teeth.

The gears arrangement can be divided into two basic categories:

A.1.1. Gears with parallel or intersecting axis, where cylindrical or conical pitch cylinders or cone surfaces are in rolling contact without any relative sliding motion. Spur and helical gears have parallel axes and cylindrical pitch surfaces, bevel gears have intersecting axes and conical pitch surfaces.

A.1.2. Gears with crossed or nonintersecting axis, in theory, should have pitch surfaces in hyperbolic form so the rolling motion between the surfaces is accomplished by sliding along their line of contact.

A.2 Properties of Involute

An involute is the locus of a point on a tight cord unwinding from the circumference of a “stationary circular disc” (base circle).

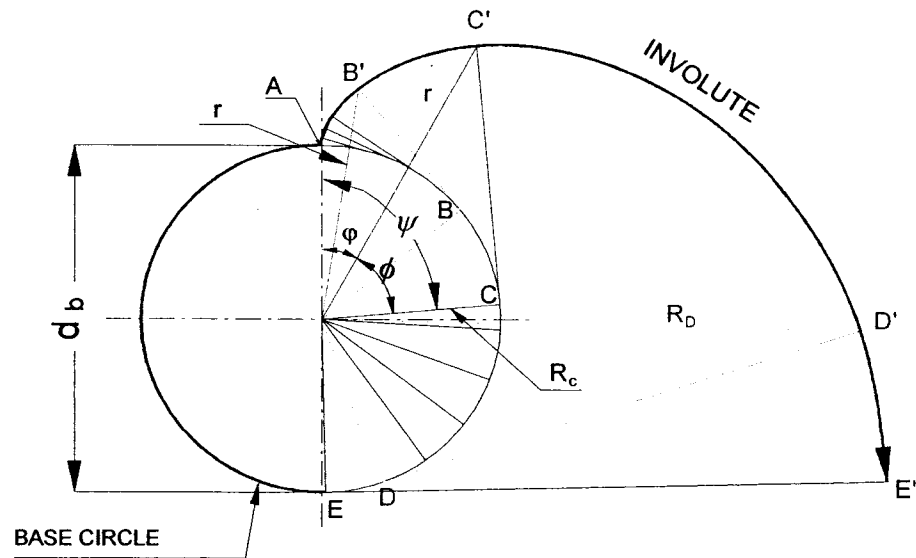


Figure A.1 Base circle and involute

Length of base circle arc \widehat{AB} = length of tangent BB' ;

Length of base circle arc \widehat{AC} = length of tangent AC' , etc.

The parametric equations for the polar coordinates of the involute are:

$$\phi = \tan \psi - \psi (\text{rad}) \quad \text{A.1}$$

$$R = \frac{d_b}{2 \times \cos \psi} \quad \text{A.2}$$

with the angle ψ as a parameter.

The “stationary circular disc” of diameter d_b , as shown in Figure 1, represents the base circle for the involute tooth profile.

With mating involute gears, tooth contact takes place along the line of action.

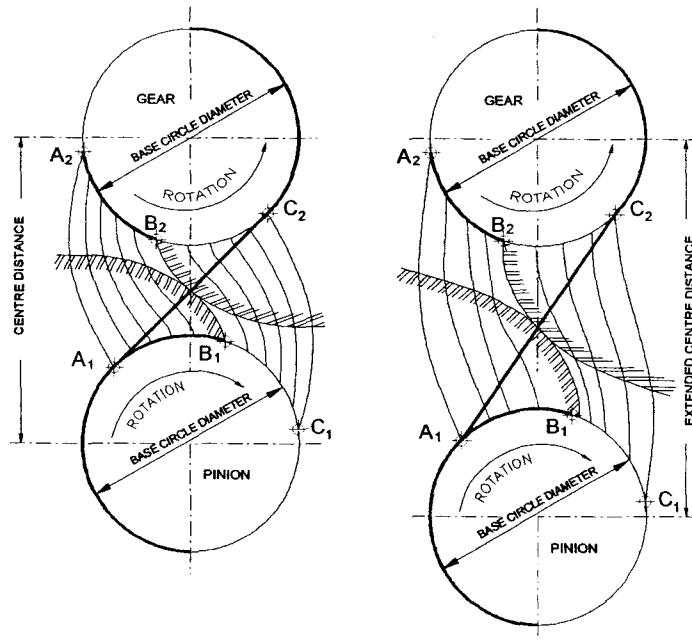


Figure A.2. Analogy and comparison of involute and rope drive and line of action A_1C_2

The transmission of movement (rotation) by the involute tooth flanks could be analogous to that of a crossed inelastic rope drive having pulley diameters the same as the base circle, where the rope is wound from the driven pulley onto the driving pulley.

The wound and unwound lengths of rope are equal and correspond to the length of the tangent to the base circle from the point of contact involute:

$$\text{Arc length } \widehat{A_1B_1} = \widehat{A_2B_2}$$

$$\text{Arc length } \widehat{B_1C_1} = \widehat{B_2C_2}$$

The analogy between involute gears and rope drive can extend further. The system is tied to a fixed center distance so that the centre distance can be increased or decreased with either system without jeopardizing its function. Similarly, the gear ratio is given by the base circle or pulley diameter ratio in each case. For a better visualization of extending the center, distance gives involute gears an advantage over gears with other tooth profiles.

The extent of the modification of the center distance is limited, in practice, by the limits imposed on the tip and root circles of the involute profile.

The minimum and maximum center distances are determined by two conditions:

- Meshing interference must not occur at the root of the tooth; and
- The next tooth must have already entered into engagement before the previous tooth leaves engagement - transverse contact ratio must be greater than 1.

A.3. Basic Gear Tooth Data

Involute helicoids is the surface generated by a straight line inclined at a constant angle to the axis of stationary cylinder (base cylinder) and contained in a plane and pure rolling without slip on the surface of the cylinder.

The base helix angle β_b is the sensitive angle between this straight line generator and the line parallel to the cylinder axis, which is also contained in the rolling plane.

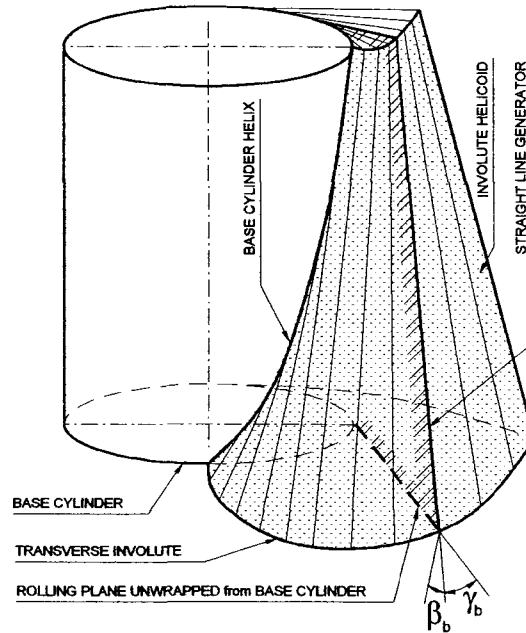


Figure A.3. Involute helicoids tooth flank surface of a helical gear with base helix angle β_b and base lead angle γ_b

Every individual tooth could be right and left hand involute flank joined by the surface on the tip of the cylinder at the crest, and determined by the base diameter d_b , and the base helix angle β_b .

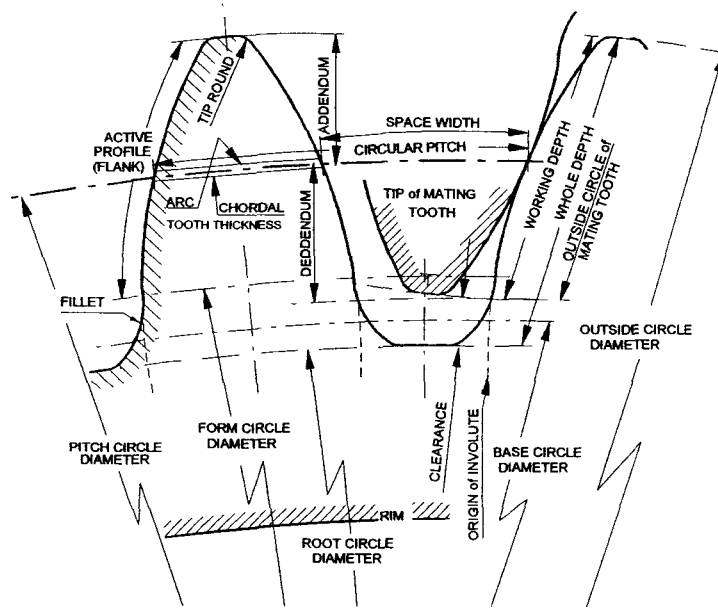


Figure A.4. Gear tooth nomenclature

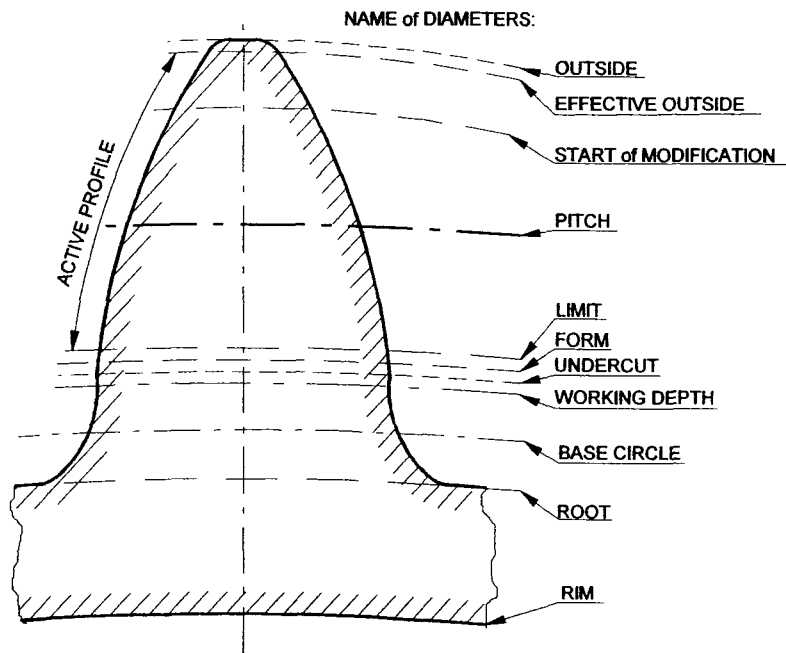


Figure A.5. Gear diameters nomenclature

Data required for specifying a spur or helical gear:

Table A.1. List the basic parameters

ITEM	PARAMETER	SPUR	HELICAL
1	Number of teeth	Z	Z
2	Base diameter	d_b	d_b
3	Base helix angle	NA	β_b
4	Base tooth thickness	s_b	s_b
5	Tip diameter	d_a	d_a
6	Root diameter	d_f	d_f

Data for items 1, 5, and 6 could be determined from basic design parameters; e.g. from Equation (24), (23), and (22) (Table No. A.1).

Data for items 2 and 3 required special tools and measuring equipment but “base tooth thickness” s_b , could be found indirectly from measurements of the base tangent length. For more details, see Appendix F.

The data for generating the gear can be calculated once the above data has been established.

A.4.Data for Generating Gears

Geometric properties of involute gears is produced by the generating process.

A rack type cutter with an infinite number of teeth can produce spur gears.

Internal spur gear and helical can be produced by a pinion type cutter.

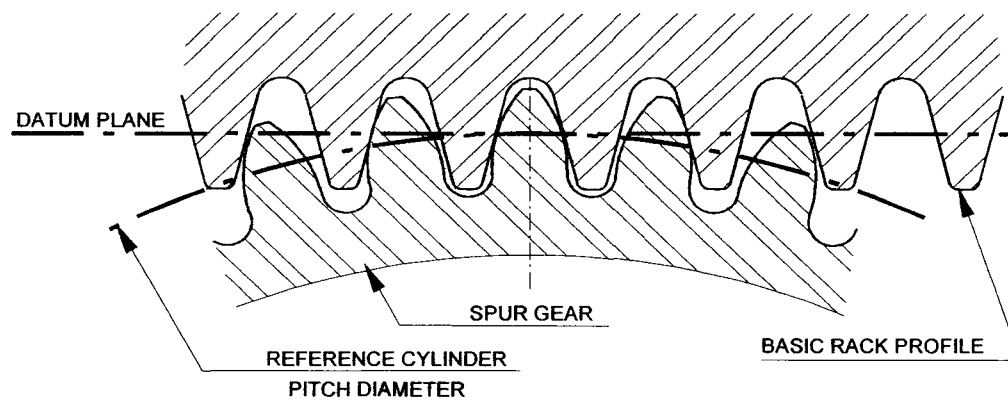


Figure A.6. Relation of spur gear, basic rack and rack cutter

For spur and helical gears, the tooth traces are the lines of intersection between the tooth flanks and the reference cylinder surface.

These lines are helixes on the reference cylinder and they will be straight lines when the surface of the reference cylinder developed in the pitch plane.

The sharp angle between the developed tooth trace and the straight-line generator of the reference cylinder is the helix angle β .

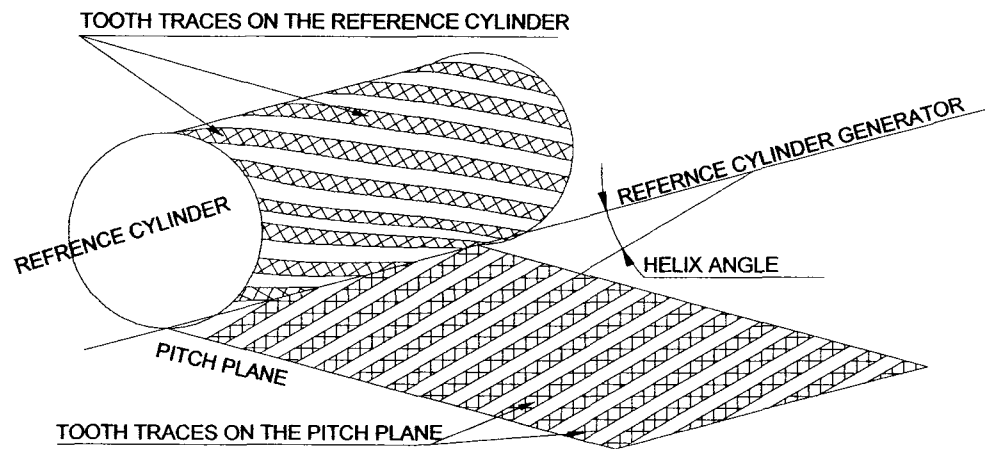


Figure A.7. Tooth traces on the reference cylinder and pitch plane

A distinction has been made between transverse and normal dimensions for pitch.

The following description applies:

- Transverse pitch p_t - distance between the tooth traces of adjacent corresponding flanks in the pitch plane measured at right angles to the reference cylinder generator.
- Normal pitch – distance between tooth traces of adjacent corresponding flanks in the pitch plane measured at right angles to the tooth traces.

Considering ISO standard the diameter of the reference cylinder (diameter d) can be calculated from the module – m from following equations:

$$m = \frac{P}{\pi} [mm] \quad A.3$$

$$d = \frac{z * m}{\cos \beta} [mm] \quad A.4$$

In the imperial system, pitch is specified in terms – diametral pitch P_{nd} ,

where:

$$p = \frac{\pi}{P_{nd}} [inch] = \frac{25.4 * \pi}{P_{nd}} [mm] \quad A.5$$

The relationship between module “m” and P_{nd} expressed by equation:

$$m = \frac{25.4}{P_{nd}} \quad A.6$$

The basic rack profile is fundamental to the specification of involute gears. It determines the tooth profile on the gear, the generating rack profile, and associated rack shaped cutter tool.

The basic rack profile is the normal section through the teeth of the basic rack that corresponds to external gear with number of teeth $z = \infty$ and diameter $d = \infty$.

The tooth of the basic rack profile is bound by the tipped line at the top and by the parallel root line at the bottom. The fillet between the straight tooth flank and root line is usually a circular arc.

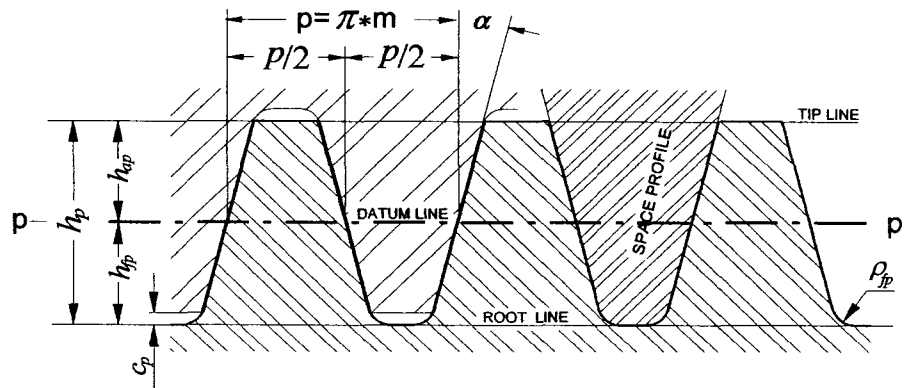


Figure A.8. Basic rack profile

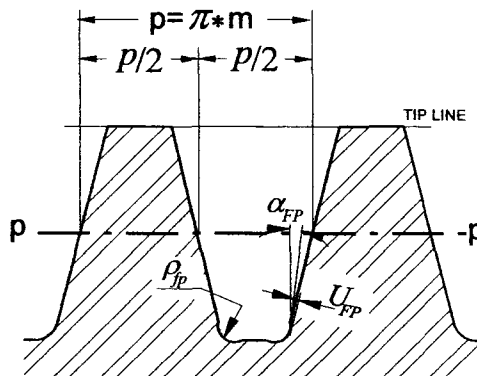


Figure A.9. Basic rack profile with undercut

Characteristics parameters of a basic rack are:

- Basic rack profile with module m has pitch $p = \pi \times m$;
- Datum line –pp- is the line drawn parallel to the tip and root lines;
- Tooth thickness = tooth space = half the *pitch* $= \frac{p}{2}$;
- Dimensions of the basic rack profile are given relative to the datum line and are quoted as a multiple of module - m . Dimensions relating to module $m = 1.0$ are identified by * h_{ap} * ;
- Mating rack profile is symmetrical to the basic rack profile about the datum line (pp), and displaced by half a pitch relative to it;
- The parts of the flank are inclined at the profile angle α to line normal to the datum line. This angle is the same as the pressure angle α (α_n) at the reference cylinder of the gear;
- Tooth depth h_p is divided by the datum line into the addendum h_{ap} and dedendum h_{fp} ;
- Dedendum h_{fp} is the sum of addendum h_{ap} and the bottom clearance c_p ;
- Bottom clearance determines the greatest possible fillet radius $\rho_{fp\max}$; the radius must not be greater than that resulting in the full fillet root;
- The condition for this is:

$$\rho_{fp\max} = \frac{c_p}{1 - \sin \alpha} \leq \left(\frac{\pi * m}{4} - h_{fp} * \tan \alpha \right) * \tan \left(\frac{90^\circ + \alpha}{2} \right) \quad A.7$$

- The basic rack profile with fillet undercut with depth U_{fp} and profile angle α_{fp} is used for gear cutting by sharp or other similar finishing by grinding.

A.5. Addendum Modification

During the manufacturing of the gears by a generating process, the datum line of the basic rack profile does not necessarily need to form a tangent to the reference circle. The tooth profile could be alternated by shifting the datum line from the tangential position.

The involute shape of the tooth profile is retained and affected to the tooth profile.

The displacement is:

- Positive when in the direction is away from the centre of the gear ($x \cdot m > 0$); and,
- Negative when in the direction is towards the centre of the gear ($x \cdot m < 0$.) This relation also applied to internal and helical gears.

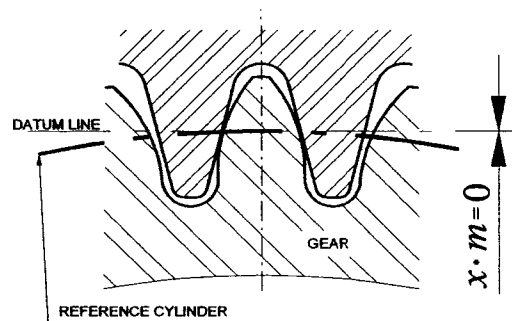


Figure A.10. Tooth profile without modification addendum $x \cdot m = 0$

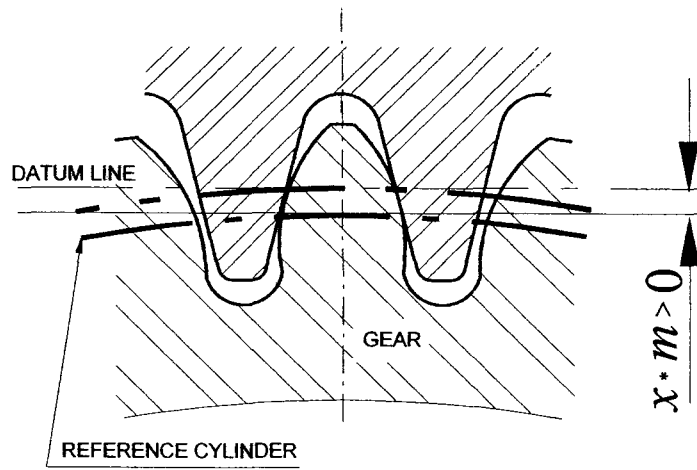


Figure A.11. Tooth profile with addendum modification $x \cdot m > 0$
 (Tooth thicker and stronger)

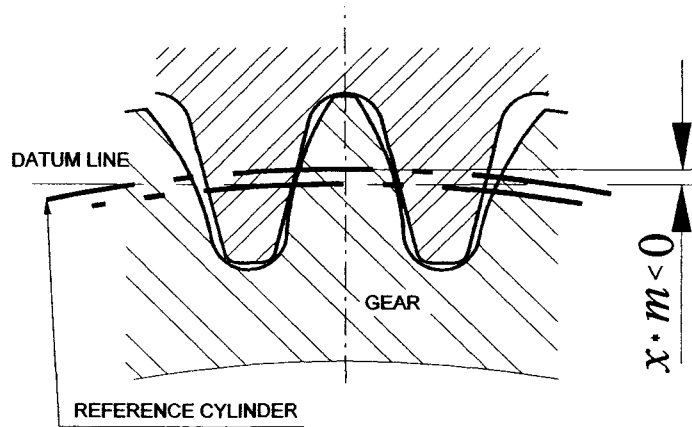


Figure A.12. Tooth profile with addendum modification $x \cdot m < 0$
 (Tooth thinner and weaker)

The addendum modification coefficient – x – is the amount of the addendum modification divided by module.

The following characteristics of a generated tooth form are extremely significant for its load carrying capacity:

- A.5.1. The profile angle α ; the relationship between the mean radius of curvature of the tooth flanks and the contact load capacity.
- A.5.2. The tooth root thickness; the relationship between the modulus of section and the bending strength at the root of the tooth.
- A.5.3. The fillet radius at the critical point for bending, as at this point, the rapidly changing cross section result is high and could be an excessive stress concentration factor.
- A.5.4. The crest width; excessive shear stress at the tip is unwanted in surface hardened gears.

Two tooth profile zones have to be distinguished:

- Involute zone; and
- Root fillet.

The fillet form is affected by the choice of the basic rack profile. The tooth depth has to be increased slightly where the fillet form continues – a semicircular arc.

The tooth root thickness and the fillet radius improved with increasing bending strength, while the bending strength was affected by addendum modification.

The process of generating rack profiles and the tooth form generated are shown in Figure 13. The course of generating the tooth, the generating rack profile rolls to the right on reference circle 'd' from the position shown and the gear, being cut out, corresponds in a clockwise rotation, point R." The line of action will be reached at the lowest point R of the straight generating rack flank it becomes engaged and cuts the bottom point R' on the involute. This point at the beginning of the involute profile has a radius r_{im} .

The fillet begins at this point on the gear and is in the form of a trochoid.

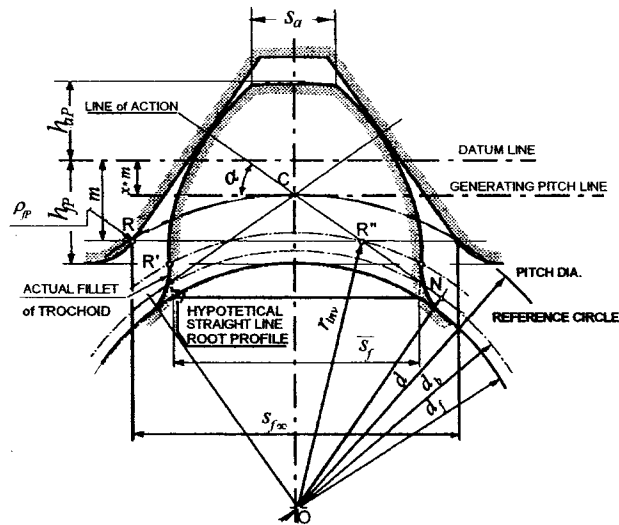


Figure A.13. Tooth form generated by the generating rack profile

The trochoid fillet needs to be blended tangentially with the involute, the point R'' on the line of action, and must be positioned above point N, the point of intersection between the line of action and the line drawn normal to it through the center of the gear.

If “R” is positioned below N, undercut will occur and the trochoid fillet no longer blends tangentially with the involute (Figure A.14).

A.6. Cutter Interference Point

Cutter is the interference as results of its exit from the tooth space endpoint of the straight flank of the generating rack profile generate trochoid fillet, which intersects the involute. Part of the involute, as could be seen in Figure A.14, is cut away with a large reduction of tooth usable profile.

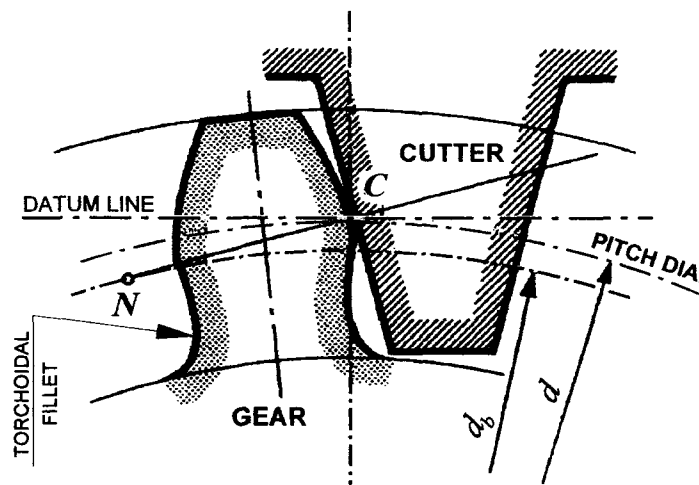


Figure A.14. Generated tooth profile without adequate addendum modification,
cutter interference

The bending strength of the tooth is also reduced by trochoid concentration.

When undercutting occurs, an angle is formed at the junction between involute tooth flank and the fillet, rather than a continuous curve.

At the beginning of the cutter interference, R'' and N match the involute, still blending with the trochoid at the point of inflexion on the base circle see Figure A15.

On gears without addendum modification, the start of the cutter interference depends on the pressure angle and the number of teeth.

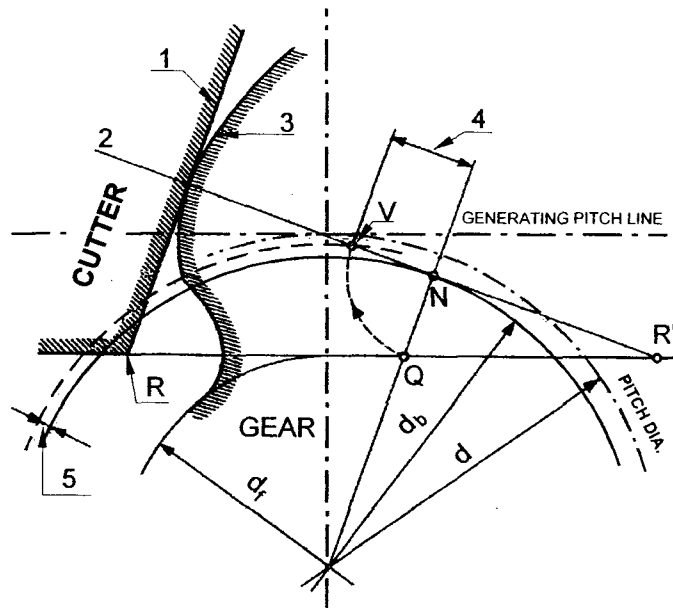


Figure A.15. Approximate determination of loss of involute due to cutter interference, where:

1. Flank of generating cutter (rack) profile, for clarity shown without fillet
2. Line of action
3. Involute flank of the gear
4. Loss of involute profile measured along line of action
5. Loss of involute profile measured radially at the gear tooth flank

The minimum number of teeth z_g without cutter interference with $h_{ap} = 1 * m$ and full fillet root is given by the equation:

$$z_g = \frac{2}{\sin^2 \alpha} \quad \text{A.8}$$

Table A.2. List the minimum number of teeth vs. pressure angle

Pressure angle	α	15°	17°30'	20°	22°30'	25°
Minimum Number of teeth	z_g	29.9	22.1	17.1	13.7	11.2

The minimum addendum modification coefficient 'x' to avoid cutter interference on spur gears is expressed by the equation:

$$x_{\min} = 1 - \frac{z}{2} * \sin^2 \alpha \quad \text{A.9}$$

B. GEOMETRY of MATING GEARS

The tooth form of mating gears could be involute, cycloidal, or connected with special production processes. The second category includes gears with crossed, non-intersection axes; e.g. worm gears, and hypoid bevel gears. The relationships for mating of external spur (and helical) gears are considered and applied to internal gears and pinions.

The following conditions apply only to gears with involute and with parallel axes:

B.1. Basic Conditions to be met by mating gears

1st Condition

The ratio of the gear and pinion base diameters must be equal to the gear ratio:

$$u = \frac{z_2}{z_1} = \frac{d_{b2}}{d_{b1}} \quad \text{B.10}$$

Consequently,

$$\frac{d_{b2}}{z_2} = \frac{d_{b1}}{z_1}, \frac{p_{bt2}}{\pi} = \frac{p_{bt1}}{\pi}; p_{bt1} = p_{bt2} \quad \text{B.11}$$

This means that transverse base pitches of mating gears must be equal.

2nd Condition

The normal base pitches must be equal:

$$p_{b1} = p_{b2} \quad \text{B.12}$$

Hence, the line of contact, and the base of helix angles of gear and pinion must be equal:

$$\beta_{b1} = \beta_{b2} \quad \text{B.13}$$

3rd Condition

For a smooth transition of tooth contact from one pair of teeth to another, there must be at least one theoretical point of contact in the zone of action. Because of strength considerations, there is an auxiliary requirement in case of mating helical gears that all points of contact along the minimum required path of teeth contact should be corresponding to, along the contact line over face.

The following condition must apply:

$$\text{Transverse contact ratio } \varepsilon_{\alpha} = \frac{\text{length of path of contact } g_{\alpha}}{\text{transverse base pitch } p_{bt}} \geq 1 \quad \text{B.14}$$

$$\text{Overlap ratio } \varepsilon_{\beta} = \frac{b * \tan \beta}{P_{bt}} \geq 1 \quad \text{B.15}$$

According to the manufacturer's recommendation, gear and transverse contact ratio should be greater than 1.

4th Condition

The sum of the theoretical transverse tooth thickness of gear and pinion must be equal to the transverse working pitch:

$$s_{i1}' + s_{i2}' = p_i' = \pi * \frac{2 * a}{z_1 + z_2} \quad \text{B.16}$$

5th Condition

The pinion and gear must provide an adequate bottom clearance beyond the tip circle of mating gear to avoid interference:

$$d_{a1} + d_{f2} + 2 * c = 2 * a \quad \text{B.17}$$

$$d_{a2} + d_{f1} + 2 * c = 2 * a \quad \text{B.18}$$

where: $a = \text{centre distance}$,

$c = \text{bottom clearance}$

B.2 Principles of Addendum Modification

If the sum of the addendum modification coefficients $x_1 + x_2 \neq 0$, then the center distance does not equal the sum of the reference radii.

The working pressure angle α'_t see Figure B 16, at that time differs from the generating pressure angle α_t . The amount by which the centre distance deviates from the sum of the reference circle diameter is known as the centre distance modification $y * m$ and the working pressure angle α'_t is given by the following equations:

$$y * m = a - \frac{d_1 + d_2}{2} \quad \text{or} \quad \text{B.19}$$

$$y * m = \frac{d_1 + d_2}{2} * \left(\frac{\cos \alpha_t}{\cos \alpha'_t} - 1 \right) \quad \text{B.20}$$

For mating external spur and helical gears, the center distance modification is always smaller than the sum of addendum modification.

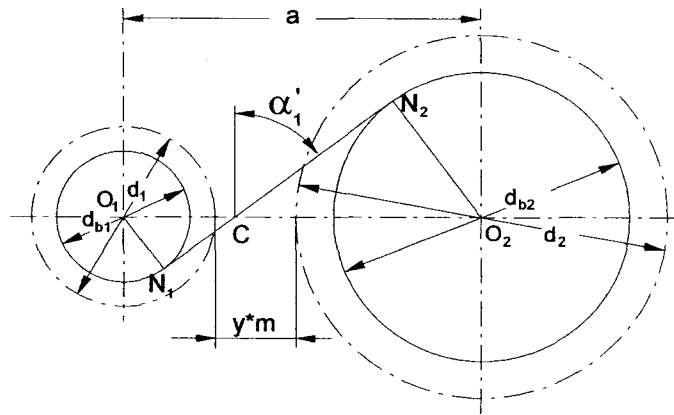


Figure B.16. Mating gears with center distance modification $y * m$

Addendum shortening of $k * m$ is necessary to maintain the basic rack profile bottom clearance c_p :

$$k * m = \frac{(z_1 + z_2) * m}{2} \left[\frac{\text{inv} \alpha'_t - \text{inv} \alpha_t}{\tan \alpha} - \frac{1}{\cos \beta} \left(\frac{\cos \alpha_t}{\cos \alpha'_t} - 1 \right) \right] \quad \text{B.21}$$

The geometrical relationship of involute teeth by choosing relatively large addendum modifications with addendum shortening needs to be large enough to avoid excessively pointed teeth. This has resulted in a tooth form with high bending strength.

See Figures A10, A11 and A12.

B.3. Basic equations for mating gears with addendum modifications

The following basic data for each of the mating gears is important;

- Pressure angle α
- Module m
- Number of pinion teeth z_1
- Number of gear teeth z_2
- Addendum of basic rack profile per unit $m = 1$ h_{ap}^*
- Dedendum of basic rack profile per unit $m = 1$ h_{fp}^*
- Helix angle β

In the case of involute gears, with a choice of the center, distance a could be different than the reference center distance expressed by following equation:

$$a_d = \frac{d_1 + d_2}{2} \quad \text{B.22}$$

Two of the following three variables must always specify to correct the tooth geometry:

- Addendum modification coefficient of pinion x_1
- Addendum modification coefficient of gear x_2
- Center distance $(x_1 + x_2)$ a

Unrestrained choice of the center distance a , with the above dimensional criteria for the sum of the addendum modification coefficient is possible with a very close graduated series of modules.

B.3.1 Mating spur and helical external gears and pinions

The three following cases are used in gear industries:

Case A

Determination of gear addendum, modification coefficient x_2 , for known pinion addendum modification coefficient x_1 , and the center distance a :

$$\cos \alpha'_t = \frac{d_{b1} + d_{b2}}{2 * a} \quad \text{B.23}$$

$$(x_1 + x_2) = \frac{z_1 + z_2}{2} * \frac{\text{inv} \alpha'_t - \text{inv} \alpha_t}{\tan \alpha} \quad \text{B.24}$$

$$x_2 = (x_1 + x_2) - x_1 \quad \text{B.25}$$

Case B

Determination of center distance a , for given pinion and gear addendum modification coefficient x_1 , and x_2 :

$$\text{inv} \alpha'_t = \text{inv} \alpha_t + \frac{2 * \tan \alpha * (x_1 + x_2)}{z_1 + z_2}, \quad \text{B.26}$$

$$a = \frac{d_{b1} + d_{b2}}{2 * \cos \alpha'_t}. \quad \text{B.27}$$

Case C

Determination of the pinion addendum modification coefficient x_1 ,
for known the gear addendum modification coefficient x_2 and the center
distance a :

$$\cos \alpha'_t = \frac{d_{b1} + d_{b2}}{2 * a} \quad \text{B.28}$$

$$(x_1 + x_2) = \frac{z_1 + z_2}{2} * \frac{\text{inv} \alpha'_t - \text{inv} \alpha_t}{\tan \alpha} \quad \text{B.29}$$

$$x_1 = (x_1 + x_2) - x_2 \quad \text{B.30}$$

The appropriate diameters can be calculated for:

Pinion:

Pinion (pitch) reference diameter $d_1 = \frac{z_1 * m}{\cos \beta}$ B.31

Theoretical pinion root diameter $d_{f1tho} = d_1 - 2 * m (h_{fp}^* - x_1)$ B.32

Pinion tip diameter $d_{a1} = d_1 + 2 * m (h_{ap}^* + x_1) - 2 * k * m$ B.33

Gear

Gear (pitch) reference diameter $d_2 = \frac{z_2 * m}{\cos \beta}$ B.34

Theoretical gear root diameter $d_{f2tho} = d_2 - 2 * m (h_{fp}^* - x_2)$ B.35

Gear tip diameter $d_{a2} = d_2 + 2 * m (h_{ap}^* + x_2) - 2 * k * m$ B.36

For verification and cross check the following equation held:

$$c = c_p = m(h_{fp}^* - h_{ap}^*) \quad \text{B.37}$$

$$c = a - 0.5(d_{f1tho} + d_{a2}) \quad \text{B.38}$$

$$c = a - 0.5(d_{f2tho} + d_{a1}) \quad \text{B.39}$$

B.3.2. Mating spur and helical internal gears and pinions

In generally, gear addendum modification coefficient x_2 has to be determined for known pinion addendum modification coefficient x_1 and center distance a :

$$\cos \alpha'_t = \frac{d_{b2} - d_{b1}}{2 * a} \quad \text{B.40}$$

$$(x_2 - x_1) = \frac{z_2 + z_1}{2} * \frac{\text{inv} \alpha'_t - \text{inv} \alpha_t}{\tan \alpha_t} \quad \text{B.41}$$

$$x_2 = (x_2 - x_1) + x_1 \quad \text{B.42}$$

Where diameters of:

Pinion reference diameter $d_1 = \frac{z_1 * m}{\cos \beta} \quad \text{B.43}$

Theoretical pinion root diameter $d_{f1tho} = d_1 - 2 * m(h_{fp}^* - x_1) \quad \text{B.44}$

Pinion tip circle diameter $d_{a1} = d_1 + 2 * m(h_{ap}^* + x_1) \quad \text{B.45}$

Gear reference diameter $d_2 = \frac{z_2 * m}{\cos \beta} \quad \text{B.46}$

The exact calculation of the theoretical gear root circle diameter require of knowledge of the number of cutter teeth z_0 , with cutter addendum coefficient x_0 , and the theoretical gear root diameter these parameters can be calculated as:

$$d_{f2tho} = \frac{d_{b2} - d_{b1}}{\cos \alpha_{gt}} + \frac{z_0 * m}{\cos \beta} + 2 * m(h_{fp}^* - x_0) \quad B.47$$

Then, the theoretical gear root diameter can be calculated with approximation from:

$$d_{f2} \approx d_2 + 2 * m(h_{ap}^* + x_1) \quad B.48$$

Gear tip diameter could be calculated from:

$$d_{a2} = d_2 - 2 * m(h_{ap}^* - x_2) \quad B.49$$

The addendum shortening for internal gear and pinion can be obtained:

$$k * m = \frac{(z_2 - z_1) * m}{2} \left[\frac{\text{inv} \alpha'_i - \text{inv} \alpha_i}{\tan \alpha} - \frac{1}{\cos \beta} \left(\frac{\cos \alpha_i}{\cos \alpha'_i} - 1 \right) \right] \quad B.50$$

When the addendum shortening value is negative as tooth depth is increased.

B.4. Interference on spur external gears

Interference caused by contact with non-involute parts of the tooth flank of the mating gear results in severe shock during rotation of pinion and gear transmission.

B.4.1. Interference at roots for mating external gears

The path of contact at the tip of the gear tooth (see Figure B.17) makes contact within the involute part of the pinion tooth dedendum. The involute profile generated on the pinion must start at radius r_{inv} (point A), which is smaller than the actual radius r_{inv}' at which the path of contact ends. Related distances are g_{inv} and g_{inv}' . (see Figure B17)

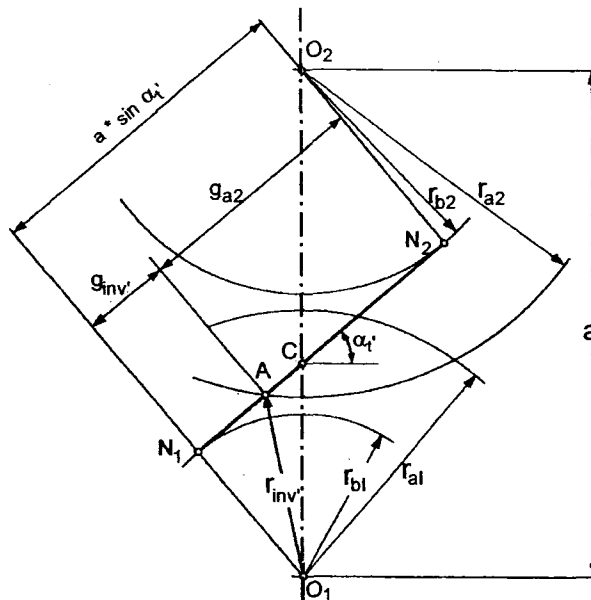


Figure B.17. Distance g_{inv}' along the line of action defined by geometry mating gears

C. NOTATION, SYMBOLS and ABBREVIATIONS,
on base of AGMA 6123-A88.

SYMBOL	UNITS	DESCRIPTION
A	--	Arrangements constant
b	mm	Face width, Total
b'	mm	Face width, Engaged
C	mm	Center distance
C_a	--	Application Factor for Pitting Resistance
C_L	--	Life Factor for Pitting Resistance
c	mm	Clearance
D	mm	Diameter
d	mm	Diameter at Half Working Depth
d'	mm	Operating Pitch Diameter of Gear
e	--	Pump efficiency
f_{Σ}	radians	Misalignment Angle
H_R	--	Hardness, Rockwell C
j	--	Bearing Power Loss Coefficient
K	--	Load Intensity
K_a	--	Application Factor for Bending Strength
K_L	--	Life Factor for Bending Strength

AGMA 6123-A88

SYMBOL	UNITS	DESCRIPTION
K_m	--	Load Distribution Factor
L	mm	Bearing Length
L_f	--	Load Share per Planet
M	--	Mechanical Advantage Factor
m_n	--	Normal Module
n	rpm	Shaft Speed
n'	rpm	Relative rpm of Member for which Torque is Specified
n_i	rpm	Input Shaft
n_{iR}	rpm	Input Speed, Ring Gear
n_{iS}	rpm	Input Speed, Sun Gear
n_o	rpm	Output Speed
P	kW	Power
P_A	kW	Application Power of Enclosed Drive
P_{Bh}	kW	Hydrodynamic Bearing Power Loss
P_{Br}	kW	Rolling Bearing Power Loss
P_{Bt}	kW	Thrust bearing Power Loss
P_M	kW	Mesh Power Loss

AGMA 6123-A88

SYMBOL	UNITS	DESCRIPTION
P_{mc}	kW	Minimum Component Power
P'_R	--	Lowest Common Denominator of Ratio Fraction
P'_S	--	Lowest Common Numerator of Ratio Fraction
P_S	kW	Seal Power Loss
P_w	kW	Windage Power Loss
p	kPa	Operating Lube Pressure
Q	L/min	Oil Flow
r_{iR}	mm	Ring Gear Inside Radius
r_{oP}	mm	Planet Outside Radius
r_{oS}	mm	Inside Radius
r_i	mm	Inside Radius of Thrust Bearing
r_o	mm	Outside Radius of Thrust Bearing
r_P'	mm	Planet Operating Pitch Radius
r_R'	mm	Ring Gear Operating Pitch Radius
r_S'	mm	Sun Operating Pitch Radius
S_F	--	Service Factor

AGMA 6123-A88

SYMBOL	UNITS	DESCRIPTION
T_p	N*m	Torque per Mesh on Planet Gear
T_s	N*m	Torque per Mesh on Sun Gear
t	mm	Oil Film Thickness
v	m/s	Pitch Line Velocity
v_{iR}	m/s	Specific Sliding Velocity at Ring Gear Tip
v_{oP}	m/s	Specific Sliding Velocity at Planet Tip
v_{oS}	m/s	Specific Sliding Velocity at Sun Tip
w	kPa	Load per Unit Area
x	--	Numerical Remainder
y	--	Number of Planet Groups with Different Meshing Conditions
μ	MPa*s	Outlet oil Viscosity (Absolute, millipascal second)
z_{CP}	--	Number of Planets
z_{GP}	--	Number of Planets in a Group
z_p	--	Number of Teeth in Planet Gear
z_{PR}	--	Number of Teeth in Planet Meshing with Ring Gear
z_{PS}	--	Number of Teeth in Planet Meshing with Sun Gear

AGMA 6123-A88

SYMBOL	UNITS	DESCRIPTION
z_R	--	Number of Teeth in Ring Gear
z_S	--	Number of Teeth in Sun Gear
α'	--	Operating Transverse Pressure Angle
α'_n	--	Operating Normal Pressure Angle
β'	--	Helix Angle at Operating Pitch Diameter
μ	--	Coefficient of Friction
ρ	--	Radius of Curvature

Subscripts

1	first number in gear train
2	second number in a gear train
...	etc. for any additional members
e	external mesh feature
i	internal mesh feature, ring tip
l	for light weight oil
m	for medium weight oil
o	outside feature
P	feature of a planet gear
R	feature of a ring gear
S	feature of a sun gear

D. NOTATION, SYMBOLS and ABBREVIATIONS,
on base ISO 6336-1, 1996.

SYMBOL	UNITS	DESCRIPTION
a	mm	Center distance
a_d	mm	Reference circle centre distance
b	mm	Face width
c	mm	Bottom clearance
c_p	mm	Bottom clearance of basic rack profile
$d(r)$	mm	Reference circle diameter (radius)
$d'(r')$	mm	Working pitch circle diameter (radius)
$d_a(r_a)$	mm	Tip diameter (radius)
$d_b(r_b)$	mm	Base diameter (radius)
$d_f(r_f)$	mm	Root diameter (radius)
$d_n(r_n)$	mm	Virtual reference diameter (radius)
e, e_n	mm	Space width (normal)
e_t	mm	Transverse space width
g_a	mm	Length of path of addendum contact
g_α	mm	Length of path of contact
h	mm	Tooth depth
h_a	mm	Addendum

ISO 6336-1, 1996

SYMBOL	UNITS	DESCRIPTION
h_a	mm	Chordal height of tooth
h_{ap}	mm	Addendum of basic rack profile
h_f	mm	Dedendum
h_{fp}	mm	Dedendum of basic rack profile
h_p	mm	Tooth depth of basic rack profile
inv	rad	Involute function
j, j_n	mm	Backlash, normal backlash
$\Delta j, \Delta j_n$	mm	Backlash allowance, normal backlash allowance
j_r	mm	Radial backlash
j_t	mm	Circumferential backlash
k	--	Addendum shortening coefficient
k	--	Number of teeth spanned for base tangent length
k_A	--	Contact parameter at gear tooth tip
k_{AZ}	--	Contact parameter at rack tooth tip
k_E	--	Contact parameter at pinion tooth tip
k_{EZ}	--	Contact parameter at pinion tooth tip in rack and pinion drive
l	mm	Length along profile, general

ISO 6336-1, 1996

SYMBOL	UNITS	DESCRIPTION
l_a	mm	Length of profile on addendum flank
l_f	mm	Length of profile on dedendum flank
l_α	mm	Active length of profile
m, m_n	mm	Module, (normal)
m_t	mm	Transverse module
p, p_n	mm	Pitch (normal)
p_b, p_{bn}	mm	Base pitch (normal)
p_{bt}	mm	Transverse base pitch
p_t	mm	Transverse pitch
r	mm	Radius general
s, s_n	mm	Tooth thickness (normal)
s_a, s_{an}	mm	Tooth crest width (normal)
s_{at}	mm	Transverse tooth crest thickness
s_b, s_{bn}	mm	Base tooth thickness (normal)
s_{bt}	mm	Transverse base tooth thickness
$\overline{s}, \overline{s}_n$	mm	Chordal tooth thickness (normal)
u	--	Gear ratio

ISO 6336-1, 1996

SYMBOL	UNITS	DESCRIPTION
v	m/sec	Velocity, general
v'	m/sec	Pitch line velocity
v_b	m/sec	Velocity at base circle
v_g	m/sec	Sliding velocity
v_r	m/sec	Rolling velocity
v_ρ	m/sec	Tangential velocity, normal to line of action
$x^{(1)}$	--	Addendum modification coefficient
x_{eff}	--	Addendum modification coefficient include backlash allowance
y	--	Centre distance modification coefficient
$z^{(2)}$	--	Number of teeth
z_g	--	Minimum number of teeth to avoid cutter interference
z_n	--	Virtual number of teeth
A	--	Gear tooth tip
AW_k	mm	Actual base tangent length
B	--	Lowest point of single pair contact
C	--	Pitch point
D	--	Highest point of single pair contact

ISO 6336-1, 1996

SYMBOL	UNITS	DESCRIPTION
D_M	mm	Diameter of ball used for measurements
N	--	Point of tangency of line of action with base circle
O	--	Centre of gear
(1)		On spur and helical gear external and internal gears, 'x' is positive, if the profile datum line is displaced in the direction away from the centre of the gear
(2)		The number of teeth 'z' is always positive on both external and internal spur and helical gears
P	--	Point, point on involute, general
P_{nd}	$\frac{1}{inch}$	Normal diametral pitch
U_{FP}	mm	Depth of undercut on basic rack profile
W_k	mm	Base tangent length measured over 'k' teeth
α, α_n	deg	Profile angle, pressure angle, normal pressure angle
α_a	deg	Transverse profile angle at tooth tip
α_{FP}	deg	Profile angle of undercut flank
α_{gt}	deg	Transverse generating pressure angle
α_{kt}	deg	Transverse pressure angle at ball centre radius
α_t	deg	Transverse pressure angle

ISO 6336-1, 1996

SYMBOL	UNITS	DESCRIPTION
α'	deg	Working transverse pressure angle
β	deg	Helix angle on reference cylinder
β_b	deg	Base helix angle
β'	deg	Helix angle on pitch cylinder
γ	---	Specific sliding
γ	--	Reference cylinder lead angle
γ_b	deg	Base lead angle
ε	--	Addendum contact ratio
ε_a	--	Transverse contact ratio
ε_β	--	Overlap ratio
ε_γ	--	Total contact ratio
η	--	Gear efficiency
μ	--	Coefficient of friction
ρ_{fp}	mm	Fillet radius of basic rack profile
φ	rad	Roll angle, polar angle involute
ψ	rad	Angular parameter, general
Δ_j, Δ_{jn}	mm	backlash normal backlash

Suffix

<i>inv</i>	Involute, point on involute
<i>max</i>	Maximum
<i>min</i>	Minimum
<i>troch</i>	Trochoid, point on trochoid
<i>theo</i>	Theoretical
<i>y</i>	Any point on involute
<i>A</i>	Gear tooth tip
<i>E</i>	Pinion tooth tip
<i>P</i>	Basic rack profile
<i>O</i>	Tool
1	Pinion, smaller gear in gear pair
2	Gear, larger gear in a gear pair
'	Relating to working conditions
*	Factor for expressing dimensions as a multiple or submultiples of the normal module; e.g. $h_{ap} = h_{ap}^* \times m$

Appendix E; FORMULAS RELATING to INDIVIDUAL GEARS

Table E1. Formulas related to individual gears

		Equation	Eq. Number
Normal pitch (on reference cylinder)		$p = \pi \times m$	(1)
Transverse module		$m_t = \frac{m}{\cos \beta}$	(2)
Transverse pitch		$p_t = \pi \times m_t$	(3)
Reference diameter, (pitch diameter)		$d = \frac{z \times m}{\cos \beta} = z \times m_t$	(4)
Transverse pressure angle	(5a) $\tan \alpha_t = \frac{\tan \alpha}{\cos \beta}$	(5c) $\cos \alpha_t = \frac{\cos \alpha \times \cos \beta}{\cos \beta_b}$	(5a)
	(5b) $\sin \alpha_t = \frac{\sin \alpha}{\cos \beta_b}$		(5b)
			(5c)
Base pitch		$p_b = \pi \times m \times \cos \alpha$	(6)
Transverse base pitch		$p_{bt} = \pi \times m \times \frac{\cos \alpha}{\cos \beta_b}$	(7)
Base helix angle	(8a) $\sin \beta_b = \sin \beta \times \cos \alpha$	(8b) $\tan \beta_b = \tan \beta \times \cos \alpha$	(8a)
			(8b)
Base diameter	$d_b = z \times m \times \frac{\cos \alpha}{\cos \beta_b}$	$d_b = d \times \cos \alpha_t$	(9a)
			(9b)

Table E1. Formulas relating to individual gears - continued

		Equation	Eq. Number
Transverse profile angle at tooth tip		$\cos \alpha_a = \frac{d_b}{d_a}$	(10)
Virtual number of teeth		$z_n = \frac{z}{\cos^2 \beta_b \cdot \cos \beta}$	(11)
Involute function		$inv \alpha = \tan \alpha - \alpha(rad)$	(12)
Angle in radians		$\alpha(rad) = \frac{\pi}{180} \times \alpha^\circ$	(13)
Overlap ratio	(14a) $\varepsilon_\beta = \frac{b \times \tan \beta_b}{p_{bt}}$	(14b) $\varepsilon_\beta = \frac{b \times \sin \beta_b}{p_b}$	(14a)
		(14c) $\varepsilon_\beta = \frac{b \times \sin \beta}{p}$	(14b) (14c)
Normal tooth thickness on reference cylinder		$s_n = m \left(\frac{\pi}{2} + 2 \times x \times \tan \alpha \right)$	(15)
Transverse tooth thickness on reference cylinder		$s_t = \frac{m}{\cos \beta} \left(\frac{\pi}{2} + 2 \times x \times \tan \alpha \right)$	(16)
Normal base tooth thickness		$s_{bn} = z \times m \times \cos \alpha \left(\frac{s_n}{z \times m} + inv \alpha_t \right)$	(17)
Transverse tooth crest width		$s_{at} = d_a \left(\frac{s_n}{z \times m} + inv \alpha_t - inv \alpha_a \right)$	(18)
Base tangent length $W_k = m \left[(k - 0.5) \pi \times \cos \alpha + z \times inv \alpha_t \times \cos \alpha + 2 \times x \times \sin \alpha \right]$			(19)
Actual base tangent length		$AW_k = W_k - \Delta j_n$	(20)

Table E2. Formulas relating to external spur and helical gear pairs

	Equation	Eq. number
Bottom clearance of basic rack profile	$c_p = m(h_{fp}^* - h_{ap}^*)$	(21)
Root diameter	$d_t = d - 2 \times m(h_{fp}^* - x)$	(22)
Tip diameter	$d_{a1,2} = 2 \times a - d_{f1,2} - 2 \times c_p$	(23)
Gear ratio	$u = \frac{z_2}{z_1}$	(24)
Working pitch diameter, pinion	$d_1' = \frac{2 \times a}{u + 1}$	(25)
Working pitch diameter, gear	$d_2' = \frac{2 \times u \times a}{u + 1}$	(26)
Transverse working pressure angle	$\cos \alpha_t' = \frac{d_{b1} + d_{b2}}{2 \times a}$	(27)
Sum of addendum modification coefficient	$x_1 + x_2 = \frac{z_1 + z_2}{2} \times \frac{\text{inv} \alpha_t' - \text{inv} \alpha_t}{\tan \alpha}$	(28)
Length of path addendum contact of pinion	$g_{a1} = \frac{d_{b1}}{2} (\tan \alpha_{a1} - \tan \alpha_{at}')$	(29)
Length of path addendum contact of gear	$g_{a2} = \frac{d_{b2}}{2} (\tan \alpha_{a2} - \tan \alpha_{at}')$	(30)
Length of path of contact	$g_a = g_{a1} + g_{a2}$	(31a)
or		(31b)
$g_a = \sqrt{r_{a1}^2 - r_{b1}^2} + \sqrt{r_{a2}^2 - r_{b2}^2} - \sqrt{a^2 (r_{a2}^2 - r_{b2}^2)}$		

Table E2. Formulas relating to external spur and helical gear pairs

Active length of profile below tooth tip	$l_{\alpha} = g_{\alpha} \left(\tan \alpha_a - \frac{g_a}{d_b} \right)$	(32)
Addendum contact ratio of pinion	$\varepsilon_1 = \frac{z_1}{2 \times \pi} (\tan \alpha_{a1} - \tan \alpha_t')$	(33)
Addendum contact ratio of gear	$\varepsilon_2 = \frac{z_2}{2 \times \pi} (\tan \alpha_{a2} - \tan \alpha_t')$	(34)
Transverse contact ratio	$\varepsilon_a = \varepsilon_1 + \varepsilon_2 \quad \text{or} \quad \varepsilon_a = \frac{g_a}{p_{bt}}$	(34)
Total contact ratio	$\varepsilon_{\gamma} = \varepsilon_a + \varepsilon_{\beta}$	(35)
Helix angle on pitch cylinder	$\tan \beta' = \frac{d'}{d} \times \tan \beta$	(36)
Circumferential backlash	$j_t = \frac{j_n}{\cos \alpha_t' \times \cos \beta_b}$	(37)
Radial backlash	$j_r = \frac{j_n}{2 \times \sin \alpha_t' \times \cos \beta_b}$	(38)
Sum of base tangent lengths	$W_{k1} + W_{k2} = (z_1 + z_2) \times m \times \cos \alpha \left(\text{inv} \alpha_t' + \frac{\pi}{z_1 + z_2} \right) + (k_1 + k_2 - 2) \times p_b$	(39)
Contact parameter of pinion	$k_E = \frac{u+1}{u} \left(1 - \frac{\tan \beta_t'}{\tan \alpha_{a1}} \right)$	(40)
Contact parameter of gear	$k_A = u+1 \left(1 - \frac{\tan \alpha_t'}{\tan \alpha_{a2}} \right)$	(41)

Appendix F, TOOTH THICKNESS and MEASUREMENTS

Determination of base tooth thickness, tools, and measurements for d_b , β_b and s_b

This is an indirect measure of the tooth thickness.

General definition of the base tangent line:

The distance between two parallel planes tangential to two opposite tooth flanks, e.g. left and right tooth flank. The property of the involute, the points of intersection of tangent to the base circle with a right and left hand involute flank. That makes the use of the property of involute; points of intersection of tangent to the base circle with both (right/left) involute flanks are equidistance to the position of the tangent. (see Figure F1)

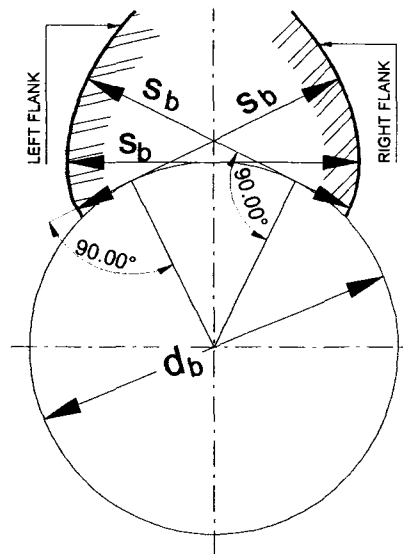


Figure F1. Equidistant base thickness involute tooth

In case of the opposed involutes forming a tooth, this constant distance is transverse base tooth thickness s_b and is equal to the length of arc between origins of involutes on the base circle. (Figure F1).

The parallel planes tangential to the tooth flanks, (left and right) are at angle β_b to the axis of the gear and the distance between them is s_b . Practically the measurement is over tooth flanks spanning a number of teeth k instead of the single tooth.

Note: The number of k depends on the tooth geometry:

- pressure angle;
- number of teeth; and
- addendum modification coefficient.

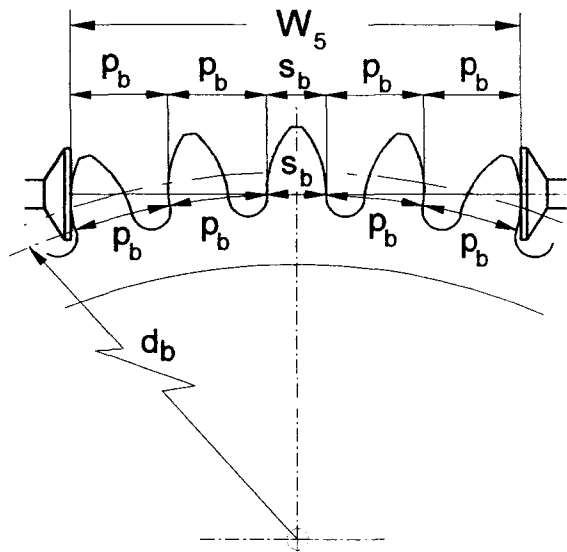


Figure F2. Base tangent length W_5 on a spur gear

The tooth thickness measured along the arc of the base cylinder on spur or helical gears, could be calculated as follow:

$$s_n = m * \left(\frac{\pi}{2} + 2 * x * \tan \alpha \right) \quad \text{F1.}$$

The tooth base thickness measured along the arc of the base cylinder is expressed by equations:

$$\text{For spur gears} \quad s_b = z * m * \cos \alpha \left(\frac{s_n}{z * n} + \text{inv} \alpha \right) \quad \text{F2}$$

$$\text{For helical gears} \quad s_{bn} = z * m * \cos \alpha \left(\frac{s_n}{z * n} + \text{inv} \alpha_t \right) \quad \text{F3.}$$

The theoretical base tangent length - without taking into account any tolerances - for gears without backlash is:

$$\text{For spur gears} \quad W_k = s_b + (k - 1) * p_b \quad \text{F4.}$$

$$\text{For helical gears} \quad W_k = s_{bn} + (k - 1) * p_b \quad \text{F5.}$$

Combined formula for base tangent length W_k as follows:

$$W_k = m \left[(k - 0.5) \pi * \cos \alpha + z * \text{inv} \alpha_t * \cos \alpha + 2 * x * \sin \alpha \right] \quad \text{F6.}$$

The number teeth k it calculates from following equations:

$$k = \frac{s_x - W_1}{\pi * m * \cos \alpha} + 1 \quad \text{F7}$$

Value of k must be rounded to the nearest whole number

Where:

$$s_x = \frac{d_b * \tan \alpha_x}{\cos \beta_b} \quad \text{F8.}$$

$$\cos \alpha_x = \frac{d_b}{d_a - 2 * m} \quad \text{F9.}$$

$$W_1 = m \left(\frac{\pi}{2} * \cos \alpha + \text{inv} \alpha, * \cos \alpha * z * 2 * x * \sin \alpha \right) \quad \text{F10}$$

Note, all the above equations apply to external spur and helical gears and also to the tooth space profile of internal spur and helical gears.

Appendix G; CALCULATIONS

Nomenclature as per AGMA 1012-F90 and 6123-AB8

BASE GEOMETRY of SUN GEAR $z_{S1} = 17$

Given	$z_{S1} = 17$	$p = 24 \cdot \text{in}^{-1}$	
Pitch diameter;	$D_{s1} := \frac{z_{S1}}{p}$		$D_{s1} = 17.992 \text{ mm}$
Number of teeth;	$z_{S1} := D_{s1} \cdot p$		$z_{S1} = 17$
Circular tooth thk.;	$t_{s1} := \frac{\pi}{2 \cdot p}$		$t_{s1} = 1.662 \text{ mm}$
Clearance min, basic;	$c := \frac{0.2000}{p} + 0.051 \cdot \text{mm}$		$c = 0.263 \text{ mm}$
Whole depth, min (basic);	$h_t := \frac{2.200}{p} + 0.051 \cdot \text{mm}$		$h_t = 2.3793 \text{ mm}$
Pressure angle;			$\phi := 25 \cdot \text{deg}$
Addendum, basic;	$a := \frac{1.000}{p}$		$a = 1.058 \text{ mm}$
Dedendum, min(basic);	$b := \frac{1.00}{p} + 0.051 \cdot \text{mm}$		$b = 1.109 \text{ mm}$
Working depth;	$h_k := \frac{2.000}{p}$		$h_k = 2.117 \text{ mm}$
Outside diameter;	$D_{os1} := D_{s1} + 2 \cdot a$		$D_{os1} = 20.1083 \text{ mm}$
Root diameter;	$D_{Rs1} := D_{os1} - 2 \cdot h_t$		$D_{Rs1} = 15.350 \text{ mm}$
Basic circle diameter;	$D_{bs1} := D_{s1} \cdot \cos(\phi)$		$D_{bs1} = 16.306 \text{ mm}$
Circular pitch;	$p_1 := \frac{\pi \cdot D_{s1}}{z_{S1}}$		$p_1 = 3.325 \text{ mm}$
Base pitch	$P_{bs1} := p_1 \cdot \cos(\phi)$		$P_{bs1} = 3.013 \text{ mm}$

CTM Planet geometry

Nomenclature as per AGMA 1012-F90 and 6123-A88

BASE GEOMETRY of PLANET GEAR $z_p = 19$

Given $z_{p1} = 19$ $p = 24 \cdot \text{in}^{-1}$

Pitch diameter; $D_{p1} := \frac{z_{p1}}{p}$ $D_{p1} = 20.108 \text{ mm}$

Number of teeth; $z_{p1} := D_{p1} \cdot p$ $z_{p1} = 19$

Circular tooth thk.; $t_{p1} := \frac{\pi}{2 \cdot p}$ $t_{p1} = 1.662 \text{ mm}$

Clearance min, basic; $c := \frac{0.2000}{p} + 0.051 \cdot \text{mm}$ $c = 0.263 \text{ mm}$

Whole depth, min (basic); $h_t := \frac{2.200}{p} + 0.051 \cdot \text{mm}$ $h_t = 2.3793 \text{ mm}$

Pressure angle; $\phi := 25 \cdot \text{deg}$

Addendum, basic; $a := \frac{1.000}{p}$ $a = 1.058 \text{ mm}$

Dedendum, min(basic); $b := \frac{1.00}{p} + 0.051 \cdot \text{mm}$ $b = 1.109 \text{ mm}$

Working depth; $h_k := \frac{2.000}{p}$ $h_k = 2.117 \text{ mm}$

Outside diameter; $D_{op1} := D_{p1} + 2 \cdot a$ $D_{op1} = 22.225 \text{ mm}$

Root diameter; $D_{Rp1} := D_{op1} - 2 \cdot h_t$ $D_{Rp1} = 17.466 \text{ mm}$

Basic circle diameter; $D_{bp1} := D_{p1} \cdot \cos(\phi)$ $D_{bp1} = 18.2243 \text{ mm}$

Circular pitch; $p_1 := \frac{\pi \cdot D_{p1}}{z_{p1}}$ $p_1 = 3.325 \text{ mm}$

Base pitch $p_{bs1} := p_1 \cdot \cos(\phi)$ $p_{bs1} = 3.013 \text{ mm}$

CTM Ring geometry

Nomenclature as per AGMA 1012-F90 and 6123-A88

BASE GEOMETRY of RING GEAR $z_R = 55$

Given	$z_R = 55$	$p := 24 \cdot \text{in}^{-1}$	
Pitch diameter;	$D_R := \frac{z_R}{p}$		$D_R = 58.208 \text{ mm}$
Number of teeth;	$z_R := D_R \cdot p$		$z_R = 55$
Circular tooth thk.;	$t_R := \frac{\pi}{2 \cdot p}$		$t_R = 1.662 \text{ mm}$
Clearance min, basic;	$c := \frac{0.2000}{p} + 0.051 \cdot \text{mm}$		$c = 0.263 \text{ mm}$
Whole depth, min (basic);	$h_t := \frac{2.200}{p} + 0.051 \cdot \text{mm}$		$h_t = 2.3793 \text{ mm}$
Pressure angle;			$\phi := 25 \cdot \text{deg}$
Addendum, basic;	$a := \frac{1.000}{p}$		$a = 1.058 \text{ mm}$
Dedendum, min(basic);	$b := \frac{1.00}{p} + 0.051 \cdot \text{mm}$		$b = 1.109 \text{ mm}$
Working depth;	$h_k := \frac{2.000}{p}$		$h_k = 2.117 \text{ mm}$
Inside diameter;	$D_{oR} := D_R - 2 \cdot a$		$D_{oR} = 56.0917 \text{ mm}$
Root diameter;	$D_{RR} := D_{oR} + 2 \cdot h_t$		$D_{RR} = 60.850 \text{ mm}$
Basic circle diameter;	$D_{bR} := D_R \cdot \cos(\phi)$		$D_{bR} = 52.7547 \text{ mm}$
Circular pitch;	$p_1 := \frac{\pi \cdot D_R}{z_R}$		$p_1 = 3.325 \text{ mm}$
Base pitch	$p_{bs} := p_1 \cdot \cos(\phi)$		$p_{bs} = 3.013 \text{ mm}$

CTM - Sun gear and planet $N_s = 17$ & $N_p = 19$, Contact Ratio

Given $p := 24 \cdot \text{in}^{-1}$ $z_s := 17$ $z_p := 19$ $z_R := 55$

1. Number of teeth;	$z_s = 17$	$m := 1.0583$	$z_p = 19$	
2. Pitch diameter;	$D_s := \frac{z_s}{p}$	$D_s = 17.992 \text{ mm}$	$D_p := \frac{z_p}{p}$	$D_p = 20.108 \text{ mm}$
3. Addendum, (basic);	$a_s := \frac{1.00}{p}$	$a_s = 1.058 \text{ mm}$	$a_p := \frac{1.00}{p}$	$a_p = 1.058 \text{ mm}$
4. Outside diameter, [2/(2x3)]	$D_{os} := D_s + 2 \cdot a_s$	$D_{os} = 20.108 \text{ mm}$	$D_{op} := D_p + 2 \cdot a_p$	$D_{op} = 0.022 \text{ m}$
5. Pressure angle, transverse;	$\phi := 25 \cdot \text{deg}$			
6. Base diameter, cos(5)x(2)	$D_{bs} := \cos(\phi) \cdot D_s$	$D_{bs} = 16.306 \text{ mm}$	$D_{bp} := \cos(\phi) \cdot D_p$	$D_{bp} = 18.2243 \text{ mm}$
7. Gear ratio	$r := \frac{z_p}{z_s}$	$r = 1.11765$		
8. Inverse ratio 1.0/7	$r_{inv} := \frac{1}{r}$	$r_{inv} = 0.895$		
9. Arccos [6/4]	$A_{rs} := \arccos\left(\frac{D_{bs}}{D_{os}}\right)$	$A_{rs} = 0.625$	$A_{rp} := \arccos\left(\frac{D_{bp}}{D_{op}}\right)$	$A_{rp} = 0.609$
10. O.D. roll, tan (9)x rad	$OD_s := \tan(A_{rs}) \cdot 57.29578$	$OD_s = 41.346$	$OD_p := \tan(A_{rp}) \cdot 57.29578$	$OD_p = 39.994$
11. P.D. roll tan (5)x rad	$PD := \tan(\phi) \cdot (57.29578)$	$PD = 26.717$		
12. Addendum roll, [10 - 11]	$A_{rbs} := OD_s - PD$	$A_{rbs} = 14.629$	$A_{rpb} := OD_p - PD$	$A_{rpb} = 13.276$
13. Sun gear roll [12s + (12px7)]	$A_s := A_{rbs} + (A_{rpb} \cdot r)$	$A_s = 29.467$		
14. Gear Roll [12p+(12sx8)]	$A_p := A_{rpb} + (A_{rbs} \cdot r_{inv})$	$A_p = 26.365$		
15. L.D. Roll sun [10-13]	$Ld_s := OD_s - A_s$	$Ld_s = 11.879$		
16. L.D. Roll plant. [10-14]	$Ld_p := OD_p - A_p$	$Ld_p = 13.628$		

17. Arctan[15/rad]	$A_{atgs} := \text{atan}\left(\frac{Ld_{ts}}{57.29578}\right)$	$A_{atgs} = 0.204$	
18. L.D. sun [6/cos(17)]	$Ld_s := \frac{D_{bs}}{\cos(A_{atgs})}$	$Ld_s = 16.653 \text{ mm}$	
19. Arctan[16/rad]	$A_{atgp} := \text{atan}\left(\frac{Ld_p}{57.29578}\right)$	$A_{atgp} = 0.234$	
20. L.D. planet [6/cos(19)]	$Ld_p := \frac{D_{bp}}{\cos(A_{atgp})}$	$Ld_p = 18.733 \text{ mm}$	
21. Circular pitch $\pi \times (2/1)$	$Cp_s := \pi \cdot \frac{D_s}{z_s}$	$Cp_s = 3.325 \text{ mm}$	$Cp_p := \pi \cdot \frac{D_p}{z_p}$ $Cp_p = 3.325 \text{ mm}$
22. Extra involute, [0.016x21]	$I_{ex} := 0.00016 \cdot Cp_s$	$I_{ex} = 0.001 \text{ mm}$	$I_{exp} := 0.00016 \cdot Cp_p$ $I_{exp} = 0.001 \text{ mm}$
23. Form Diameter sun [18 - 22]	$Fd_s := Ld_s - I_{ex}$	$Fd_s = 16.652 \text{ mm}$	
24. Arccos sun [6 /23]	$A_{coss} := \text{acos}\left(\frac{D_{bs}}{Fd_s}\right)$	$A_{coss} = 0.204$	
25. F.D. Roll sun = tan(24)x rad	$Fd_{rs} := \tan(A_{coss}) \cdot 57.29578$	$Fd_{rs} = 11.870$	
26. Form Dia. planet , [20 - 22]	$Fd_p := Ld_p - I_{ex}$	$Fd_p = 18.732 \text{ mm}$	
27. Arccos planet [6/26]	$A_{cosp} := \text{acos}\left(\frac{D_{bp}}{Fd_p}\right)$	$A_{cosp} = 0.233$	
28. F.D. Roll planet = tan(27)x rad	$Fd_{rp1} := \tan(A_{cosp}) \cdot 57.29578$	$Fd_{rp1} = 13.621$	
29. Roll per tooth, [360 / (1)]	$R_{ts} := \frac{360}{z_s}$ $R_{ts} = 21.176$	$R_{tp} := \frac{360}{z_p}$ $R_{tp} = 18.947$	
30. Contact ratio S/P [13 / 29]	$e_{sp} := \frac{A_s}{R_{ts}}$ $e_{sp} = 1.392$		

CTM - Gear Ring and planet $N_r = 55$ & $N_p = 19$, Contact Ratio

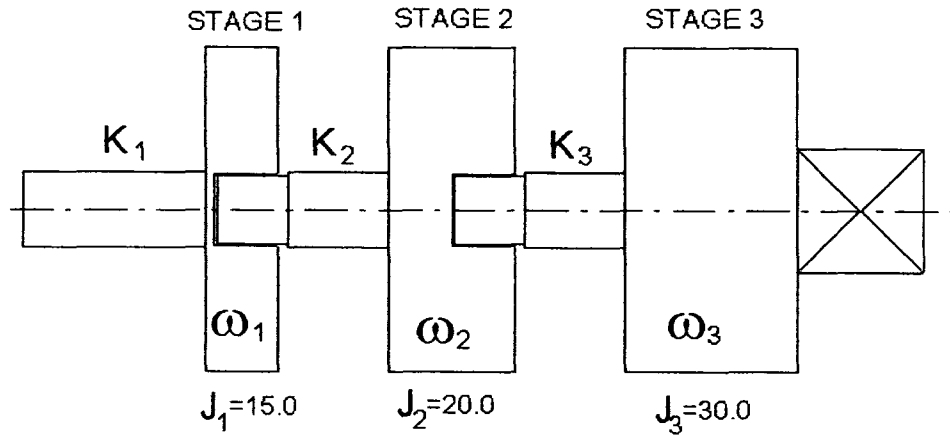
Given $p = 24 \cdot \text{in}^{-1}$ $z_s = 17$ $z_p = 19$ $z_R = 55$

1. Number of teeth;	$z_R = 55$	$m := 1.0583333$	$z_R = 55$	
2. Pitch diameter;	$D_R := \frac{z_R}{p}$	$D_R = 58.208 \text{ mm}$	$D_p := \frac{z_p}{p}$	$D_p = 20.108 \text{ mm}$
3. Addendum, (<i>basic</i>);	$a_t := \frac{1.00}{p}$	$a_t = 1.058 \text{ mm}$	$a_p := \frac{1.00}{p}$	$a_p = 1.058 \text{ mm}$
4. Outside diameter; [2/(2x3)]	$D_{oR} := D_R + 2 \cdot a_t$	$D_{oR} = 60.325 \text{ mm}$	$D_{op} := D_p + 2 \cdot a_p$	$D_{op} = 22.225 \text{ mm}$
5. Pressure angle, transverse;	$\phi := 25 \cdot \text{deg}$			
6. Base diameter, cos(5)x(2)	$D_{bR} := \cos(\phi) \cdot D_R$	$D_{bR} = 52.755 \text{ mm}$	$D_{bp} := \cos(\phi) \cdot D_p$	$D_{bp} = 18.224 \text{ mm}$
7. Gear ratio	$r := \frac{z_p}{z_R}$	$r = 0.34545$		
8. Inverse ratio 1.0/7	$r_{inv} := \frac{1}{r}$	$r_{inv} = 2.89474$		
9. Arccos [6/4]	$A_{rR} := \arccos\left(\frac{D_{bR}}{D_{oR}}\right)$	$A_{rR} = 0.50638$	$A_{rp} := \arccos\left(\frac{D_{bp}}{D_{op}}\right)$	$A_{rp} = 0.6094$
10. O.D. roll, tan (9)x rad	$OD_r := \tan(A_{rR}) \cdot 57.29578$	$OD_r = 31.7769$	$OD_p := \tan(A_{rp}) \cdot 57.29578$	$OD_p = 39.99378$
11. P.D. roll tan (5)x rad	$PD := \tan(\phi) \cdot (57.29578)$	$PD = 26.71746$		
12. Addendum roll, [10 - 11]	$A_{rx} := OD_r - PD$	$A_{rx} = 5.059$	$A_{rxp} := OD_p - PD$	$A_{rxp} = 13.27632$
13. Ring gear roll [12s + (12px7)]	$A_r := A_{rx} + (A_{rxp} \cdot r)$	$A_r = 9.6458$		
14. Ring Gear Roll [12p+(12sx8)]	$A_p := A_{rxp} + (A_{rx} \cdot r_{inv})$	$A_p = 27.922$		
15. L.D. Roll Ring [10-13]	$Ld_r := OD_r - A_r$	$Ld_r = 22.131$		
16. L.D. Roll plant. [10-14]	$Ld_p := OD_p - A_p$	$Ld_p = 12.072$		

17. Arctan[15/rad]	$A_{atR} := \text{atan}\left(\frac{Ld_R}{57.29578}\right)$	$A_{atR} = 0.369$		
18. L.D. Ring Ring [6/cos(17)]	$Ld_R := \frac{D_{bR}}{\cos(A_{atR})}$	$Ld_R = 0.053 \text{ mm}$		
19. Arctan[16/rad]	$A_{atp} := \text{atan}\left(\frac{Ld_p}{57.29578}\right)$	$A_{atp} = 0.20765$		
20. L.D. planet [6/cos(19)]	$Ld_p := \frac{D_{bp}}{\cos(A_{atp})}$	$Ld_p = 18.624 \text{ mm}$		
21. Circular pitch $\pi \times (2/1)$	$CpR := \pi \cdot \frac{D_R}{z_R}$	$CpR = 3.325 \text{ mm}$	$Cp_p := \pi \cdot \frac{D_p}{z_p}$	$Cp_p = 3.325 \text{ mm}$
22. Extra involute, [0.016x21]	$I_{ex} := 0.00016 \cdot CpR$	$I_{ex} = 0.001 \text{ mm}$	$I_{exp} := 0.00016 \cdot Cp_p$	$I_{exp} = 0.001 \text{ mm}$
23. Form Diameter Ring [18 - 22]	$Fd_R := Ld_R - I_{ex}$	$Fd_R = 56.553 \text{ mm}$		$Fd_R = 56.553 \text{ mm}$
24. Arccos Ring [6 /23]	$A_{cosR} := \text{acos}\left(\frac{D_{bR}}{Fd_R}\right)$	$A_{cosR} = 0.369$		
25. F.D. Roll Ring = tan(24)x rad	$Fd_{tR} := \tan(A_{cosR}) \cdot 57.29578$	$Fd_{tR} = 22.129$		
26. Form Dia. planet , [20 - 22]	$Fd_p := Ld_p - I_{exp}$	$Fd_p = 18.624 \text{ mm}$		$Fd_p = 18.624 \text{ mm}$
27. Arccos planet [6/26]	$A_{cosp} := \text{acos}\left(\frac{D_{bp}}{Fd_p}\right)$	$A_{cosp} = 0.208$		
28. F.D. Roll planet = tan(27)x rad	$Fd_{tp} := \tan(A_{cosp}) \cdot 57.29578$	$Fd_{tp} = 12.0636$		
29. Roll per tooth, [360 / (1)]	$R_{tr} := \frac{360}{z_R}$	$R_{tr} = 6.545$	$R_{tp} := \frac{360}{z_p}$	$R_{tp} = 18.947$
30. Contact ratio S/P [13 / 29]	$e_{SP} := \frac{A_r}{R_{tr}}$	$e_{SP} = 1.47366$		$e_{SP} = 1.474$

CRITICAL SPEEDS by HOLZER METHOD

The torsional-frequency curve and establishes the first lateral critical speed by applying the Holzer method for sun gears input from 1 to 3 .



Number of stages along the planetary gear set: stage = 3

Rotational axis in case of planetary gears are fixed; fixed = 0

Stiffness and moment: a := if[fixed = 1, stage, (stage - 1)] n := 1.. a j := 1.. stage

Boundary conditions: k := 0.. points i := 1.. (stage - 2)

Frequency: $\omega_k = \omega_{min} + k \cdot \frac{\omega_{max} - \omega_{min}}{points}$ $\lambda_k = (\omega_k)^2$

Material properties and sun gears stiffnesses:

Frequency range and number of points to be plotted:

Stiffnesses of subsections of the torsional system:

Moments of inertia of sun gears:

points = 400

$$\omega_{max} = 185 \cdot \frac{rad}{sec}$$

$$\omega_{min} = 1.65 \cdot \frac{rad}{sec}$$

$K_j :=$

$1 \cdot 10^6 \cdot \frac{gm \cdot mm}{rad}$
$2 \cdot 10^6 \cdot \frac{gm \cdot mm}{rad}$
$3 \cdot 10^6 \cdot \frac{gm \cdot mm}{rad}$

$J_n :=$

$85 \cdot gm \cdot mm \cdot sec^2$
$115 \cdot gm \cdot mm \cdot sec^2$
$185 \cdot gm \cdot mm \cdot sec^2$

Boundary conditions:

$$\begin{pmatrix} P_{1,k} \\ \theta_{1,k} \\ Trd_{1,k} \end{pmatrix} = \begin{pmatrix} 1 \\ 1 \\ -\lambda_k \cdot J_1 \end{pmatrix}$$

Torque equations:

$$\begin{pmatrix} P_{i+1,k} \\ \Theta_{i+1,k} \\ \text{Trq}_{i+1,k} \end{pmatrix} := \begin{pmatrix} i+1 \\ \Theta_{i,k} + \frac{\text{Trq}_{i,k}}{K_{P_{i,k+1}}} \\ \text{Trq}_{i,k} - \lambda_k \cdot J_{(P_{i,k})+1} \left(\Theta_{i,k} + \frac{\text{Trq}_{i,k}}{K_{P_{i,k+1}}} \right) \end{pmatrix}$$

$$\Theta_{\text{stage},k} := \Theta_{(\text{stage}-1),k} + \frac{\text{Trq}_{(\text{stage}-1),k}}{K_{\text{stage}}}$$

$$\text{null} := 0 \cdot \text{gm} \cdot \text{mm}$$

$$\text{Trq}_{\text{stage},k} := \text{if}[\text{fixed} = 1, \text{Trq}_{(\text{stage}-1),k} - \lambda_k \cdot J_a \cdot \Theta_{\text{stage},k}, \text{null}]$$

Cubic spline interpolation:

$$\text{freq}_k := \omega_k$$

$$\text{Trq1}_k := \text{if} \left(\text{fixed} = 0, \Theta_{\text{stage},k}, \frac{-\text{Trq}_{\text{stage},k}}{10^6 \cdot \text{lb} \cdot \text{in}} \right)$$

$$\text{derivative} := \text{cspline}(\text{freq}, \text{Trq1})$$

$$\text{Torsional_curve}_k := \text{interp}(\text{derivative}, \text{freq}, \text{Trq1}, \omega_k)$$

$$\text{aux}_0 := 0$$

$$d := 0..(\text{points} - 1)$$

$$\text{Trq2}_d := \text{Trq1}_{d+1}$$

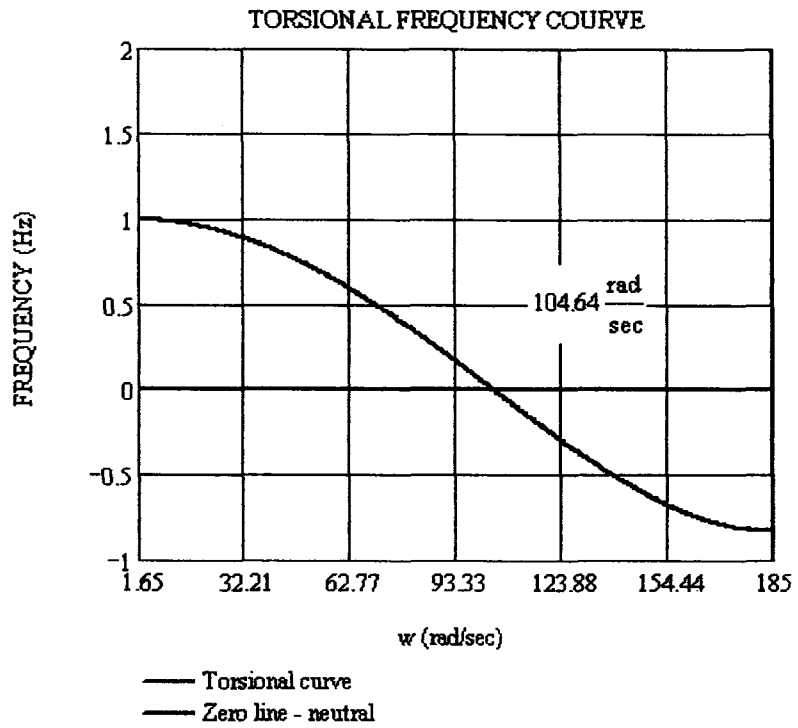
$$\text{aux}_{d+1} := \text{if}[(\text{Trq1}_d \cdot \text{Trq2}_d) < 0, \text{if}[(\text{aux}_d = 0), (d + 1), \text{aux}_d], \text{aux}_d]$$

$$\text{index} := \text{aux}_{\text{points}}$$

Linear interpolation and calculate first natural frequency:

$$\omega_{\text{nat1}} := \omega_{\text{index}-1} + \frac{\text{Trq1}_{\text{index}-1}}{\text{Trq1}_{\text{index}} - \text{Trq1}_{\text{index}-1}} \cdot (\omega_{\text{index}-1} - \omega_{\text{index}})$$

The critical speeds of the system correspond to those frequencies which result zero in the torsional-frequency curve.

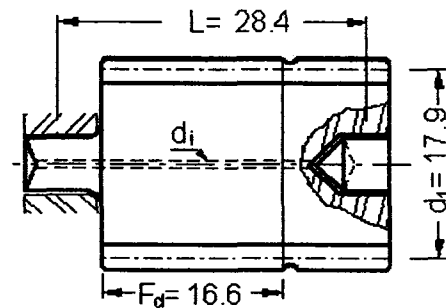


The first natural frequency of the system in this frequency range is: $\omega_{nat1} = 104.64 \frac{\text{rad}}{\text{sec}}$

CTM -Torsional and bending deformation last sun gear

Given

$$\begin{aligned}
 z_p &:= 19 & n_{out} &:= 98.7 \text{rpm} & p &:= 24 \text{in}^{-1} \\
 F_d &:= 16.6 \text{mm} & L &:= 28.4 \text{mm} & \text{rpm} &:= \text{min}^{-1} \\
 \phi &:= 25 \text{deg} & i_o &:= 4.235^3 & \mu\text{m} &:= 1 \cdot 10^{-6} \cdot \text{m} \\
 \eta_o &:= 0.985^3 & C &:= 19.05 \text{mm} & d_o &:= 0.01 \text{mm} \\
 z_s &:= 17 & T_{in} &:= 15.0 \text{N}\cdot\text{m} & T_o &:= i_o \cdot \eta_o \cdot T_{in}
 \end{aligned}$$



$$T_o = 1.089 \times 10^3 \text{ N}\cdot\text{m} \quad \text{or } 1 \mu\text{m} = 1/1000 \text{mm}$$

Modulus of elasticity for VascoMax C-350 MPa $E = 2670 \text{MPa}$

Poisson ratio $\nu = 0.3$

Gear ratio $u = 0.895$

Pitch diameter of sun gear $d_1 = \frac{2 \cdot C}{u + 1}$

Pitch diameter of planet gear $d_2 = \frac{2 \cdot u \cdot C}{u + 1}$

Pitch line velocity $v_1 = \frac{d_1 \cdot \pi \cdot n_{out}}{60 \cdot 1000}$

Tangential force on pitch circle $W_{t3} = 2000 \cdot \frac{T_o}{d_1}$

Specific tooth load on pitch circle $w = \frac{W_{t3}}{L}$

For hollow gears required to use of coefficient $e = \frac{1}{1 - \frac{d_o}{d_1}}$

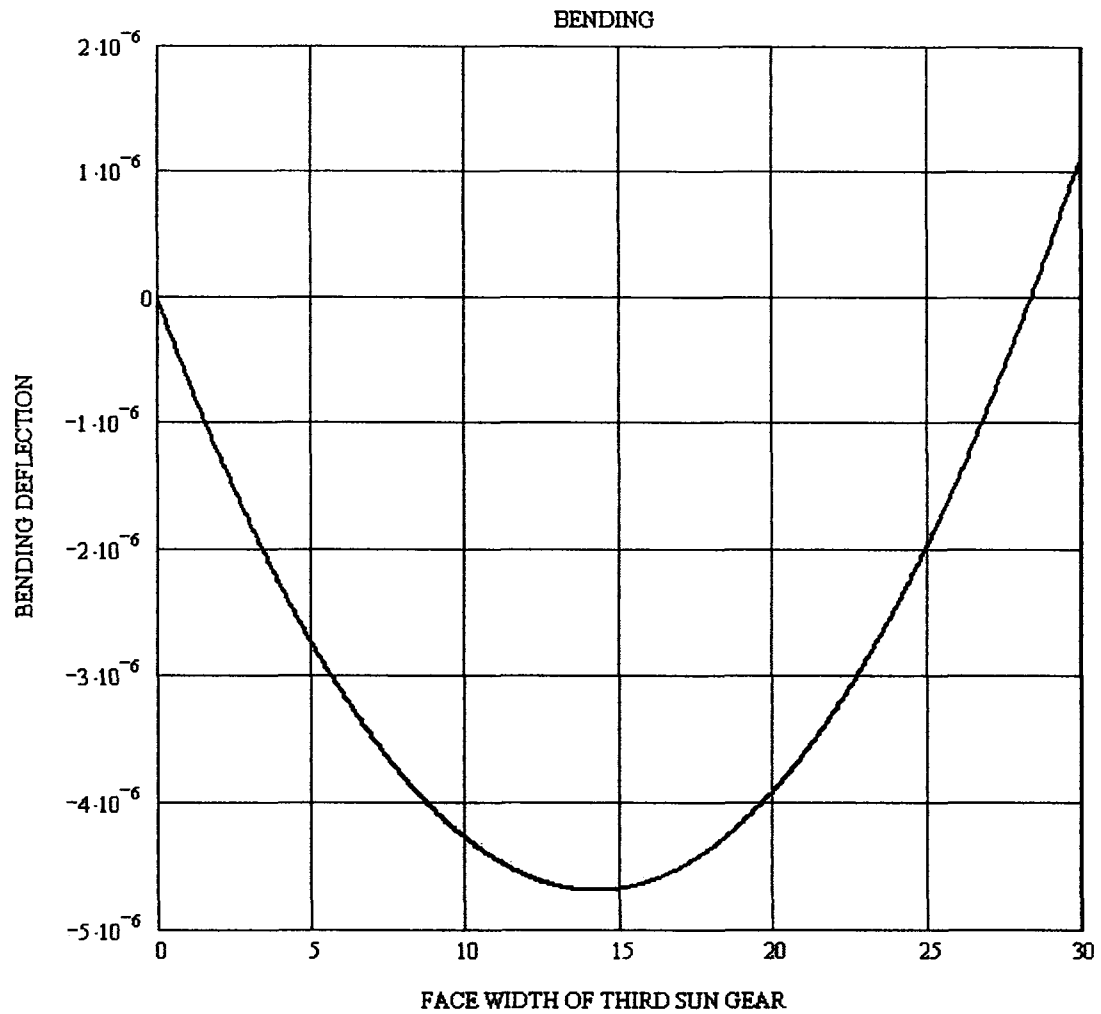
Width/pitch diameter ratio $\kappa = \frac{L}{d_1}$

Bearing distance ratio $\eta = \frac{F_d}{L}$

Modulus of rigidity $G = \frac{E}{2 \cdot (1 + \nu)} \quad G = 1026.9 \text{MPa}$

Bending effect f_b over inter length l ; $l := 0.0\text{-mm}, 05\text{-mm}.. 30\text{-mm}$

$$f_b(l) := \left[\frac{w \cdot 2000 \cdot \left(\eta - \frac{7}{12} \right) \cdot \kappa^4}{\cos(\phi) \cdot E \cdot \pi} \left[1 - \left(\frac{\frac{L}{2} - l}{\frac{L}{2}} \right)^2 \right] \right] \cdot e$$

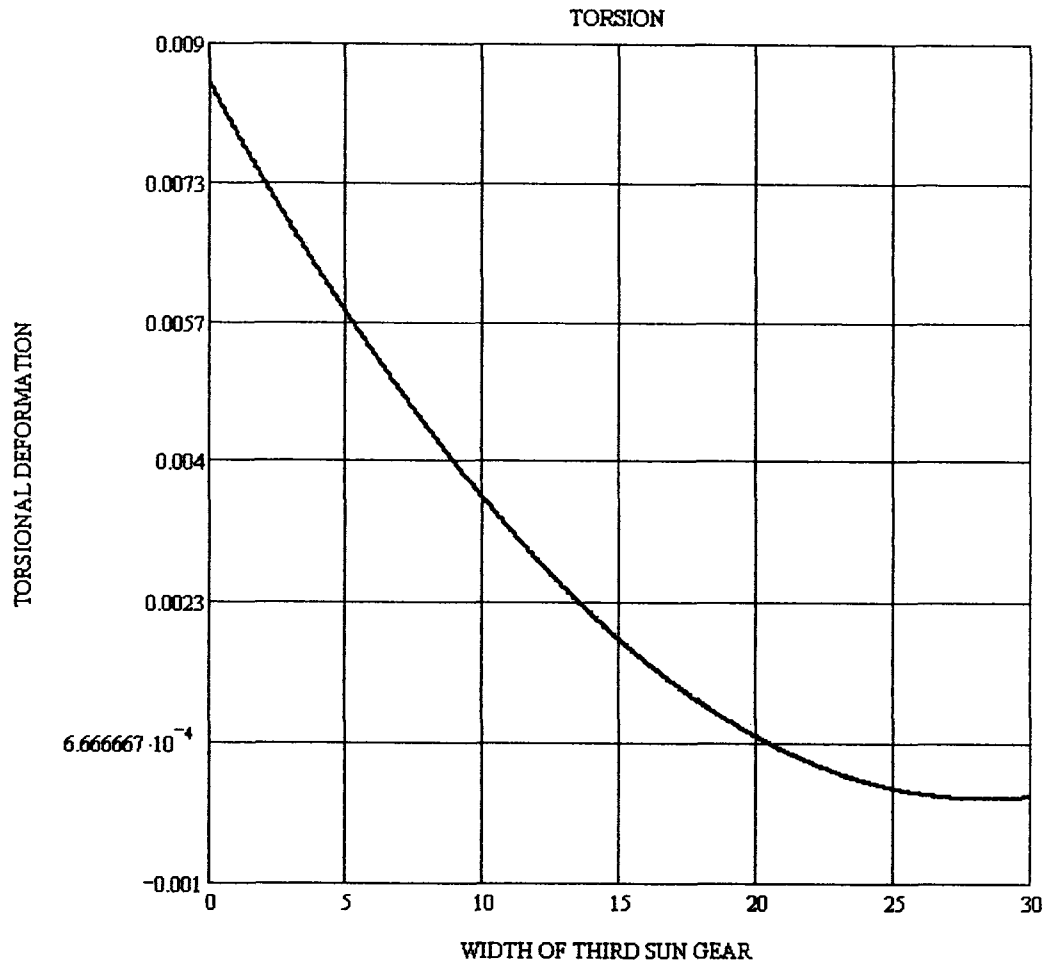


Maximum bending deformation @ 8.0 mm

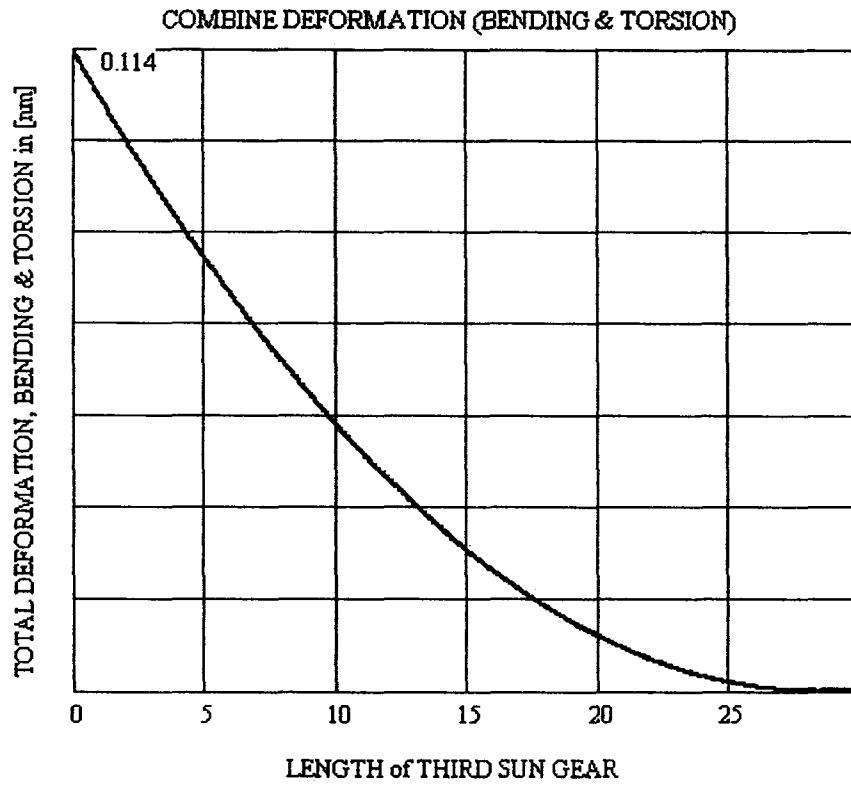
$$f_b := -6.263 \times 10^{-8} \mu\text{m}$$

Torsional effect f_t :

$$f_t(D) = \frac{w \cdot \cos(\phi) \cdot 1000 \cdot \kappa^2}{G \cdot \pi} \left[4 \left(\frac{L-1}{L} \right) - \left[1 - \left(\frac{\frac{L}{2}-1}{\frac{L}{2}} \right)^2 \right] \right] \cdot \varepsilon$$



Maximum Torsional deformation @ 0.0 mm $f_t = 1.13 \times 10^{-4} \mu\text{m}$



Deflection and torsional affect at maximum width of 3rd sun gear F; $\Delta_{\max} = 0.114\text{mm}$

Maximum allow clearance $c = \frac{0.2000}{p} + 0.051 \cdot \text{mm}$ $c = 0.263 \text{mm}$

CTM - STAGE ANALYSIS

Preliminary consideration

Outside diameter maximum	$D_o = 70\text{mm}$
Torque input minimum	$T_{in} = 15.0\text{ Nm}$
Input shaft speed	$n_{in} = 7500\text{ r/min}$
Output shaft speed minimum	$n_{out} = 100\text{ r/min}$

Efficiency spur gears	$\eta_g = 0.985$	$\eta_g := 0.985$
Coefficient of friction - needle bearings, (SKF data)	$\mu_n = 0.9995$	$\mu_n := 0.9995$
Coefficient of friction - ball bearings, (SKF data)	$\mu_b = 0.9999$	$\mu_b := 0.9999$
Frictional moment of needle bearings	$M_n = \text{Nm}$	
Frictional moment of ball bearings	$M_b = \text{Nm}$	

$$p := 24 \cdot \text{in}^{-1}$$

$$\text{rpm} := \text{min}^{-1}$$

Input data

Torque generating from air motor	$T_{in} = 15\text{Nm}$	$T_{in} := 15 \cdot \text{N} \cdot \text{m}$
Input shaft speed	$n_{in} = 7500\text{r/min}$	$n_{in} := 7500\text{rpm}$
Number of teeth of gear ring	$z_R = 55$	$z_R := 55$
Number of teeth of sun gear	$z_s = 17$	$z_{s1} := 17$
Number of teeth of planet	$z_p = 19$	$z_s := 17$ $z_{p1} := 19$
Number of planets	$z_{CP} = 2$	$z_p := 19$ $z_{s2} := 17$
		$z_{CP} := 3$ $z_{p2} := 19$

ASSEMBLY REQUIREMENTS

1. Assembly ; $\frac{z_R + z_s}{z_{CP}} = T$

Resultant must be integer $\frac{z_R + z_{s1}}{z_{CP}} = 24$ $\frac{z_R + z_{s2}}{z_{CP}} = 24$ $\frac{z_R + z_s}{z_{CP}} = 24$

2. Parallelism; $a_{SP} = -a_{PR}$

Distance between center line of sun-planet and planet-gear ring must be equal

Pitch Diameters; $D_{s1} := \frac{z_{s1}}{p}$ $D_{p1} := \frac{z_{p1}}{p}$ $D_{p2} := \frac{z_{p2}}{p}$ $D_{s2} := \frac{z_{s2}}{p}$ $D_p := \frac{z_p}{p}$ $D_s := \frac{z_s}{p}$

Arms;

1 st STAGE	$a_{SP1} := \frac{D_{s1} + D_{p1}}{2}$	$a_{SP1} = 19.05 \text{ mm}$	$a_{PR1} := \frac{\frac{z_R}{p} - D_{p1}}{2}$	$a_{PR1} = 19.05 \text{ mm}$
2 nd STAGE	$a_{SP2} := \frac{D_{s2} + D_{p2}}{2}$	$a_{SP2} = 19.05 \text{ mm}$	$a_{PR2} := \frac{\frac{z_R}{p} - D_{p2}}{2}$	$a_{PR2} = 19.05 \text{ mm}$
3 rd STAGE	$a_{SP3} := \frac{D_s + D_p}{2}$	$a_{SP3} = 19.05 \text{ mm}$	$a_{PR3} := \frac{\frac{z_R}{p} - D_p}{2}$	$a_{PR3} = 19.05 \text{ mm}$

3. Locat. of planets: $(z_{p1} + z_s) \cdot \sin\left(\frac{\pi}{z_{CP}}\right) > z_{p1} + 2$

$(z_{p1} + z_{s1}) \cdot \sin\left(\frac{\pi}{z_{CP}}\right) = 31.177$	$(z_{p2} + z_{s1}) \cdot \sin\left(\frac{\pi}{z_{CP}}\right) = 31.177$	
		$31.177 > 21$
$z_{p1} + 2 = 21$	$z_{p2} + 2 = 21$	

$i_{21} := \frac{z_R}{z_{s1}} + 1$ $i_{21} = 4.235$

$\eta_1 = .985$

Torque; $T_{o1} := i_{21} \cdot T_m \cdot \eta_1$ $T_{o1} = 62.576 \text{ N}\cdot\text{m}$

Outs. dia. D_{outs} $D_r := \frac{z_R}{p}$ $D_r = 58.21 \text{ mm}$

Modulus of elasticity MPa $E = 199948 \text{ MPa}$

Stresses on Sun, Planetary and Ring Gear, 1st stage

Torque on 1st stage $T_m := T_{in} \cdot i_{21}$ $T_m = 63.5 \text{ N}\cdot\text{m}$ $P := \frac{T_{in} \cdot \omega_{in}}{9549.3}$ +

Tangential driving force W_t $W_t := 2000 \cdot \frac{T_m}{D_{s1}}$ $W_t = 1667438.6 \text{ N}$ $W_{t1} = T_{in} \cdot \frac{1}{D_s}$

$$Q = \frac{P}{\omega_{in}} \cdot \frac{\left[\left(\frac{z_{p1}}{z_{s1}} \right) + 1 \right]^3}{\frac{z_{p1}}{z_{s1}}}$$

$$K_{sm} = \frac{35550 \cdot Q \cdot \left(\frac{z_{p1}}{z_{s1}} + 1 \right)}{C_1^3}$$

Face width sun gear $F_1 := 31500 \cdot \frac{Q}{C_1^2 \cdot K_{sm}}$ $F_1 = 8 \text{ mm}$

For Sun

Maximum compressive stress S_{c1} $s_{cs1} := \sqrt{\frac{0.70}{\left(\frac{1}{E} + \frac{1}{E} \right) \cdot \cos(\phi) \cdot \sin(\phi)}} \cdot \sqrt{\frac{W_{t1}}{F_1 \cdot D_{s1}} \cdot \frac{\frac{z_{p1}}{z_{s1}} + 1}{\frac{z_{p1}}{z_{s1}}}}$ $s_{cs1} = 1418.6 \text{ MPa}$

Maximum shear stress S_s $s_{ss1} := 0.295 \cdot s_{cs1}$ $s_{ss1} = 418.5 \text{ MPa}$

For Planet

Maximum compressive stress S_c $s_{cp1} := \sqrt{\frac{0.70}{\left(\frac{1}{E} + \frac{1}{E} \right) \cdot \cos(\phi) \cdot \sin(\phi)}} \cdot \sqrt{\frac{W_{t1}}{F_1 \cdot D_{p1}} \cdot \frac{\frac{z_{p1}}{z_{s1}} + 1}{\frac{z_{p1}}{z_{s1}}}}$ $s_{cp1} = 1341.9 \text{ MPa}$

Maximum shear stress S_s $s_{sp1} := 0.295 \cdot s_{cp1}$ $s_{sp1} = 395.9 \text{ MPa}$

For Ring

Maximum compressive stress S_c $s_{cr1} := \sqrt{\frac{0.70}{\left(\frac{1}{E} + \frac{1}{E} \right) \cdot \cos(\phi) \cdot \sin(\phi)}} \cdot \sqrt{\frac{W_{t1}}{F_1 \cdot D_r} \cdot \frac{\frac{z_{p1}}{z_{s1}} + 1}{\frac{z_{p1}}{z_{s1}}}}$ $s_{cr1} = 788.7 \text{ MPa}$

Maximum shear stress S_s $s_{sr1} := 0.295 \cdot s_{cr1}$ $s_{sr1} = 232.7 \text{ MPa}$

Stresses on Sun, Planetary and Ring Gear, 2nd stage

Torque on 1st stage $T_m = T_{in} \cdot i_{21}$ $T_m = 63.5 \text{ N}\cdot\text{m}$ $P := \frac{T_m \cdot n_m}{9549.3}$

Tangential driving force W_t $W_t := 2000 \cdot \frac{T_m}{D_{s1}}$ $W_{t2} := T_m \cdot \frac{1}{D_s}$

$$Q := \frac{P}{n_m} \cdot \frac{\left[\left(\frac{z_{p1}}{z_{s1}} \right) + 1 \right]^3}{\frac{z_{p1}}{z_{s1}}}$$

$$K_{hm} := \frac{13350 \cdot Q \cdot \left(\frac{z_{p1}}{z_{s1}} + 1 \right)}{C_2^3}$$

Face width sun gear $F_2 := 31500 \cdot \frac{Q}{C_2^2 \cdot K_{hm}}$ $F_2 = 21.2 \text{ mm}$

For Sun

Maximum compressive stress S_{c1} $s_{cs1} := \sqrt{\frac{0.70}{\left(\frac{1}{E} + \frac{1}{E} \right) \cdot \cos(\phi) \cdot \sin(\phi)}} \cdot \sqrt{\frac{\frac{z_{p1}}{z_{s1}} + 1}{F_2 \cdot D_{s1} \cdot \frac{z_{p1}}{z_{s1}}}} \cdot W_{t2}$ $s_{cs1} = 1789.1 \text{ MPa}$

Maximum shear stress S_s $s_{ss1} := 0.295 \cdot s_{cs1}$ $s_{ss1} = 527.8 \text{ MPa}$

For Planet

Maximum compressive stress S_c $s_{cp1} := \sqrt{\frac{0.70}{\left(\frac{1}{E} + \frac{1}{E} \right) \cdot \cos(\phi) \cdot \sin(\phi)}} \cdot \sqrt{\frac{\frac{z_{p1}}{z_{s1}} + 1}{F_2 \cdot D_{p1} \cdot \frac{z_{p1}}{z_{s1}}}} \cdot W_{t2}$ $s_{cp1} = 1692.3 \text{ MPa}$

Maximum shear stress S_s $s_{sp1} := 0.295 \cdot s_{cp1}$ $s_{sp1} = 499.2 \text{ MPa}$

For Ring

Maximum compressive stress S_c $s_{cr1} := \sqrt{\frac{0.70}{\left(\frac{1}{E} + \frac{1}{E} \right) \cdot \cos(\phi) \cdot \sin(\phi)}} \cdot \sqrt{\frac{\frac{z_{p1}}{z_{s1}} + 1}{F_2 \cdot D_r \cdot \frac{z_{p1}}{z_{s1}}}} \cdot W_{t2}$ $s_{cr1} = 994.7 \text{ MPa}$

Maximum shear stress S_s $s_{sr1} := 0.295 \cdot s_{cr1}$ $s_{sr1} = 293.4 \text{ MPa}$

Stresses on Sun, Planetary and Ring Gear, 3rd stage

Torque on 3rd stage $T_3 := T_m \cdot i_{21} \cdot i_{21} \quad T_3 = 269.1 \text{ N}\cdot\text{m} \quad P := \frac{T_3 \cdot n_m}{9549.3}$

Tangential driving force $W_t \quad W_{t3} := 2000 \cdot \frac{T_3}{D_{s1}} \quad W_{t3} := T_3 \cdot \frac{1}{D_{s1}}$

$$Q := \frac{P}{n_m} \cdot \frac{\left[\left(\frac{z_{p1}}{z_{s1}} \right) + 1 \right]^3}{\frac{z_{p1}}{z_{s1}}} \quad K_{zm} := \frac{10050 \cdot Q \cdot \left(\frac{z_{p1}}{z_{s1}} + 1 \right)}{C_3^3}$$

Face width sun gear $F_3 := 31500 \cdot \frac{Q}{C_3^2 \cdot K_{zm}} \quad F_3 = 28.2 \text{ mm}$

For Sun

Maximum compressive stress $s_{cs1} \quad s_{cs1} := \sqrt{\frac{0.70}{\left(\frac{1}{E} + \frac{1}{E} \right) \cdot \cos(\phi) \cdot \sin(\phi)}} \cdot \sqrt{\frac{W_{t3}}{F_3 \cdot D_{s1}} \cdot \frac{\frac{z_{p1}}{z_{s1}} + 1}{\frac{z_{p1}}{z_{s1}}}} \quad s_{cs1} = 3194.6 \text{ MPa}$

Maximum shear stress $s_{ss1} \quad s_{ss1} := 0.295 \cdot s_{cs1} \quad s_{ss1} = 942.4 \text{ MPa}$

For Planet

Maximum compressive stress $s_{cp1} \quad s_{cp1} := \sqrt{\frac{0.70}{\left(\frac{1}{E} + \frac{1}{E} \right) \cdot \cos(\phi) \cdot \sin(\phi)}} \cdot \sqrt{\frac{W_{t3}}{F_3 \cdot D_{p1}} \cdot \frac{\frac{z_{p1}}{z_{s1}} + 1}{\frac{z_{p1}}{z_{s1}}}} \quad s_{cp1} = 3021.8 \text{ MPa}$

Maximum shear stress $s_{sp1} \quad s_{sp1} := 0.295 \cdot s_{cp1} \quad s_{sp1} = 891.4 \text{ MPa}$

For Ring

Maximum compressive stress $s_{cr1} \quad s_{cr1} := \sqrt{\frac{0.70}{\left(\frac{1}{E} + \frac{1}{E} \right) \cdot \cos(\phi) \cdot \sin(\phi)}} \cdot \sqrt{\frac{W_{t3}}{F_3 \cdot D_r} \cdot \frac{\frac{z_{p1}}{z_{s1}} + 1}{\frac{z_{p1}}{z_{s1}}}} \quad s_{cr1} = 1776.1 \text{ MPa}$

Maximum shear stress $s_{sr1} \quad s_{sr1} := 0.295 \cdot s_{cr1} \quad s_{sr1} = 523.9 \text{ MPa}$

WINDAGE LOSS as per AGMA 6123-A88, section 9.2.2

where:

P_w = windage power loss per gear, kW
 d = operating pitch diameter of gear, mm
 n = gear speed, rpm
 b = total face width, mm
 β = operating helix angle, deg
 m_n = normal module
 A = arrangement constant, from 1000 to 4000,
 base on arrangement

$$p := 24 \cdot \text{in}^{-1} \quad \text{rpm} := \text{min}^{-1}$$

$$T_{in} := 15 \cdot \text{N} \cdot \text{m} \quad C := 19.05 \text{mm}$$

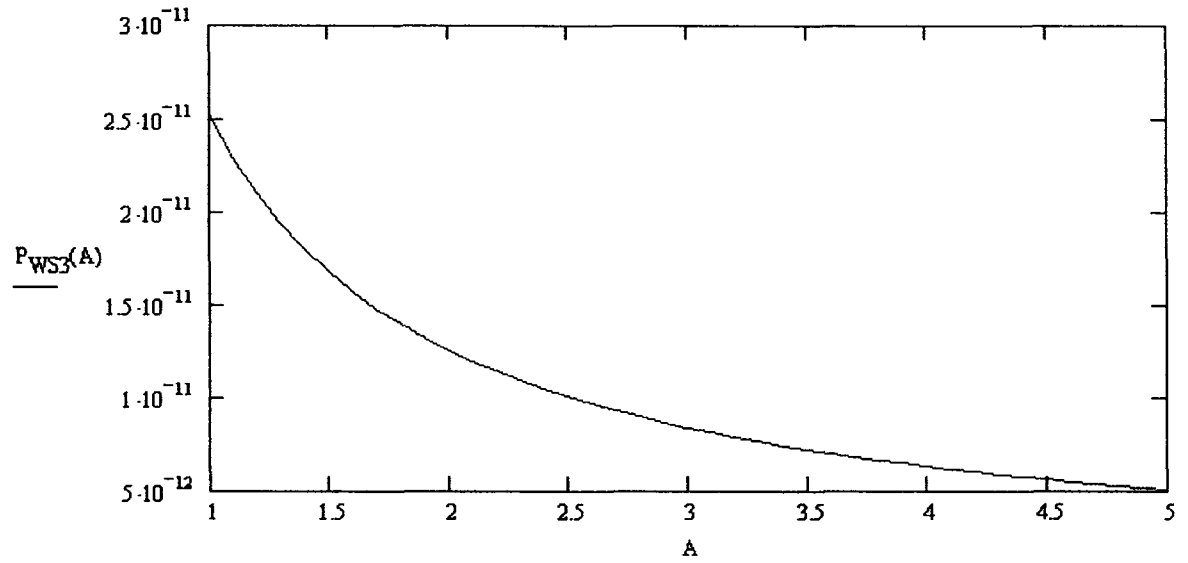
$$n_S := 7500 \text{rpm} \quad \beta := 0 \cdot \text{deg}$$

$$z_P := 19 \quad z_R := 55 \quad z_S := 17$$

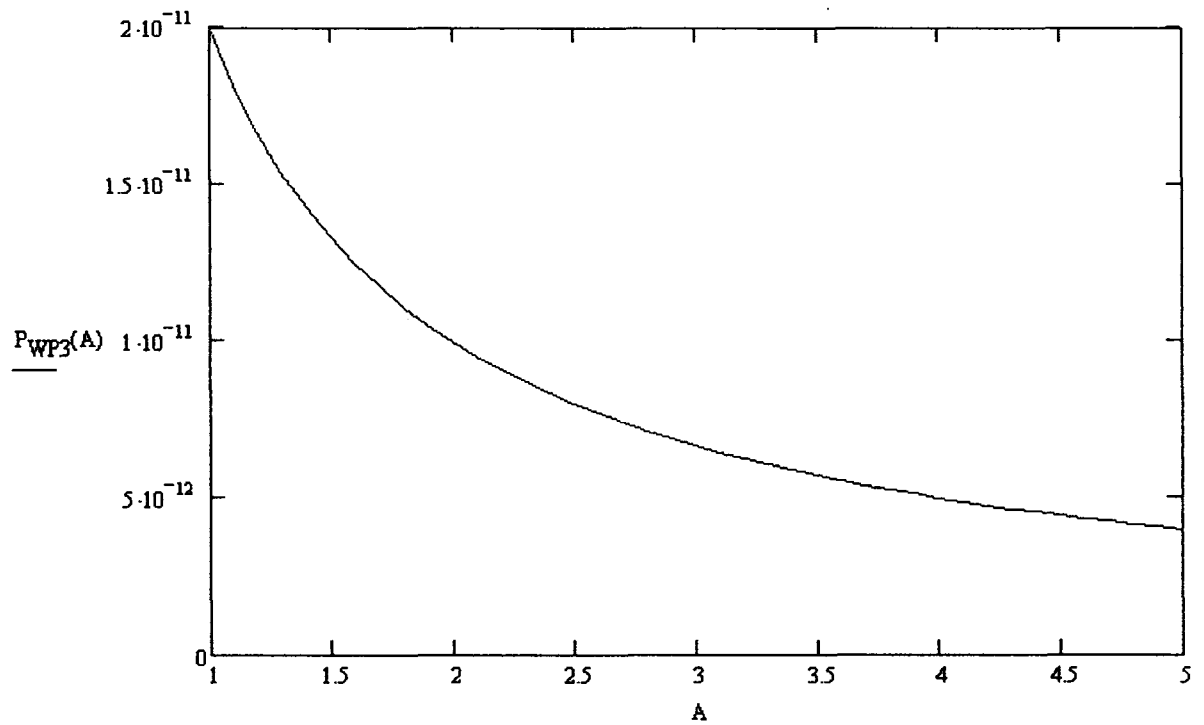
$$\alpha := 25 \text{deg} \quad z_{CP} := 3$$

	SUN GEAR	PLANET GEAR	RING GEAR
Pitch diameter;	$D_S := z_S \cdot p^{-1}$	$D_P := z_P \cdot p^{-1}$	$D_R := z_R \cdot p^{-1}$ $D_R = 58.208 \text{mm}$
Number of teeth;	$z_S := D_S \cdot p$	$z_P := D_P \cdot p$	$z_R := D_R \cdot p$
Circular tooth thk.;	$t_S := \pi \cdot 2 \cdot p^{-1}$	$t_P := \pi \cdot 2 \cdot p^{-1}$	$t_R := \pi \cdot 2 \cdot p^{-1}$ $p = 0.945 \frac{1}{\text{mm}}$
Clearance min, basic;		$c := 0.2000 \cdot p^{-1} + 0.051 \cdot \text{mm}$	
Whole depth, min (basic);		$h_t := 2.200 \cdot p^{-1} + 0.051 \cdot \text{mm}$	
Addendum, basic;		$a := 1.000 \cdot p^{-1}$	
Dedendum, min(basic);		$b := 1.00 \cdot p^{-1} + 0.051 \cdot \text{mm}$	$\cos(\alpha) = 0.906$
Working depth;		$h_k := 2.000 \cdot p^{-1}$	
Outside diameter;	$D_{oS} := D_S + 2 \cdot a$	$D_{oP} := D_P + 2 \cdot a$	$D_{iR} := D_R - 2 \cdot a$
Root diameter;	$D_{rS} := D_{oS} - 2 \cdot h_t$	$D_{rP} := D_{oP} - 2 \cdot h_t$	$D_{rR} := D_{iR} - 2 \cdot h_t$
Basic circle diameter;	$D_{bS} := D_S \cdot \cos(\alpha)$	$D_{bP} := D_P \cdot \cos(\alpha)$	$D_{bR} := D_R \cdot \cos(\alpha)$

Sun gear @ 3rd stage $P_{WS3}(A) = D_S \cdot n_{S3} \cdot b_{S3} \cdot \cos(\beta)^3 \cdot p \cdot \frac{1.42 \cdot 10^{-11}}{A}$ $b_{S3} \equiv 15 \text{ mm}$ $i_0 = (i_1 \cdot i_2 \cdot i_3)$ $i_t = \frac{1}{i_0}$



Planet gear @ 3rd stage $P_{WP3}(A) = 3D_P \cdot n_{P3} \cdot b_{P3} \cdot \cos(\beta)^3 \cdot p \cdot \frac{1.42 \cdot 10^{-11}}{A}$ $b_{P3} \equiv 15 \text{ mm}$ $n_{P3} = n_S \cdot i_t$



BEARING LOSS as per AGMA 6123-A88, section 9.2.3

where:

n_b = bearing speed, rpm

f = bearing coefficient of friction

w = bearing load,

d_o = bearing outside diameter,

d_i = bearing bore

$$f := 0.0011$$

$$d_o := 7\text{mm}$$

$$d_i := 5\text{mm}$$

$$n_b := 7500\text{rpm}$$

$$W_b := 5500\text{N}$$

Sun gear @ 1st stage

$$T_{bS} := f \cdot W_b \cdot \frac{d_o + d_i}{4000}$$

$$P_{BS1} := T_{bS} \cdot \frac{n_b}{9549} \quad P_{BS1} = 2.376 \times 10^{-10} \text{ kW}$$

Planet gear @ 1st stage

$$T_{bP1} := 2f \cdot W_b \cdot \frac{d_o + d_i}{4000}$$

$$n_{P1} := n_S \cdot \frac{D_S}{D_P} \quad n_{P1} = 6.711 \times 10^3 \text{ rpm}$$

$$P_{BP1} := 2T_{bP1} \cdot \frac{n_{P1}}{9549} \quad P_{BP1} = 8.503 \times 10^{-10} \text{ kW}$$

Planet gear @ 2nd stage

$$T_{bP2} := 2f \cdot W_b \cdot \frac{d_o + d_i}{4000}$$

$$n_{P2} := n_{S2} \cdot \frac{D_S}{D_P} \quad n_{P2} = 1.584 \times 10^3 \text{ rpm}$$

$$P_{BP2} := 2T_{bP2} \cdot \frac{n_{P2}}{9549} \quad P_{BP2} = 2.008 \times 10^{-10} \text{ kW}$$

$$n_{P3} := n_S \cdot i_t$$

Planet gear @ 3rd stage

$$T_{bP3} := 3f \cdot W_b \cdot \frac{d_o + d_i}{4000}$$

$$n_{P3} := n_{S3} \cdot \frac{D_S}{D_P} \quad n_{P3} = 374.101 \text{ rpm}$$

$$P_{BP3} := 3T_{bP3} \cdot \frac{n_{P3}}{9549} \quad P_{BP3} = 1.067 \times 10^{-10} \text{ kW}$$

Output square

$$W_{bs} := 15000\text{N} \quad d_{os} := 32\text{mm} \quad d_{is} := 30\text{mm} \quad n_{psq} := n_S \cdot i_t$$

$$T_{bP3s} := f \cdot W_{bs} \cdot \frac{d_{os} + d_{is}}{4000}$$

$$P_{BP3s} := T_{bP3s} \cdot \frac{n_{psq}}{9549} \quad P_{BP3s} = 4.407 \times 10^{-11} \text{ kW}$$

$$n_{psq} = 98.735 \text{ rpm}$$

$$P_{tot} := P_{BS1} + P_{BP3s} + (2P_{BP1} + 2P_{BP2} + 3P_{BP3})$$

$$P_{tot} = 2.704 \times 10^{-9} \text{ kW}$$

H. MATERIAL and LUBRICANT



Allvac

An Allegheny Technologies Company

TECHNICAL DATA SHEET

VASCOMAX[®] C-200/C-250/C-300/C-350

GENERAL

VascoMax alloys (18% nickel maraging steels) are divided into two broad classes depending on the primary strengthening element in the chemical analysis. The original maraging steels, introduced in the early 1960's, depend on cobalt (7-12% cobalt depending on grade) as their strengthening agent; they are cobalt strengthened 18% nickel maraging steels. In the early 1980's, Allvac introduced a new type of maraging steel which contains no cobalt and has titanium as a primary strengthening agent; they are titanium-strengthened 18% nickel maraging steels.

Cobalt-strengthened grades, or "C-type 18 Ni maraging", are designated by the letter "C" in the grade identification (example: VascoMax C-250). Titanium-strengthened grades, or "T-type 18Ni maraging", are designated by the letter "T" in the grade identification (example: VascoMax T-250).

This data sheet covers the C-type 18Ni maraging steels manufactured by Allvac: VascoMax C-200, VascoMax C-250, VascoMax C-300, and VascoMax C-350. Information on the T-type VascoMax grades is available in a separate Technical Data Sheet. Allvac continues to be a leading producer of the titanium-strengthened alloys. It should be emphasized that the essential difference between C-type and T-type maraging steels is the chemical analysis. In terms of mechanical properties and recommended processing, there are few, if any, significant differences. Since high purity melting is essential to assure optimum mechanical properties, Allvac employs double vacuum melting - under strictest quality control - for all VascoMax grades.

Numerical designations for each grade, while not direct correlations in all cases, are generally representative of the ultimate tensile strength of that grade, expressed in ksi. For example, VascoMax C-350 has a nominal ultimate tensile strength of 350 ksi (350,000 psi). This variety in property levels among the four grades allows flexibility in selecting the property combination which best suits a given application. Mechanical properties of the four VascoMax C-grades are reported in Table 1 on page 3 illustrating briefly their properties and highlighting their outstanding values.

An additional benefit of the VascoMax alloys is the age hardening reaction of these nickel maraging steels. In the solution annealed condition (as supplied to the customer), they are very tough, relatively soft (30/35 Rc), and therefore, readily machined and formed. After machining or forming, a precipitation hardening (aging) process, which requires no protective atmosphere and relatively low furnace temperatures, raises the hardness to a level sufficient for many tooling applications.

APPLICATIONS

Allvac produces the VascoMax alloys in a full range of "long" mill product forms including billet, bar, rod, rod coil, and wire.

Extensive laboratory and field testing, plus numerous production applications of VascoMax C-250, have proven that this family of maraging steels is equivalent to, or slightly better than, the cobalt-bearing grades. Typical applications for the maraging steels are missile and rocket motor cases, wind tunnel models, recoil springs, flexures, actuators, landing gear components, high performance shafting, gears, and fasteners. The alloys are used in extrusion tooling, and in the die casting industry for long-run dies and also as core pins.

DEVELOPMENT

Aerospace demands for ultra-high performance materials led to the development of the C-type 18% nickel maraging steels by the International Nickel Company (INCO) in the early 1960's. Vasco was instrumental in assisting INCO in this development and pioneered these alloys in the specialty steel industry.

NI-253/154/156/173

Data are typical and should not be construed as maximum or minimum values for specification or for final design. Data on any particular piece of material may vary from those shown herein. Allvac[®] and VascoMax[®] are registered trademarks of ATI Properties, Inc. © Copyright, Allvac 2000.

Page 1 of 12

2020 Ashcraft Ave • PO Box 5030 • Monroe, NC 28110-5030 • (704) 289-4511 • Fax (704) 289-4018 • www.allvac.com



Allvac

An Allegheny Technologies Company

TECHNICAL DATA SHEET

VASCOMAX[®] C-200/C-250/C-300/C-350

RECOMMENDED HEAT TREATMENT

All VascoMax steels are furnished in the solution annealed condition. They are very tough, relatively soft (28 to 32 Rc) and, therefore, readily machined and formed. They achieve full properties through martensitic precipitation aging (hence the name maraging steels) - a relatively simple, low temperature heat treatment. As is true of other heat treating procedures, aging is a time/temperature dependent reaction. Of these two factors, temperature is more important than time.

Because the VascoMax steels are essentially carbon-free, protective atmospheres are not required during annealing or aging. This is one of several VascoMax advantages over carbon-strengthened high-strength steels which are subject to carburization and decarburization, and thus require a protected or neutral environment.

The VascoMax steels are also exceptionally stable during annealing and aging, offering predictable, uniform shrinkage on all dimensions. This distortion-free (nonwarping) characteristic is a significant advantage over many other high-strength steels.

The VascoMax C-steels should be aged at 900° to 925°F (480° to 495°C) for three to six hours. Air cool. Very large cross sections should be aged for longer periods.

RECOMMENDED PROCEDURES FOR PROCESSING/FABRICATION

The VascoMax C-steels are processed essentially the same as the titanium-bearing 18% nickel maraging steels. Detailed procedures for machining, cold working, warm working, hot working, welding, nitriding, plating, forging, rolling, solution annealing, as well as recommendations for die casting applications, can be found in the VascoMax C Recommended Procedures for Processing and Fabrication Data Sheet.

ADVANTAGES OF VASCOMAX

Allvac prepared this technical data sheet to assist both the engineer and the less technically oriented individual in understanding the tremendous benefits of VascoMax alloys as both structural and a tooling material. Here is a summary of those advantages

- **Excellent Mechanical Properties**
 - High yield and ultimate tensile strengths
 - High toughness, ductility, and impact strengths
 - High fatigue strength
 - High compressive strength
 - Hardness and wear resistance sufficient for many tooling applications
- **Excellent Workability**
 - Easily machined
 - Readily formed - cold, warm, or hot (without in-process anneals)
 - High resistance to crack propagation
 - Excellent polishability
 - Good weldability
- **Excellent Heat Treatment Characteristics**
 - Low furnace temperatures required
 - Precipitation hardening, aging heat treatment
 - Uniform, predictable shrinkage during heat treatment
 - Minimal distortion during heat treatment
 - Through-hardening without quenching
 - No protective atmosphere required
 - Freedom from carburization or decarburization
- **Advantages During Application**
 - Low coefficient of expansion minimizes heat checking
 - Pitting and corrosion resistance superior to common tool steel
 - Good repair weldability
 - Excellent mechanical properties have led to longer tool life
 - Easily reworked and retreated for secondary tool life

NI-253/154/156/173

Data are typical and should not be construed as maximum or minimum values for specification or for final design. Data on any particular piece of material may vary from those shown herein. Allvac[®] and VascoMax[®] are registered trademarks of ATI Properties, Inc. © Copyright, Allvac 2000.

Page 2 of 12

2020 Ashcraft Ave • PO Box 5030 • Monroe, NC 28110-5030 • (704) 289-4511 • Fax (704) 289-4018 • www.allvac.com

VASCOMAX® C-350
Physical Properties

Average Coefficient of Thermal Expansion (70-900° F)	6.3×10^{-4} in/in/°F
Modulus of Elasticity	29×10^6 psi
Density	.292 lbs/cu. in. (8.1 g/cc)
Thermal Conductivity at 68° F	14.6 BTU/(ft)(hr)(°F)
at 122° F	14.9 BTU/(ft)(hr)(°F)
at 212° F	15.6 BTU/(ft)(hr)(°F)

Nominal Annealed Properties

Hardness	35 Rc
Yield Strength	120 ksi
Ultimate Strength	165 ksi
Elongation	18%
Reduction of Area	70%

Nominal Room Temperature Properties after Aging

Size	Direction	Hardness Rockwell "C"	Tensile Strength ksi	0.2% Yield Strength ksi	Elongation in 4.5 \sqrt{A} %	Reduction of Area %
5/8" Round	Longitudinal	57.8	350.2	342.7	7.5	35.4
1 1/4" Round	Longitudinal	58.4	346.8	340.6	7.6	33.8
3" Round	Longitudinal	58.2	342.2	336.5	6.2	28.6
.250" Sheet	Transverse	57.7	355.5	347.3	3.0	15.4

Effect of Stress Concentration Factor, K_t , on Tensile Properties

K_t	Notch Tensile Strength		Notch-To-Smooth Tensile Strength Ratio*
	Average ksi	Range ksi	
2.0	433.7	427.4 - 437.3	1.20
6.25	334.3	331.7 - 337.6	0.93
9.0	333.0	326.7 - 338.6	0.92

* Based on smooth bar tensile strength of 362.8 ksi

All samples solution annealed for one hour at 1500° F, air cooled and aged at 900° F for three hours.

Effect of Test Temperature on Tensile Properties

Test Temp °F	0.2% Yield Strength ksi	Ultimate Tensile Strength ksi	Elongation in 4.5 \sqrt{A} %	Reduction of Area %
600 °F	295.4	310.2	12.3	54.9
800 °F	277.3	288.4	15.6	57.6
900 °F	251.9	270.4	17.4	60.3
1000 °F	233.6	251.8	20.0	70.9

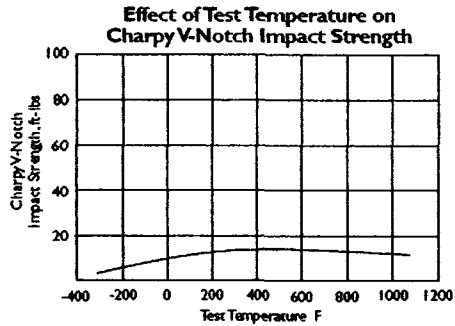
All samples solution annealed for one hour at 1500° F, air cooled and aged at 900° F for six hours.

Condition	Compressive Strength		Rockwell "C" Hardness
	Proportional Limit ksi	0.2% Offset Yield Strength ksi	
Solution Annealed	108.0	160.5	34.3
Aged	349.3	388.1	59.6

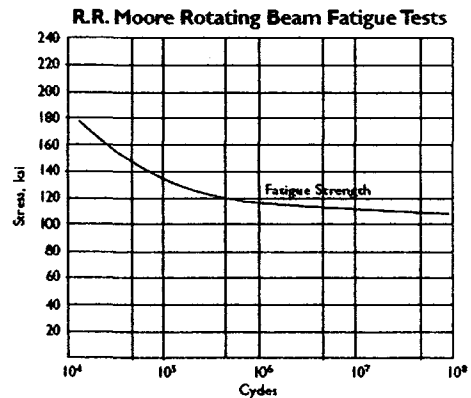
Samples solution annealed for 30 minutes at 1500° F, air cooled and aged 3 hours at 900° F as indicated. Average of 3 tests per condition.



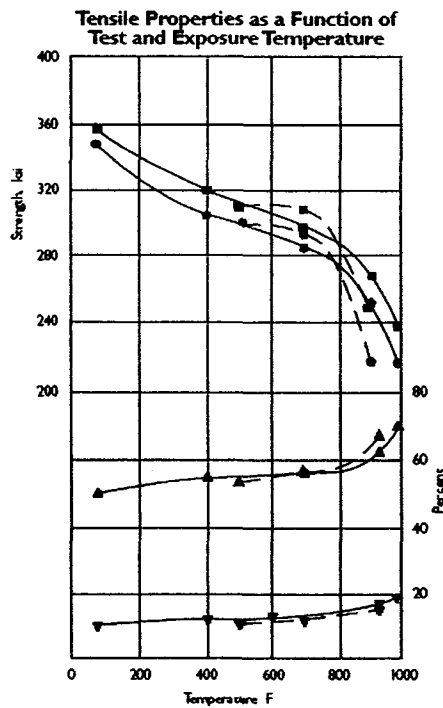
VASCOMAX® C-350



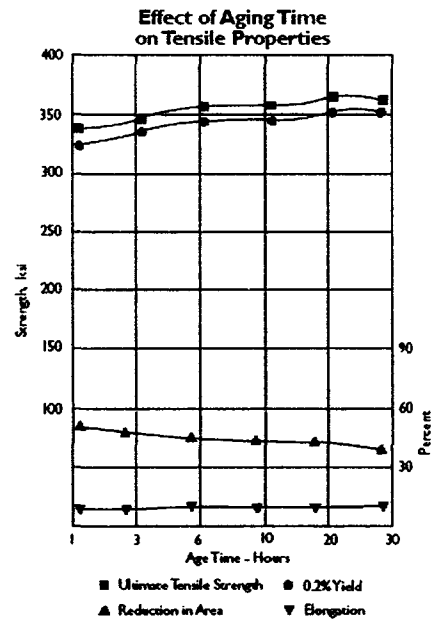
All samples solution annealed for 30 minutes at 1500° F, air cooled and aged at 900° F for three hours.



All samples solution annealed for 30 minutes at 1500° F, air cooled and aged at 900° F for three hours.



All samples annealed for one hour at 1475° F, air cooled and aged at 900° F for three hours.



All specimens solution annealed for one hour at 1500° F, air cooled and aged at 900° F for the times indicated.

No.253/154/156/173 Data are typical and should not be construed as maximum or minimum values for specification or for final design. Data on any particular piece of material may vary from those shown herein. Allvac® and VascoMax® are registered trademarks of ATI Properties, Inc. © Copyright, Allvac 2000. Page 12 of 12



DURON® XL SYNTHETIC BLEND ENGINE OILS

DURON XL Synthetic Blend Engine Oils are super premium, heavy duty engine oils specially formulated to meet the rigors of cold, harsh winters and are recommended for year-round use in vehicles operating in both highway and off-highway applications.

DURON XL Synthetic Blend 15W-40 possesses the superior soot dispersing properties required by the latest low emission engine designs – beyond that of API CI-4, Caterpillar ECF-1, Mack EO-N Premium Plus and Cummins 20078. It is especially recommended for use in extremely demanding operations, running in both highway and off-highway applications

DURON XL Synthetic Blend 10W-40 delivers the same high temperature performance as the SAE 15W-40 grade, but with superior low-temperature fluidity for easier winter operation.

DURON XL Synthetic Blend 0W-30 is fully approved against the demanding requirements of API CH-4, Caterpillar ECF-1, Mack EO-M Plus and Cummins 20076. It permits unassisted start-ups down to - 45°C. It is also an excellent hydraulic fluid for mobile equipment, where a motor oil is specified.

Typical Characteristics are shown below:

SAE Grade	DURON XL Synthetic Blend		
	15W-40	10W-40	0W-30
Viscosity cSt @ 40°C	110	107	68.7
cSt @ 100°C	15.3	15.6	12.1
SU @ 100°F	566	546	348
SU @ 210°F	80	81	67
Viscosity Index	146	158	176
Flash Point, °C / °F	235/455	231/448	231/448
Pour Point, °C / °F	-42/-44	-42/-44	<-51/<-60
Cold Crank Viscosity,			
cP @ -15°C / +5°F	2,534	-	-
cP @ -20°C / -4°F	4,305	2,918	-
cP @ -25°C / -13°F	-	5,411	-
cP @ -30°C / -22°F	-	-	2,911
cP @ -35°C / -31°F	-	-	5,249
Border Line Pumping Viscosity, cP @ °C	13,988@-25	20,500@-30	18,113@-40
Sulphated Ash, % Wt	1.37	1.18	1.18
Total Base No.	10.5	9.0	9.1

For DURON XL Synthetic Blend Performance Specifications, Refer to Table AL-1 (see Page 56)